

**THE ROLE OF APOLIPOPROTEIN E IN TRAUMATIC BRAIN INJURY AS
DETERMINED BY ISOFORM AND *ApoE* HAPLODEFICIENCY**

by

Emilie L. Castranio

BA, Washington & Jefferson College, 2013

Submitted to the Graduate Faculty of
the Department of Environmental and Occupational Health
Graduate School of Public Health in partial fulfillment
of the requirements for the degree of
Doctor of Philosophy

University of Pittsburgh

2018

UNIVERSITY OF PITTSBURGH
GRADUATE SCHOOL OF PUBLIC HEALTH

This dissertation was presented

by

Emilie L. Castranio

It was defended on

July 12th, 2018

and approved by

Aaron Barchowsky, PhD, Professor, Department of Environmental and Occupational Health,
Graduate School of Public Health, University of Pittsburgh

Radosveta Koldamova, MD, PhD, Associate Professor, Department of Environmental and
Occupational Health, Graduate School of Public Health, University of Pittsburgh

C. Edward Dixon, PhD, Professor, Department of Neurological Surgery, School of Medicine,
University of Pittsburgh

Dissertation Advisor: Iliya Lefterov, MD, PhD, Research Professor, Department of
Environmental and Occupational Health, Graduate School of Public Health, University of
Pittsburgh

Copyright © by Emilie L. Castranio

2018

THE ROLE OF APOLIPOPROTEIN E IN TRAUMATIC BRAIN INJURY AS DETERMINED BY ISOFORM AND *Abca1* HAPLODEFICIENCY

Emilie L. Castranio, PhD

University of Pittsburgh, 2018

ABSTRACT

Traumatic brain injury (TBI) is a significant public health concern as one of the leading causes of death and disability in the United States. TBI is due to the head forcibly contacting another object, or other mechanisms causing displacement of the brain within the skull. TBI is a complex multimodal disease process associated with high heterogeneity in outcomes, which suggests significant influence by genetic factors. Recent studies implicate the apolipoprotein E (*APOE*) gene in modulating TBI outcomes in an isoform-specific manner, specifically with inheritance of the *APOE4* allele conferring worse outcome. The isoform-specific effect may be modulated by ATP-binding cassette transporter A1 (ABCA1), a transmembrane protein that mediates the transport of lipids and cholesterol onto APOE, impacting its lipidation and stability.

First, we examined whether there is an APOE isoform-specific response to TBI using mice expressing human *APOE3^{+/+}* or *APOE4^{+/+}* isoforms. At 3-months-old, TBI-treated mice received a craniotomy followed by a controlled cortical impact in the left hemisphere, whereas sham-treated mice received only a craniotomy. We found that both isoforms demonstrated similar cognitive impairments and transcriptional profiles following moderate TBI. We then examined the impact of ABCA1 deficiency on the response to traumatic brain injury using human *APOE3^{+/+}* and *APOE4^{+/+}* targeted replacement mice with only one functional copy of the *Abca1* gene (*E3/Abca1^{+/-}*; *E4/Abca1^{+/-}*). We observed a common transcriptional response to TBI

among the genotypes – *E3/Abca1*^{+/+}, *E4/Abca1*^{+/+}, *E3/Abca1*^{+/-}, *E4/Abca1*^{+/-} – however, *E4/Abca1*^{+/-} had the highest proportion of unique transcripts. Additionally, we found that *Abca1* haploinsufficiency increased the expression of microglia sensome genes among only *APOE4* injured mice. Our results suggest that the *APOE4* isoform is more susceptible to the consequences of *Abca1* haploinsufficiency.

To identify modules, or interconnected gene clusters, correlated to TBI, *APOE* isoform, and *Abca1* haploinsufficiency, we performed Weighted Gene Co-expression Network Analysis (WGCNA). We determined that the module most correlated to TBI, regardless of *APOE* isoform or *Abca1* deficiency, represented “immune response” with major hub genes including microglia-specific genes *Trem2*, *Tyrobp*, and *Cd68*. Unique modules were also associated with *APOE* isoform, and *Abca1* haploinsufficiency. Our results identify genes with a potential to become useful targets for future research.

TABLE OF CONTENTS

PREFACE.....	XIV
1.0 INTRODUCTION.....	1
1.1 TRAUMATIC BRAIN INJURY	1
1.1.1 The pathophysiology of traumatic brain injury	2
1.1.2 Inflammation is a key pathological feature of TBI.....	3
1.1.3 Prognosis of TBI	4
1.1.4 Factors influencing TBI outcomes	5
1.2 APOLIPOPROTEIN E: A GENETIC MODIFIER OF TBI OUTCOMES. 5	
1.2.1 Apolipoprotein E Structure and Function	5
1.2.2 APOE and its isoform specific role in TBI.....	7
1.2.3 ATP-binding Cassette Transporter A1: An important regulator of APOE	8
1.2.4 APOE, ABCA1 and neuroinflammation	9
1.3 DISSERTATION OBJECTIVES.....	10
2.0 MATERIALS & METHODS.....	11
2.1 MOUSE MODELS	11
2.1.1 Transgenic lines	11
2.1.2 Breeding.....	12

2.2	CRANIOTOMY AND CONTROLLED CORTICAL IMPACT SURGERY .	
	12
2.3	BEHAVIORAL TESTING	13
2.3.1	Elevated Plus-maze test.....	13
2.3.2	Morris Water Maze test	13
2.4	ANIMAL TISSUE PROCESSING	14
2.5	TRANSCRIPTOME ANALYSIS.....	15
2.5.1	RNA Isolation, RT-qPCR and Sequencing	15
2.5.2	Principle Component Analysis	16
2.5.3	Functional Pathway Analysis	16
2.5.4	Weighted Gene Co-expression Network Analysis	16
2.6	WESTERN BLOT	17
2.7	IMMUNOHISTOCHEMISTRY & QUANTIFICATION.....	18
2.8	STATISTICS.....	19
3.0	GENE CO-EXPRESSION NETWORKS IDENTIFY TREM2 AND TYROBP AS MAJOR HUBS IN HUMAN APOE EXPRESSING MICE FOLLOWING TRAUMATIC BRAIN INJURY.....	20
3.1	ABSTRACT.....	20
3.2	INTRODUCTION	21
3.3	METHODS.....	24
3.3.1	Animals	24
3.3.2	Controlled Cortical Impact.....	25
3.3.3	Elevated-Plus Maze	25

3.3.4	Morris Water Maze	26
3.3.5	Animal Tissue Processing	27
3.3.6	Immunohistochemistry	27
3.3.7	RNA isolation and mRNA sequencing	28
3.3.8	Principle Component analysis	29
3.3.9	Functional Pathway analysis	29
3.3.10	Weighted Gene Co-expression Network Analysis	29
3.3.11	Western blot	30
3.3.12	Statistical Analyses	30
3.4	RESULTS	31
3.4.1	TBI causes anxiety-related changes and spatial learning deficits	31
3.4.2	Changes in transcriptome induced by TBI reflect stimulated immune response and decreased neuronal functionality	32
3.4.3	Transcriptome analysis demonstrates a higher expression of markers for resident microglia versus peripheral macrophages	35
3.4.4	Integrated system approach identifies correlated gene networks associated with TBI	38
3.4.5	Networks associated with expressed APOE isoform	44
3.5	DISCUSSION	47
3.6	SUPPLEMENTAL MATERIALS & FIGURES	53
3.6.1	TBI consistently affects biological processes in both APOE isoforms	53
3.6.2	Gene Set Enrichment Analysis identifies biological processes commonly effected by injury in both isoforms	58

3.6.3	WGCNA identifies correlations between modules	60
3.6.4	ME brown strongly correlates with injury regardless of APOE isoform	61
3.6.5	Microglia localize to the injury site in TBI brains.....	61
3.6.6	Gene-network associated with ‘transport’ is downregulated in injured mice	64
3.6.7	ME Darkred and ME Salmon both correlate with APOE isoform	64
4.0	ABCA1 HAPLODEFICIENCY AFFECTS THE BRAIN TRANSCRIPTOME FOLLOWING TRAUMATIC BRAIN INJURY IN MICE EXPRESSING HUMAN APOE ISOFORMS	67
4.1	ABSTRACT.....	67
4.2	INTRODUCTION	68
4.3	MATERIALS & METHODS	72
4.3.1	Animals.....	72
4.3.2	Traumatic Brain Injury	72
4.3.3	Tissue Processing	73
4.3.4	RNA Isolation and RNA Sequencing.....	73
4.3.5	Weighted Gene Co-expression Network Analysis (WGCNA).....	74
4.3.6	Functional Pathway Analysis	75
4.4	RESULTS	75
4.4.1	TBI induces changes to the transcriptome that are common among both <i>Abca1^{+/+}</i> and <i>Abca1^{+/-}</i> mice expressing human APOE isoforms	75

4.4.2	TBI significantly alters the expression of transcripts unique to each genotype, with the highest proportion of unique transcripts among E4/ <i>Abca1</i> ^{+/-} mice	78
4.4.3	<i>Abca1</i> haploinsufficiency upregulates microglia sensome genes in injured APOE4 mice.....	80
4.4.4	WGCNA reveals interconnected gene clusters associated with each trait of interest- <i>APOE</i> isoform, <i>Abca1</i> copy number, and injury status.....	82
4.5	DISCUSSION.....	88
4.6	CONCLUSIONS	91
5.0	FINAL CONCLUSIONS.....	93
5.1	GENERAL SUMMARY	93
5.1.1	Strengths and Limitations.....	95
	BIBLIOGRAPHY.....	97

LIST OF TABLES

Table 1. Gene-network modules represent various biological functions associated with injury and APOE isoform.....	40
Table 2. Differentially expressed genes of interest and their corresponding coefficients.....	55
Table 3. TBI increases the expression of genes related to immune response and inflammation in both APOE3 and APOE4 mice.....	56
Table 4. TBI decreases the expression of genes related to transport and ion transmembrane transport in APOE3 and APOE4 mice.....	57

LIST OF FIGURES

Figure 1. TBI significantly affected behavior performance in mice expressing human APOE3 and APOE4 isoforms.	32
Figure 2. TBI significantly affected the transcriptome demonstrating increases in immune response and decreases in neuronal functionality.	34
Figure 3. mRNA-seq data reveal that microglia are predominant source of inflammation.	37
Figure 4. WGCNA identified modules that correlated to TBI and or APOE isoform.	39
Figure 5. ME Brown correlates to TBI and is associated with Immune Response.	41
Figure 6. TREM2 protein level and Astrocytosis are increased by TBI.	43
Figure 7. ME darkred correlates to APOE isoform and is associated with innate immunity.	46
Figure 8. Gene-network module salmon correlates to APOE isoform in injury groups and is associated with myelination.	47
Figure 9. Gene set enrichment analysis of injury.	59
Figure 10. (Related to Fig. 4) WGCNA identified correlations between modules.	60
Figure 11. (Related to Fig. 5) Module related to injury was identified by relationship between gene significance and module membership.	62
Figure 12. Microglia are significantly higher in TBI animals and concentrated at the injury site.	63

Figure 13. Gene-network module green is downregulated in TBI animals and reflects biological process “transport” 65

Figure 14. (Related to Figure 7-8). Modules related to APOE isoform were identified by relationship between gene significance and module membership..... 66

Figure 15. TBI increases the expression of genes associated with immune response, and decreases the expression of genes connected to ion transmembrane transport. 77

Figure 16. TBI affects a greater proportion of unique genes in E4/Abca1^{+/-} mice. 79

Figure 17. Abca1 deficiency affects the microglial response to TBI in an APOE isoform-dependent manner. 81

Figure 18. WGCNA identified modules correlated to TBI and Abca1 haploinsufficiency..... 84

Figure 19. ME turquoise consists of two sub-modules correlated to injury status. 87

PREFACE

ACKNOWLEDGEMENTS

This dissertation would not have been possible without the support and assistance of many people, and I am sincerely grateful to all of them. In particular, my thanks go out to my advisors, Dr. Iliya Lefterov and Dr. Radosveta Koldamova for providing this opportunity to grow as a scientist. I am grateful to the entire Koldamova-Lefterov lab for their contributions to the articles within this dissertation, however, Drs. Kyong Nyon Nam, Anaïs Mounier, and Alexis Carter, as well as soon-to-be Dr. Cody Wolfe, will always stand out in my mind for their support, understanding and friendship throughout this process. I would also like to thank the entire Environmental and Occupational Health department, and my committee members, Dr. Barchowsky and Dr. Dixon. I would also like to thank my previous mentors from Washington & Jefferson College and Emory University, Dr. Ronald J. Bayline, Dr. Constance Harrell and Dr. Neigh, who helped get me to this point through their training and support.

Finally, I would like to thank my family, particularly my parents, Richard and Lorraine Castranio. Their endless support and encouragement was necessary to the completion of my dissertation and Ph.D. Last, but not least, I thank my husband, Ethan J. Guswiler, whose love, support, and patience was the most necessary of all. I dedicate this dissertation to you.

1.0 INTRODUCTION

1.1 TRAUMATIC BRAIN INJURY

Traumatic brain injury (TBI) is an acquired injury that results from the head forcibly contacting another object, or other mechanisms causing displacement of the brain within the skull (e.g. inertia) [80]. TBI is one of the leading causes of death and disability in the United States. It is estimated that 2 million people in the U.S. have suffered a TBI, and over 50,000 TBI-related deaths occur each year [31,72]. In the recent decade, the number of hospitalizations and emergency department visits increased by 11% and 70%, respectively. While the overall death rate has decreased, TBI remains a contributing factor in a third of all injury-related deaths [42].

TBI is a significant public health problem adversely impacting the individual, families, and the economy. Approximately 2% of the U.S. population suffer from a TBI-related disability, and the rate of TBIs continues to rise in vulnerable populations, including children, the elderly, contact-sport athletes, and military personnel [123,32]. Compounding the issue further is the lack of existing treatment; patients are only given supportive care for which there is a large societal toll. Caregivers face a higher burden of distress, and depression, in addition to deterioration of the family unit [4]. There is also a great economic toll of TBI; in 2010, direct and indirect medical costs totaled over \$76 billion, at \$11.5 billion and \$64.8 billion respectively [25]. To date, potential TBI treatments from preclinical studies have not translated into successful

outcomes in clinical trials. A better understanding of the pathophysiology of traumatic brain injury and the modifying factors will facilitate the development of successful therapeutics.

1.1.1 The pathophysiology of traumatic brain injury

TBI is a complex multimodal disease process, not a single pathophysiological event. Structural and functional deficits are the result of both primary and secondary injury mechanisms. The primary injury is the immediate result of the impact, as seen through the mechanical stress on cells and tissues, including contusion, hemorrhage, shearing of axons, and perforations in cells and membranes [143]. The primary injury occurs immediately after the moment of impact, and as a result is not treatable, only preventable.

The secondary injury develops over the next minutes, can extend up to years after the injury, and contributes to additional damage and cell death beyond the initial site of injury [18]. The secondary injury is comprised of a number of pathways and signaling cascades, involving metabolic, molecular, and cellular events. These include glutamate excitotoxicity, perturbed cellular calcium homeostasis, lipid peroxidation, oxidative stress, mitochondrial dysfunction, and neuroinflammation [125,8,112]. Collectively, the cascade of the secondary injury events results in neuronal and glial cell death, as well as white matter degeneration [143]. The prolonged nature of the secondary injury provides an opportunity for pharmacological intervention, however, understanding the mechanisms of the secondary injury will be necessary for the development of successful therapeutics.

1.1.2 Inflammation is a key pathological feature of TBI

Inflammation is a major component of the secondary injury and has been a recent focus of research as a means of developing therapies and improving outcomes after TBI. Inflammation is present in every case of TBI, developing within minutes, and can persist for many years following the injury [2]. It is closely associated with neuronal death, impaired cell proliferation, and severity of outcomes. [37]. Additionally, inflammation can be linked directly or indirectly to all other alterations of the secondary injury [99].

The interaction between the molecular and cellular branches of the inflammatory response may in turn perpetuate the inflammatory state of the brain [52]. The molecular component, consisting of multiple inflammatory molecules upregulated by TBI, serve to recruit and orchestrate the immune reaction, as well as contribute to neuronal cell death and blood brain barrier dysfunction. Interleukin-1 β (IL-1 β), tumor necrosis factor- α (TNF- α), chemokine C motif ligand 2 (Ccl2), and chemokine CX3C motif receptor 1 (Cx3cr1) are among those that have been intensely studied for their impact on brain pathology following TBI [36,43,51,59]. Studies have primarily shown that the expression levels of these inflammatory factors are associated with severity of injury, outcome in TBI patients, neurobehavioral impairments, as well as the survival rates in rodent models [91,144].

Microglia are the resident macrophage cells of the central nervous system and are the brain's main form of immune response to infection, disease, and injury. In normal conditions, microglia survey their surroundings for inflammatory cues, phagocytose damaged cells, but also contribute to neuronal survival and synaptic remodeling [98]. Microglia rapidly respond to injury; microglial activation in TBI patients has been shown as early as 3 days, with animal models demonstrating increased microglial activation as early as 24-hours [127]. Microglia are

capable of contributing to neurotoxicity by releasing pro-inflammatory cytokines, and reactive oxygen species (ROS). Activated microglia can persist for years after TBI and are often co-localized with areas of neuronal degeneration and axonal abnormalities, suggesting a role for microglia in the progression and long-term consequences of TBI [39].

1.1.3 Prognosis of TBI

According to the criteria outlined in the *Diagnostic and Statistical Manual of Mental Disorders*, 5th edition, TBI is accompanied by at least one of the following: loss of consciousness, amnesia, disorientation, and/or neurological signs, such as neuroimaging indicating an injury, onset of seizures, or visual field cuts [7].

TBI can lead to temporary and permanent impairments in cognitive, behavioral, emotional and physical functions. Impairments can present days, months and even years after the initial injury. Impairments in cognitive functions are a common result of TBI, and include difficulties with memory, attention, learning, and sleep disturbances [133]. In the long-term, the majority of TBI patients experience changes in personality, language and communication problems, anxiety, and depressive-like behaviors [49,105,117].

TBI is also associated with the delayed development of psychological and neurological disorders, which may contribute to long-term impairment and disability. Post-traumatic epilepsy and seizures, depression, and post-traumatic stress disorder are common examples of these disorders. Additionally, TBI is strongly linked with increased risk of developing neurodegenerative dementias, including chronic traumatic encephalopathy and Alzheimer's disease (AD) [109,27].

1.1.4 Factors influencing TBI outcomes

There are a number of factors that contribute to the variability in presentation of symptoms, as well as influence long-term consequences of TBI. Symptoms can vary based on location, severity and nature of the injury. However, individual characteristics, such as age, health, gender, and drug use, also influence the heterogeneity of the secondary injury and increase the variability in TBI outcomes. Additionally, the high level of variability in outcomes suggests a significant role for genetic influence on brain susceptibility and recovery [40,141].

1.2 APOLIPOPROTEIN E: A GENETIC MODIFIER OF TBI OUTCOMES

1.2.1 Apolipoprotein E Structure and Function

The Apolipoprotein E (*APOE*) gene encodes a 34 kDa glycoprotein consisting of 299 amino acids [81,82]. There are 3 different alleles that can be inherited at the single locus (19q13.2) for *APOE*; $\epsilon 2$, $\epsilon 3$ and $\epsilon 4$ (*APOE2*, *APOE3* and *APOE4*, respectively). *APOE2* is present at the lowest frequency in humans, followed by *APOE4*, then *APOE3* at approximately 8.4%, 13.7% and 77.9% [84]. The alleles differ at 2 amino acid positions, 112 and 158; *APOE2* has cysteine present at both positions (Cys-112 and Cys-158), and *APOE4* has arginine present at both positions (Arg-112 and Arg-158). The *APOE3* allele has a cysteine at the 112 position (Cys-112) and an arginine at the 158 position (Arg-158) [60]. The difference in amino acid sequence, due to inheritance of any allele over the other, affects protein stability and domain region conformation.

The structure consists of two structural domains, the N-terminal domain and the C-terminal domain, connected by a 20 to 30 amino acids that may serve as a flexible hinge. The C-terminal domain (approximately amino acids 225-299) contains the critical region (amino acids 244-272) for lipid binding [83]. The N-terminal domain, consisting of amino acids 1-191, forms an extended four-helix bundle. It also contains the region (amino acids 136-150) that interacts with the ligand binding domain of members of the low density lipoprotein (LDL) receptor family. The amino acid differences at the 158 position among the isoforms affects receptor binding activity, with ApoE3 and ApoE4 binding normally, and ApoE2 binding is markedly reduced [139]. Whereas the arginine present at the 112 position in ApoE4 has no effect on binding activity, it causes a difference in conformation of the arginine at the 61 position (Arg-61). The Arg-112 in ApoE4 causes the Arg-61 side chain to extend away from the four-helix bundle, which leads to an interaction with a glutamate residue at the 255 position (Glu-255), resulting in a compact structure. In contrast, due to the Cys-112 in both ApoE2 and ApoE3, the Arg-61 side chain remains tucked between the helices; therefore, no interaction can occur with the Glu-255, resulting in a more extended structure [138,150].

The brain is the most cholesterol-rich organ in the body, containing 20% of the entire body's cholesterol [15]. Within the brain, cholesterol and phospholipids are necessary for the formation and maintenance of healthy cells and synapses [106,75]. APOE is the major cholesterol and lipid transporter in the central nervous system [108]. APOE, produced primarily by astrocytes, serves as the scaffold for formation of high-density lipoprotein (HDL) particles that are responsible for trafficking of cholesterol and phospholipids throughout the brain [107,82]. APOE binds, with high affinity, to members of the low-density lipoprotein (LDL) receptor family, including the LDL receptor and the very low-density lipoprotein (VLDL)

receptor, which then internalize the lipoprotein particles, allowing for lipid and cholesterol uptake [54].

Inheritance of *APOE4* is associated with higher instability, increased likelihood of proteolytic degradation, and the protein is present at lower levels in plasma and brain [9,29,150]. The stability of the N-terminal domain is isoform-dependent, with ApoE4 being the least stable, and ApoE2 being most stable [92]. Additionally, ApoE4 preferentially binds VLDL, whereas ApoE2 and ApoE3 preferentially associate with phospholipid-rich HDL, possibly due to the domain interaction affecting the structure [150]. The decreased binding preference of ApoE4 for HDL could result in less effective transportation of lipids that are required for neuronal maintenance and repair.

1.2.2 APOE and its isoform specific role in TBI

TBI is characterized by considerable damage to neurons and axons. Regenerative processes are highly dependent on the supply of cholesterol and phospholipids, which are delivered to neurons by APOE-containing HDL-like particles. Differences between the APOE isoforms' stability and function may influence TBI outcome, specifically with APOE4 conferring worse outcome after injury. However, there is uniform agreement that more studies are needed to clarify the role of *APOE4* allele in TBI. Numerous studies have demonstrated that APOE4 carriers experience worse outcomes after TBI, including worse memory performance, slower recovery rate, and increased risk of posttraumatic seizures [34,38,6]. These results are supported by numerous animal studies demonstrating APOE4 plays a significant role in determining the pathology and recovery following TBI, however, the majority were conducted in AD mouse models [12,86,14].

In contrast, numerous *in vivo* data did not find or confirm a role for APOE4 in TBI [86,87,90,142]. For example, in adult patients with moderate to severe TBI assessed at multiple time-points, APOE4 patients did not have poorer cognitive performance, or slower improvement [110]. *In vitro* data also supports these results, with one study demonstrating that cognitive outcomes after TBI in APOE-TR mice were not influenced by APOE4 status [85]. These contradictory results emphasize the need for more research on APOE and TBI.

1.2.3 ATP-binding Cassette Transporter A1: An important regulator of APOE

ATP-binding cassette transporter A1 (ABCA1) plays a key role in cholesterol efflux and homeostasis through its effect on APOE lipidation. After secretion, APOE is always associated with lipids, and is predominantly found as a component of HDL-like particles; however, APOE is secreted as nonlipidated apolipoprotein [41]. The generation of lipidated APOE is controlled exclusively by ABCA1, and depends on efficient cholesterol efflux [69]. ABCA1 is a member of the superfamily of ABC transmembrane transporters, and is expressed in all brain cell types [70]. ABCA1 is comprised of two transmembrane domains, composed of 6 transmembrane helices, and two extracellular domains, connected by intramolecular disulfide bonds [94,101]. ABCA1 regulates the efflux of cholesterol and phospholipids to lipid-free apolipoproteins, including Apolipoprotein A-I and APOE [128]. ABCA1 translocates lipids on the plasma membrane by an ATP-dependent mechanism. After reserving sufficient phospholipids and cholesterol, ABCA1 undergoes conformational changes and dimerizes [94]. Lipid-free apolipoproteins can then bind the extracellular domains of the ABCA1 dimer, after which the apolipoprotein accepts the lipids translocated by ABCA1. The nascent APOE is lipidated first by ABCA1, which transfers cholesterol and phospholipids to the protein to form a discoidal HDL particle. ABCG1 then

transfers additional lipids onto the discoidal particle. The APOE-containing particle is then trafficked throughout the brain, both accepting and releasing lipid cargo [70].

1.2.4 APOE, ABCA1 and neuroinflammation

APOE modulates the inflammatory response in an isoform specific manner, with the APOE4 isoform eliciting a stronger pro-inflammatory response than APOE3 [68,115]. APOE4 may induce a more robust pro-inflammatory reaction from microglia and may suppress anti-inflammatory signaling, a potential mechanism for worse outcomes after TBI [77,10,79,73]. The isoform-dependent effect of APOE is possibly driven by lipidation status, which has been shown to affect its stability and degradation rate, and is regulated by ABCA1.

The effect of ABCA1 on inflammation could occur through its functional role in mediating cholesterol efflux onto lipid-poor APOE. It was previously shown that the loss of ABCA1 function results in a reduction of APOE, and data from experimental animals show that *Abca1* deficiency abolishes the lipidation of APOE [71]. However, ABCA1 may directly modulate the inflammatory response after TBI. Mice lacking brain ABCA1 saw increased inflammatory gene expression, and the microglia cultured from these mice demonstrated an increased pro-inflammatory response, as seen by higher levels of TNF α secretion and lower phagocytic activity, in response to lipopolysaccharide administration [65].

1.3 DISSERTATION OBJECTIVES

In this proposal, we plan to address the role of APOE, and its physiological regulation by ABCA1, in the outcomes of traumatic brain injury. Our first study will use mice expressing human APOE isoforms to characterize the relationship between the isoforms and TBI outcomes. We aim to determine if an interaction between APOE isoform and TBI impacts the phenotype and the transcriptome. We hypothesize that there is an APOE-isoform specific response to injury, with APOE4 mice exhibiting worsened cognitive outcomes and higher inflammatory gene expression after TBI. Our second study will examine the effect of *Abca1* haplodeficiency on the TBI response in APOE targeted replacement mice. Our goal is to identify differences in the transcriptional response to TBI due to *Abca1* deficiency.

To date, there is not a published study exploring the effect of *Abca1* deficiency and human APOE isoforms on outcomes after TBI. Additionally, these studies are the first to transcriptionally profile human APOE expressing mice following TBI using Next Generation Sequencing.

2.0 MATERIALS & METHODS

2.1 MOUSE MODELS

All animal experiments were approved through the University of Pittsburgh Institutional Animal Care and Use Committee and carried out in accordance with PHS policies on the use of animals in research. Male and female mice on the C57BL/6 background were used for all experiments. Experimental mice were kept on a 12 h light-dark cycle with *ad libitum* access to normal mouse chow diet and water.

2.1.1 Transgenic lines

Human APOE4^{+/+} (B6.129P2-*ApoE*^{tm3(APOE*4)Mae} N8) and APOE3^{+/+} (B6.129P2-*ApoE*^{tm3(APOE*3)Mae} N8) targeted replacement mice were originally purchased from Taconic (Germantown, NY). In these lines, the endogenous mouse *ApoE* gene is entirely replaced, however the human *APOE* gene remains under control of the murine *ApoE* regulatory sequences.

ABCA1 heterozygous knockout (ABCA1^{+/-}) mice (DBA/1-*Abca1*^{tm1Jdm}/J) were originally purchased from The Jackson Laboratory on a C57BL/6 × DBA/1 background. They were crossbred to pure C57BL/6 background in our laboratory for 10 generations.

2.1.2 Breeding

Abca1^{-/-} mice were bred to human ApoE4^{+/+} and ApoE3^{+/+} targeted replacement mice to generate ApoE4^{+/+}/Abca1^{+/+} (E4) and ApoE4^{+/+}/Abca1^{+/-} (E4/Abca1^{+/-}); as well as ApoE3^{+/+}/Abca1^{+/+} (E3) and ApoE3^{+/+}/Abca1^{+/-} (E3/Abca1^{+/-}).

2.2 CRANIOTOMY AND CONTROLLED CORTICAL IMPACT SURGERY

CCI model of brain injury was performed according to previous published methods [19]. Anesthesia was induced using 5% isoflurane, after which it was maintained at 1.5% isoflurane. The head was secured using a stereotaxic frame, and core body temperature was held at 37°C using a heating pad. After shaving the heads, two separate iodine - alcohol washes were performed to sterilize the surgical site. A 50% mixture of bupivacaine and lidocaine was applied to the area and ophthalmic ointment was applied to the eyes. The scalp was opened with a midline incision exposing the dorsal aspect of the skull and the skull leveled. A 4.5 mm diameter craniotomy was performed over the left parietal cortex using a dental drill. Once the bone flap was removed, mice in the CCI group received a single impact at 1.0 mm depth with a 3.0 mm diameter metal tip onto the cortex (3 m/s, 100 ms dwell time; Impact One, Leica). Sham mice received identical anesthesia and craniotomy, but did not receive impact and are considered negative controls.

Following the impact, the surgical site was sutured, triple antibiotic cream applied, Buprenex (0.1 mg/kg; IP) provided for analgesia, and sterile saline administered for rehydration.

Mice were allowed to recover on heating pad, until freely mobile, before returning to their home cage.

2.3 BEHAVIORAL TESTING

2.3.1 Elevated Plus-maze test

The elevated plus maze (EPM, San Diego Instruments) test was performed 4 days post-injury as described previously [137]. The maze consists of 4 arms in the shape of a “+”. All arms are the same length (30.5 cm) with a central square (10x10 cm); 2 arms are open on the sides, and 2 have 16 cm high walls. The entire maze is raised 40 cm off the ground. The elevated plus maze tests anxiety-related behavior by utilizing rodent’s fear of open and elevated spaces. Mice are placed into the maze within the center square facing a closed arm and are allowed to explore for 5 min. Percent time spent in each arm was tracked using the ANY-maze software (Stoelting Co.) from a camera positioned over the maze. 50% of body area within an arm was established in ANY-maze for definition of entry.

2.3.2 Morris Water Maze test

Spatial navigational learning and memory retention were assessed using Morris water maze (MWM) as described previously [44,76]; with testing performed on days 6-12 post-injury. Briefly, in a circular pool of water (diameter 122 cm, height 51 cm, temperature $21 \pm 1^\circ\text{C}$), we measured the ability of mice to form a spatial relationship between a safe but invisible platform

(submerged 1 cm below the water level; 10 cm in diameter) and several visual extra maze cues surrounding the pool of water. On day 6 post-injury, mice received a habituation trial, during which the animals were allowed to explore the pool of water without the platform present. Beginning the next day, they received four daily hidden platform training (acquisition) trials with 5-min inter-trial intervals for five consecutive days (days 7-11 post-injury). The platform remained in the center of one of the four quadrants of the pool (target quadrant). Animals were allowed 60 s to locate the platform and 20 s to remain there. Mice that failed to find the platform were lead to the platform by the experimenter and allowed to rest there for 20 s. Performance was recorded using Any-maze software (Stoelting Co.) during all trials. During the acquisition trials, escape latency (time to reach the platform) was subsequently used to analyze and compare the performance between all groups.

2.4 ANIMAL TISSUE PROCESSING

Fourteen days post-injury, mice were anesthetized using Avertin (250 mg/kg of body weight, i.p.) and perfused transcardially with 20mL of cold 0.1M PBS pH 7.4, following a blood draw from the right atrium [95]. Brains were rapidly removed and a 1.5 mm coronal section of the brain, including the injury site, was taken by slicing the brain at -2.5 mm and -4.0 from bregma. Within the coronal slice, the hemispheres were separated, and the subcortical tissue was dissected out; hippocampal and cortical tissue were snap-frozen together for mRNA-seq and RT-qPCR analysis. The remaining anterior of the brain was fixed in formalin for immunohistochemistry.

2.5 TRANSCRIPTOME ANALYSIS

2.5.1 RNA Isolation, RT-qPCR and Sequencing

All procedures were performed as before [95]. Four APOE3 and APOE4 male and female mice per sham and CCI injured group were used for mRNA-seq. RNA was isolated from frozen cortices and hippocampi at the injury site and purified using RNeasy kit (Qiagen) according to the manufacturer recommendations. Quality control of all RNA samples was performed on a 2100 Bioanalyzer instrument and samples with RIN > 8 were further used for library construction using mRNA Library Prep Reagent Set (Illumina). Libraries were generated by PCR enrichment including incorporation of barcodes to enable multiplexing. The libraries, were sequenced on Illumina HiSeq2000. For RT-qPCR, first strand cDNA was synthesized from 1 µg of total RNA using EcoDry™ Premix, Random Hexamers (Clontech). Next Generation Sequencing of libraries was performed by the Next Generation Sequencing Center (University of Pennsylvania, <http://fgc.genomics.upenn.edu/>) on *HiSeq 2500* machine. Following initial processing and quality control, the sequencing datasets were further analyzed for differential gene expression, which in all cases was calculated using Subread/featureCounts (v1.5.0; <https://sourceforge.net/projects/subread/files/subread-1.5.0/>) for read alignment and summarization and statistical package edgeR (v3.14.0; <https://bioconductor.org/packages/release/bioc/html/edgeR.html>). Lists of differentially expressed genes are further analyzed as described in the following section.

2.5.2 Principle Component Analysis

Principle component analysis (PCA) was performed to determine the principle components, which account for the highest sources of variance in the dataset, using R (v. 3.3.2) packages and visualized using “ggbiplot2” (v2.1.0, <https://github.com/vqv/ggbiplot>) [132].

2.5.3 Functional Pathway Analysis

We performed functional annotation clustering using the Database for Annotation, Visualization and Integrated Discovery (DAVID, <http://david.abcc.ncifcrf.gov/version6.7>) and Gene set enrichment Analysis (GSEA, v2.2.2, <https://www.broadinstitute.org/GSEA>) [89,126].

2.5.4 Weighted Gene Co-expression Network Analysis

After obtaining the RNA-seq libraries, the datasets were used to construct gene co-expression networks as described in previous studies with some modifications. Following sequencing, the FASTQ files containing the reads were aligned to the mouse genome using the Subread package. The resulting alignment bam files were used to construct gene co-expression networks by using the WGCNA v1.51 package in R environment (v3.2.4). A raw count exclusion was performed where any gene expression average <5 reads per million are discarded to eliminate noise. The program then clusters the remaining animals by gene expression enabling the detection of outliers. If sample outliers occur, they are removed from the source files and the networks are recreated. A scale free topology model was applied to the data, determining the power. Modules were generated automatically using a soft thresholding power, $\beta=10$, and definition parameters

included a minimum module size of 100 genes and a minimum module merge cut height of 0.25. Modules were named by conventional color scheme and then correlated with trait data (Age group, ApoE isoform, Injury). Statistical significance was determined by student's t-test, $p < 0.05$.

All the modules were summarized by module eigengenes (ME), the first principle component of each module that was calculated as a synthetic gene representing the expression profile of all the genes within a given module. Within the modules, hub genes were identified by its module membership (MM) value, which is its strength of correlation to the ME, against its intramodular connectivity. Heatmaps for modules were generated for genes represented within the module across the samples, with corresponding ME value. Gene-association networks were visualized for each module using Cytoscape 3.3.0 at a threshold of 0.02. The relationships between the modules was analyzed by heatmap generation using only the top 500 expressed gene overlaps.

2.6 WESTERN BLOT

Frozen cortices and hippocampi were homogenized in TBS homogenization buffer (250 mM sucrose, 20 mM Tris base, 1 mM EDTA, and 1 mM EGTA, 1 ml per 100 mg of tissue) and protease inhibitors cocktail (Roche) as described previously. For WB, RIPA extracted proteins were used detection of apoE, ABCA1, CLU, FYN and β -ACTIN. Thirty microgram of proteins were resolved on 4-12 % SDS-PAGE gels and transferred onto nitrocellulose membranes. Used were the following primary antibodies: Anti-ABCA1 (Ab7360, Abcam), anti-ApoE (178479, Calbiochem), anti-FYN (sc-16, Santa Cruz), and anti-CLU (sc-6419, SantaCruz).

2.7 IMMUNOHISTOCHEMISTRY & QUANTIFICATION

All procedures were as reported previously [47,61,121]. Briefly, OCT-embedded hemibrains were cut in the coronal plane at 20 μm sections and stored in a glycol-based cryoprotectant at -20°C . Five sections starting at -0.20 from Bregma, separated by 500 μm were used for staining. Sections were washed in PBS and antigen retrieval performed with Reveal Decloaker at 100°C for 30 min in a water bath. Quenching of endogenous peroxidases, blocking with 5% normal donkey serum and avidin-biotin blocking followed antigen retrieval. Sections were incubated in TREM2 primary antibody (1:100, AF179, R&D Systems) overnight at 4°C , followed by washing in PBS and labeling with biotinylated secondary antibody (1:1000, donkey α sheep; A16045) and developed with Vectastain ABC Elite kit (Vector Laboratories) and DAB substrate. Sections for GFAP and Iba1 staining were blocked in 5% serum of the requisite host and incubated in primary antibody overnight (anti-GFAP: 1:1000, Z0334, Dako; Iba1: 1:200, 19-19741, WAKO). Secondary antibodies with conjugated fluorophores were applied as appropriate. Sections were mounted on charged slides and coverslipped with Permount. All slides were examined using the Nikon Eclipse 90i at $10\times$ magnification and percent positive staining was defined as the percent area covered by staining using NIS Elements software (Nikon Instruments Inc.). The percent positive staining was determined by setting a threshold within the software. The threshold was determined using negative and positive controls to identify only stained tissue. Once set, the threshold was applied to all sections and then the ipsilateral and contralateral hemispheres were traced separately to identify the area. The software then calculates the amount of staining per area. Unless otherwise stated, analysis was conducted for ipsilateral hemispheres only. Contralateral hemispheres were identified using a pinhole made before sectioning.

2.8 STATISTICS

All results are reported as means \pm S.E.M. To determine statistical significance between groups in EPM, we used two-way ANOVA with a Sidak's multiple comparison post hoc test. To analyze MWM data, a three-way ANOVA was used. Unless otherwise indicated, all statistical analyses were performed in GraphPad Prism, version 7.0, or R, version 3.3.2 and differences were considered significant where $p < 0.05$. All differential gene expression analysis was performed by edgeR.

3.0 GENE CO-EXPRESSION NETWORKS IDENTIFY TREM2 AND TYROBP AS MAJOR HUBS IN HUMAN APOE EXPRESSING MICE FOLLOWING TRAUMATIC BRAIN INJURY

The data presented in this chapter is published in *Neurobiol Dis.* 105: 1-14 (2017).

Emilie L. Castranio¹, Anais Mounier¹, Cody M. Wolfe¹, Kyong Nyon Nam¹, Nicholas F. Fitz¹,
Florent Letronne¹, Jonathan Schug², Radosveta Koldamova¹, Iliya Lefterov¹

¹ Department of Environmental and Occupational Health, University of Pittsburgh, PA 15219, USA

² Functional Genomics Core, Department of Genetics, University of Pennsylvania, Philadelphia, PA 19104, USA

3.1 ABSTRACT

Traumatic brain injury (TBI) is strongly linked to an increased risk of developing dementia, including chronic traumatic encephalopathy and possibly Alzheimer's disease (AD). *APOEε4* allele of human Apolipoprotein E (*APOE*) gene is the major genetic risk factor for late onset AD and has been associated with chronic traumatic encephalopathy and unfavorable outcome following TBI. To determine if there is an APOE isoform-specific response to TBI we performed controlled cortical impact on 3-month-old mice expressing human APOE3

or APOE4 isoforms. Following injury, we used several behavior paradigms to test for anxiety and learning and found that APOE3 and APOE4 targeted replacement mice demonstrate cognitive impairments following moderate TBI. Transcriptional profiling 14 days following injury revealed a significant effect of TBI, which was similar in both genotypes. Significantly upregulated by injury in both genotypes were mRNA expression and protein level of ABCA1 transporter and APOJ, but not APOE.

To identify gene-networks correlated to injury and APOE isoform, we performed Weighted Gene Co-expression Network Analysis. We determined that the network mostly correlated to TBI in animals expressing both isoforms is immune response with major hub genes including *Trem2*, *Tyrobp*, *Clec7a* and *Cd68*. We also found a significant increase of TREM2, IBA-1 and GFAP protein levels in the brains of injured mice. We identified a network representing myelination that correlated significantly with APOE isoform in both injury groups. This network was significantly enriched in oligodendrocyte signature genes, such as *Mbp* and *Plp1*. Our results demonstrate unique and distinct gene networks at this acute time point for injury and APOE isoform, as well as a network driven by APOE isoform across TBI groups.

3.2 INTRODUCTION

Traumatic brain injury (TBI) is one of the leading causes of death and disability in the United States. Approximately 2 million people sustain a TBI and 50,000 TBI-related deaths occur in the United States every year. Currently, there is no treatment for TBI, patients are only given supportive care for which the cost is approximately \$60 billion annually. TBI can either be

caused when the head violently impacts with another object or when an object pierces the skull and enters the brain tissue. Studies show that following the acute phase, over the long-term, patients may develop changes in cognition, and increases in both anxiety and depression [105,49]. The high level of variability in injury outcomes suggests, to a significant extent, a strong role for genetic influence on brain susceptibility and recovery [40,141].

TBI is strongly linked to increased risk of developing dementia, including chronic traumatic encephalopathy and possibly Alzheimer's disease (AD) [62,63,88]. The *APOEε4* allele of human apolipoprotein E (*APOE*) gene is the major genetic risk factor for late onset AD and has been associated with chronic traumatic encephalopathy and unfavorable outcome following TBI. Multiple studies have identified worse outcomes following TBI based on the inheritance of *APOEε4* allele [6,38]. The role of APOE in neuronal survival and repair and in overall response to TBI, however, is not well understood. It has been suggested that APOE4 is less stable and catabolically degraded more quickly than the other APOE isoforms, possibly due to its lower lipidation level [68]. In mice, studies have identified APOE-genotype and brain-region specific genomic changes using mRNA microarrays after controlled cortical impact (CCI) [33]. Patients, carriers of *APOEε4*, experiencing TBI demonstrated worse memory performance in a verbal learning test and verbal fluency measured 6 months post-injury [34]. In contrast, other *in vivo* data did not find or confirm a role for APOE4 in TBI [86,87,90,142]. For example, in adult patients with moderate to severe TBI assessed 3, 6 and 12 months post-injury, APOE4 patients did not have poorer cognitive performance, functional outcome or slower improvement [110]. There is a uniform agreement that more studies are needed to clarify the role of *APOEε4* allele in TBI. Mechanical stress placed on the brain due to the impact is considered the primary injury. Following the impact, a secondary injury occurs leading to additional damage and cell death,

worsening the outcome. Mechanisms of secondary injury include neuronal excitotoxicity, edema, oxidative stress, and neuroinflammation. The inflammatory state in the brain can persist for many years following the injury; chronic neuroinflammation following TBI was closely associated with neuronal death and impaired cell proliferation both immediately adjacent to, and locations more distant from, site of injury [2]. Multiple inflammatory molecules are upregulated after TBI and are believed to contribute to these processes, as well as blood brain barrier dysfunction. Interleukin-1 β (IL-1 β), tumor necrosis factor- α (TNF- α), chemokine C motif ligand 2 (Ccl2), and chemokine CX3C motif receptor 1 (Cx3cr1) are among those that have been intensely studied for their impact on brain pathology following TBI [36,43,51,59]. Studies have shown that the expression levels of the majority of those inflammatory factors are associated with severity of injury and outcome in TBI patients, the reduction of neurobehavioral impairments and injury volume as well as the survival rates in rodent models [91,144].

To our knowledge, transcription profiling of APOE expressing mice following TBI using Next Generation Sequencing has not yet been performed. The aim of this study was to determine if there is an interaction between APOE isoform and the response to TBI affecting phenotype and the transcriptome. We performed controlled cortical impact on 3-month-old mice expressing human APOE3 or APOE4 isoform and following the injury, tested for anxiety and learning. Transcriptional profiling of hippocampal and cortical tissue from the injury site was performed using mRNA-sequencing (mRNA-seq). We hypothesized that there is APOE isoform-specific response to injury and APOE4 mice would have worse cognitive outcomes and higher inflammatory gene expression following TBI. We found that APOE genotype, while a significant variable in both behavioral tests, did not modulate the changes in transcriptome seen two weeks post injury. To correlate the transcriptome to the phenotype we used network-based approach

and applied Weighted Gene Co-expression Network Analysis (WGCNA). This analysis not only connects the genes within networks and identifies the most connected members of a given pathway, but elucidates the relevance of the networks to the experimental findings. Thus, we identified that TBI significantly affected immune response, with *Trem2* and *Tyrobp* being highly ranked within the interconnected gene network.

3.3 METHODS

3.3.1 Animals

All animal experiments were approved through the University of Pittsburgh Institutional Animal Care and Use Committee and carried out in accordance with PHS policies on the use of animals in research. We used human APOE4^{+/+} and APOE3^{+/+} targeted replacement mice on a C57BL/6 background [46]. Experimental male and female APOE3 or APOE4 mice were kept on a 12 h light-dark cycle with *ad libitum* access to food and water. Mice at 3 mo of age were randomly assigned to either sham or controlled cortical impact (CCI) experimental group and initially were handled for 2 days (5 min per day). Following surgical procedures, mice were allowed to recover for 3 days before starting behavioral testing. All materials were purchased through Thermo Fisher Scientific, unless otherwise noted.

3.3.2 Controlled Cortical Impact

CCI model of brain injury was performed according to previous published methods [19]. Following induction of anesthesia with 5% isoflurane, the mouse was moved to the stereotaxic frame, where the head was secured, core body temperature maintained at 37°C using a heating pad and anesthesia continued with 1.5% isoflurane. The head was shaven, surgical site sterilized with two separate iodine - alcohol washes, a 50% mixture of bupivacaine and lidocaine applied to the surgical site and ophthalmic ointment applied to the eyes. The scalp was opened with a midline incision exposing the dorsal aspect of the skull and the skull leveled. A 4.5 mm diameter craniotomy was performed over the left parietal cortex using a dental drill. Once the bone flap was removed, mice in the CCI group received a single impact at 1.0 mm depth with a 3.0 mm diameter metal tip onto the cortex (3 m/s, 100 ms dwell time; Impact One, Leica). Sham mice received identical anesthesia and craniotomy, but did not receive impact and are considered negative controls. Following the impact, the surgical site was sutured, triple antibiotic cream applied, Buprenex (0.1 mg/kg; IP) provided for analgesia, and sterile saline administered for rehydration. Mice were allowed to recover on heating pad, until freely mobile, before returning to their home cage.

3.3.3 Elevated-Plus Maze

The elevated plus maze (EPM, San Diego Instruments) test was performed 4 days post-injury as described previously [137]. The maze consists of 4 arms in the shape of a “+”. All arms are the same length (30.5 cm) with a central square (10x10 cm); 2 arms are open on the sides, and 2 have 16 cm high walls. The entire maze is raised 40 cm off the ground. The elevated plus maze

tests anxiety-related behavior by utilizing rodent's fear of open and elevated spaces. Mice are placed into the maze within the center square facing a closed arm and are allowed to explore for 5 min. Percent time spent in each arm was tracked using the ANY-maze software (Stoelting Co.) from a camera positioned over the maze. 50% of body area within an arm was established in ANY-maze for definition of entry.

3.3.4 Morris Water Maze

Spatial navigational learning and memory retention were assessed using Morris water maze (MWM) as described previously [44,76]; with testing performed on days 6-12 post-injury. Briefly, in a circular pool of water (diameter 122 cm, height 51 cm, temperature $21 \pm 1^\circ\text{C}$), we measured the ability of mice to form a spatial relationship between a safe but invisible platform (submerged 1 cm below the water level; 10 cm in diameter) and several visual extra maze cues surrounding the pool of water. On day 6 post-injury, mice received a habituation trial, during which the animals were allowed to explore the pool of water without the platform present. Beginning the next day, they received four daily hidden platform training (acquisition) trials with 5-min inter-trial intervals for five consecutive days (days 7-11 post-injury). The platform remained in the center of one of the four quadrants of the pool (target quadrant). Animals were allowed 60 s to locate the platform and 20 s to remain there. Mice that failed to find the platform were lead to the platform by the experimenter and allowed to rest there for 20 s. Performance was recorded using Any-maze software (Stoelting Co.) during all trials. During the acquisition trials, escape latency (time to reach the platform) was subsequently used to analyze and compare the performance between all groups.

3.3.5 Animal Tissue Processing

Fourteen days post-injury, mice were anesthetized using Avertin (250 mg/kg of body weight, i.p.) and perfused transcardially with 20ml of cold 0.1M PBS pH 7.4, following a blood draw from the right atrium [95]. Brains were rapidly removed and a 1.5 mm coronal section of the brain, including the injury site, was taken by slicing the brain at -2.5 mm and -4.0 from bregma. Within the coronal slice, the hemispheres were separated, and the subcortical tissue was dissected out; hippocampal and cortical tissue were snap-frozen together for mRNA-seq and RT-qPCR analysis. The remaining anterior of the brain was fixed in formalin for immunohistochemistry.

3.3.6 Immunohistochemistry

All procedures were as reported previously [47,61,121]. Briefly, OCT-embedded hemibrains were cut in the coronal plane at 20 μ m sections and stored in a glycol-based cryoprotectant at -20°C . Five sections starting at -0.20 from Bregma, separated by 500 μ m were used for staining. Sections were washed in PBS and antigen retrieval performed with Reveal Decloaker at 100°C for 30 min in a water bath. Quenching of endogenous peroxidases, blocking with 5% normal donkey serum and avidin-biotin blocking followed antigen retrieval. Sections were incubated in TREM2 primary antibody (1:100, AF179, R&D Systems) overnight at 4°C , followed by washing in PBS and labeling with biotinylated secondary antibody (1:1000, donkey α sheep; A16045) and developed with Vectastain ABC Elite kit (Vector Laboratories) and DAB substrate. Sections for GFAP and Iba1 staining were blocked in 5% serum of the requisite host and incubated in primary antibody overnight (anti-GFAP: 1:1000, Z0334, Dako; Iba1: 1:200, 19-

19741, WAKO). Secondary antibodies with conjugated fluorophores were applied as appropriate. Sections were mounted on charged slides and coverslipped with Permount. All slides were examined using the Nikon Eclipse 90i at 10× magnification and percent positive staining was defined as the percent area covered by staining using NIS Elements software (Nikon Instruments Inc.). The percent positive staining was determined by setting a threshold within the software. The threshold was determined using negative and positive controls to identify only stained tissue. Once set, the threshold was applied to all sections and then the ipsilateral and contralateral hemispheres were traced separately to identify the area. The software then calculates the amount of staining per area. Unless otherwise stated, analysis was conducted for ipsilateral hemispheres only. Contralateral hemispheres were identified using a pinhole made before sectioning.

3.3.7 RNA isolation and mRNA sequencing

All procedures were performed as before [95]. Four APOE3 and APOE4 male and female mice per sham and CCI injured group were used for mRNA-seq. RNA was isolated from frozen cortices and hippocampi at the injury site and purified using RNeasy kit (Qiagen) according to the manufacturer recommendations. Quality control of all RNA samples was performed on a 2100 Bioanalyzer instrument and samples with RIN > 8 were further used for library construction using mRNA Library Prep Reagent Set (Illumina). Libraries were generated by PCR enrichment including incorporation of barcodes to enable multiplexing. The libraries, were sequenced on Illumina HiSeq2000. For RT-qPCR, first strand cDNA was synthesized from 1 µg of total RNA using EcoDry™ Premix, Random Hexamers (Clontech). Next Generation Sequencing of libraries was performed by the Next Generation Sequencing Center (University of Pennsylvania,

<http://fgc.genomics.upenn.edu/>) on *HiSeq 2500* machine. Following initial processing and quality control, the sequencing datasets were further analyzed for differential gene expression, which in all cases was calculated using Subread/featureCounts (v1.5.0; <https://sourceforge.net/projects/subread/files/subread-1.5.0/>) for read alignment and summarization and statistical package edgeR (v3.14.0; <https://bioconductor.org/packages/release/bioc/html/edgeR.html>). Lists of differentially expressed genes are further analyzed as described in the following section.

3.3.8 Principle Component analysis

Principle component analysis (PCA) was performed to determine the principle components, which account for the highest sources of variance in the dataset, using R (v. 3.3.2) packages and visualized using “ggbiplot2” (v2.1.0, <https://github.com/vqv/ggbiplot>) [132].

3.3.9 Functional Pathway analysis

We performed functional annotation clustering using the Database for Annotation, Visualization and Integrated Discovery (DAVID, <http://david.abcc.ncifcrf.gov/version6.7>) and Gene set enrichment Analysis (GSEA, v2.2.2, <https://www.broadinstitute.org/GSEA>) [89,126].

3.3.10 Weighted Gene Co-expression Network Analysis

Network analysis was performed using WGCNA (v.1.49) [149]. Libraries are clustered by gene expression enabling the detection of outliers and the power is determined by scale free topology

model. Modules were generated automatically using a soft thresholding power, $\beta=10$, a minimum module size of 33 genes and a minimum module merge cut height of 0.25. Modules were named by conventional color scheme and then correlated with trait data (APOE isoform, Injury). Each trait was converted individually into a binary factor, (e.g. Sham=0, TBI=1; APOE3=0, APOE4=1). The modules were then correlated to the group phenotype (e.g. all APOE3 Sham mice = 0, 0; all APOE3 TBI = 0, 1) using Pearson's correlation. Statistical significance was determined by student's *t*-test, $p<0.05$. All modules were summarized by module eigengenes (ME), the first principle component of each module that was calculated as a synthetic gene representing the expression profile of all genes within a given module.

3.3.11 Western blot

Frozen cortices and hippocampi were homogenized in TBS homogenization buffer (250 mM sucrose, 20 mM Tris base, 1 mM EDTA, and 1 mM EGTA, 1 ml per 100 mg of tissue) and protease inhibitors cocktail (Roche) as described previously. For WB, RIPA extracted proteins were used detection of apoE, ABCA1, CLU, FYN and β -ACTIN. Thirty microgram of proteins were resolved on 4-12 % SDS-PAGE gels and transferred onto nitrocellulose membranes. Used were the following primary antibodies: Anti-ABCA1 (Ab7360, Abcam), anti-ApoE (178479, Calbiochem), anti-FYN (sc-16, Santa Cruz), and anti-CLU (sc-6419, SantaCruz).

3.3.12 Statistical Analyses

All results are reported as means \pm S.E.M. To determine statistical significance between groups in EPM, we used two-way ANOVA with a Sidak's multiple comparison post hoc test. To analyze

MWM data, a three-way ANOVA was used. Unless otherwise indicated, all statistical analyses were performed in GraphPad Prism, version 7.0, or R, version 3.3.2 and differences were considered significant where $p < 0.05$.

3.4 RESULTS

3.4.1 TBI causes anxiety-related changes and spatial learning deficits

To examine the effect of APOE isoforms on cognitive performance following TBI, we used mice expressing human APOE3 or APOE4 isoform. As a model of brain injury, we used CCI, performed on 3 months old mice. First, the mice were tested for anxiety-related behavior in the elevated plus maze (EPM), 4 days post injury. As shown on Fig. 1A, the injured mice of both genotypes showed an increased time spent in the open-arms of the EPM when compared to their sham counterparts. We found significant main effects of genotype and TBI, but no interaction. Due to the acute time-point at which this test was performed, increased time spent in the open arms can be interpreted as an increased risk-taking or impulsive behavior by the injured animals.

We employed Morris Water Maze (MWM) to examine the effect of TBI on spatial learning. The result shown on Fig. 1B demonstrates that for both APOE genotypes, TBI significantly increased escape latency time in APOE3 mice (compare blue open and closed circles) and in APOE4 mice (compare red open and closed squares). As seen from Fig. 1B, APOE4 mice in both groups performed significantly worse than APOE3 mice confirming previous data from our and other groups showing a significant memory impairment at baseline in

APOE4 mice [46,114,45]. The conclusion from these experiments is that TBI significantly worsens spatial learning and increases impulsive behavior in both APOE isoforms.

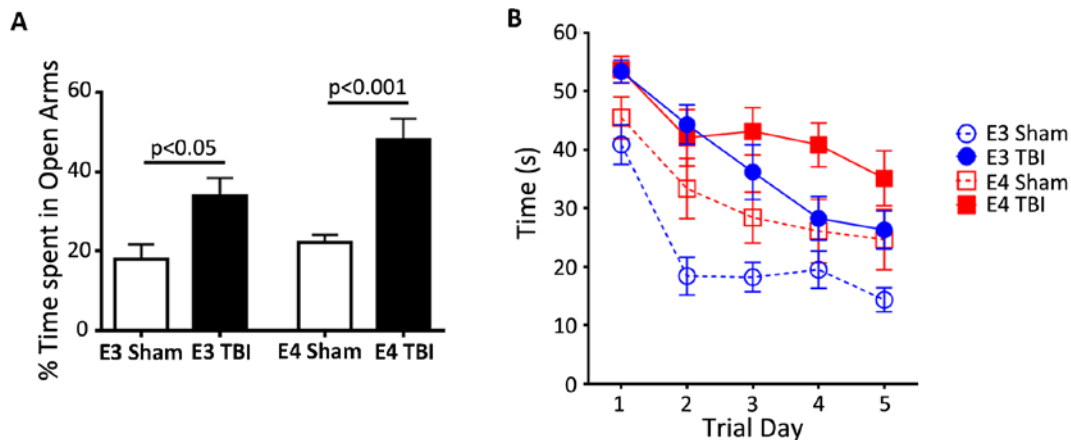


Figure 1. TBI significantly affected behavior performance in mice expressing human APOE3 and APOE4 isoforms.

Three months old APOE3 and APOE4 targeted replacement mice underwent CCI and their behavior performance was tested using Elevated Plus Maze (A) and Morris Water Maze (B) paradigms. (A) EPM was performed 4 days post injury. For both APOE isoforms, TBI significantly increased the time spent in the open arms of the maze compared to sham ($p<0.0001$). Statistics is by two-way ANOVA. There is no interaction between genotype and injury but there are significant main effects of genotype ($F_{(1, 53)} = 4.967, p=0.03$) and injury ($F_{(1, 53)} = 26.36, p<0.0001$). Sidak's multiple comparison test showed a significant difference between APOE3-Sham vs APOE3-TBI ($p<0.05$) and APOE4-Sham vs APOE4-TBI ($p<0.001$). (B) Acquisition of spatial memory was examined in APOE3 (blue) and APOE4 mice (red) on 7-11 days post injury by MWM. Time to find the hidden platform is shown for all days of training. Statistics is by three-way ANOVA. There was no interaction between any of the factors, but significant main effects of all three, training, injury and genotype. (For training: $F_{(4, 4)} = 21.35, p<0.0001$; for injury: $F_{(1, 4)} = 59.94, p<0.0001$; for genotype: $F_{(1, 4)} = 17.8, p<0.0001$)

3.4.2 Changes in transcriptome induced by TBI reflect stimulated immune response and decreased neuronal functionality

To examine how TBI affects brain transcriptome, we performed mRNA-seq using total RNA isolated from the brains of the mice tested for cognitive performance and perfused 14 days post injury. For this analysis, we used hippocampal and cortical tissue from around the injury site. The PCA was used to calculate the principal components, which account for the sources of

highest possible variance in the transcriptome. The result from the PCA shown on Fig. 2A demonstrates that the mRNA-seq data for TBI animals from both genotypes clustered together and the same was observed for sham treated mice. Thus, the result of the PCA suggests that the variance between gene expression levels in TBI vs Sham was higher than between gene expression level in APOE3 vs APOE4 transcripts.

An expression-by-expression plot [136] using the lists of differentially expressed genes (Fig. 2B) demonstrates the high number of significantly expressed transcripts in all sham versus all TBI animals. We then compared the effect of TBI on transcriptome separately for each genotype. As shown on Fig. 2C and D, a significant number of differentially expressed genes was identified in both APOE groups (genes lists shown on Table 2A and B in Suppl. Materials). We were interested whether there was a similarity between the biological processes affected by TBI in APOE3 and E4 mice. Top up-regulated categories in both genotypes were highly consistent and were associated with “Immune System Process”, “Innate Immune Response” and “Inflammatory Response” (Table 3A and B; Suppl. Materials). Top down-regulated categories in both genotypes were also similar, including “Regulation of Ion Transmembrane Transport”, and “Potassium Ion Transport” (Table 4A and B; Suppl. Materials). To further identify enriched pathways commonly affected by TBI in both isoforms, we applied Gene Set Enrichment Analysis (GSEA) [126] and compared all mice in the TBI group (E3-TBI+E4-TBI) to all sham mice (E3-sham+E4-sham). The analysis confirms the top up-regulated categories by TBI (Fig. 9; Suppl. Materials).

We were particularly interested in two genes significantly up-regulated in brains of both APOE genotypes - *Abca1* transporter (fold change=3.46) and Clusterin (*Clu/APOJ*, fold change=1.66). As shown on Fig. 2E and F, the protein level of ABCA1 and CLU was

significantly increased. In contrast, *ApoE* mRNA and APOE protein level were unaffected by TBI. Thus, these experiments confirm and validate our mRNA-seq results.

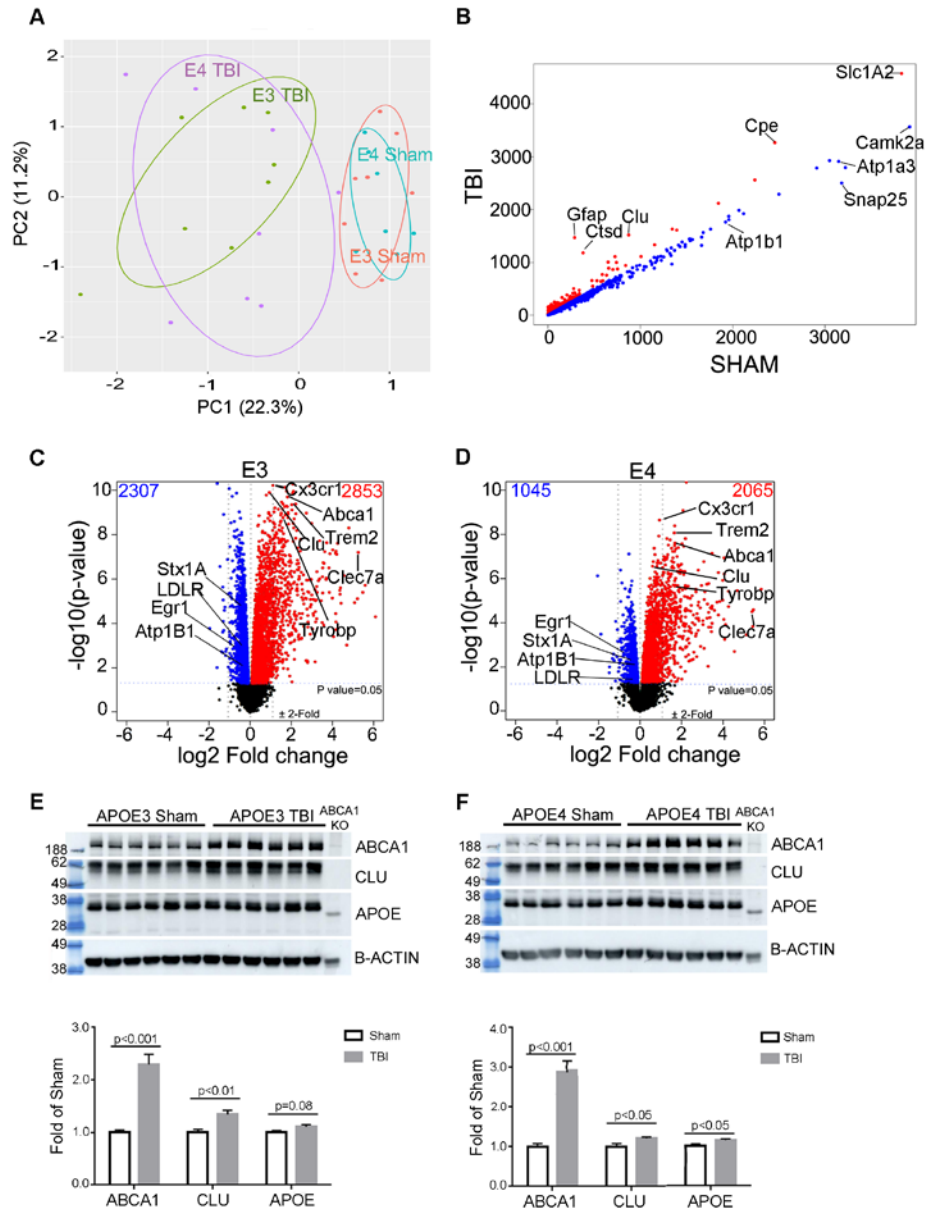


Figure 2. TBI significantly affected the transcriptome demonstrating increases in immune response and decreases in neuronal functionality.

mRNA-seq was performed on RNA isolated from the hippocampi and cortex of APOE3 and APOE4 mice shown on Fig. 1, N=8 mice per group. (A) Principle component analysis used to calculate the principal components that account for the highest possible variance in the transcriptome. N= 8 mice/group and all transcripts from each mouse. PCA plot of the transcriptome shows distinct separation based on TBI but not on APOE isoform. (B) Scatterplot for genes comparing sham and TBI reads per million. (C-D) Volcano plots representing the mRNA-seq results.

Differential gene expression analysis between sham and injured mice using EdgeR identified: in APOE3 (C): 2853 up- (red) and 2307 down-regulated genes by TBI (blue), and in APOE4 (D): 2065 up- and 1045 down-regulated genes at $p < 0.05$ cutoff. For C and D, statistics is by edgeR, $p < 0.05$. (E) Western blot results for APOE3 sham versus TBI animals for ABCA1, CLU, APOE, and β -ACTIN validate mRNA-seq results. (F) Western blot results for APOE4 sham versus TBI animals for ABCA1, CLU, APOE, and β -ACTIN validate mRNA-seq results. Proteins are normalized to levels of β -ACTIN.

3.4.3 Transcriptome analysis demonstrates a higher expression of markers for resident microglia versus peripheral macrophages

Due to the nature of the CCI model, the blood brain barrier is damaged, which allows entry to peripheral cells not normally present in the brain, such as monocytes and peripheral macrophages. We were interested in identifying which cell type was responsible for the inflammatory response in the brain at 14 days post injury. To do this, we referred to Hickman et al. (2013)[55], who demonstrated that microglia have a unique transcriptomic signature with several genes separate from that of peripheral macrophages. Thus, our RNA sequencing data point to a significant portion of genes that are considered microglia “sensitive” genes (86 of 100; Fig. 3A-B), or cellular receptors involved in the microglial function of sensing the brain environment. Several of those genes had a significantly higher expression in resident macrophages (microglia) when compared to peripheral macrophages, including *Gpr34*, *Trem2*, *Siglech*, and *P2ry12*. Additionally, a number of those genes are unique to microglia, including *Cx3cr1*, *Tmem119* and *Slco2b1*. We also looked at other receptor families involved in immune response, including the purinergic receptors (Fig. 3C-D) and sialic acid binding immunoglobulin lectins (*Siglecs*; Fig. 3E-F). Several of those were identified as being expressed at significantly higher levels in microglia compared to peripheral macrophages, including *P2rx7*, *P2ry6*, *P2ry12*, *P2ry13* and *Siglech*. As seen from Fig. 3A-F, all these groups of genes was significantly upregulated by TBI in both APOE3 and APOE4 mice. In contrast, several genes characteristic of

peripheral macrophages, such as *Alox15*, *Fabp4*, *Fcna*, *Slp1* and *Serpinb2* were not found (data not shown) or expressed at a very low level (*P2rx4*). We conclude that whereas the peripheral macrophages invade in the initial days following TBI and are likely to remain present in CNS at low levels, the resident microglia are the predominant source of inflammatory response in the brain 14 days post injury [51,56,67].

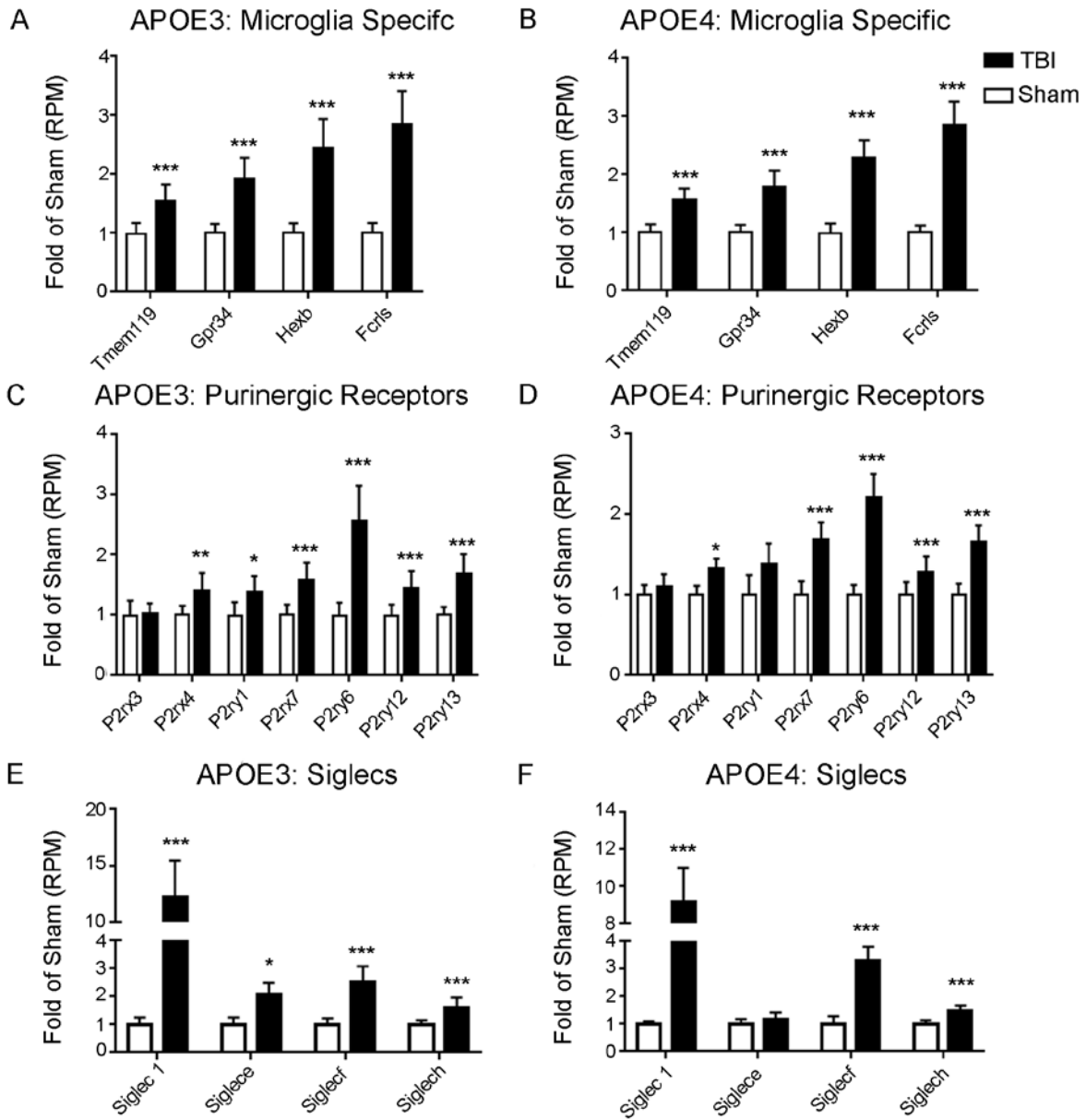


Figure 3. mRNA-seq data reveal that microglia are predominant source of inflammation.

Average expression according to mRNA-seq results for several inflammatory markers modulated by TBI were calculated as the fold of Sham reads per million for each gene. (A-B) Several microglial specific transcripts are significantly upregulated by TBI in both (A) APOE3 and (B) APOE4 mice. (C-D) Purinergic receptors in (C) APOE3 and (D) APOE4 mice, as well as (E-F) Siglecs in (E) APOE3 and (F) APOE4 mice were also upregulated following TBI. Statistics is by edgeR; * $p < 0.05$, ** $p < 0.01$, *** $p < 0.001$.

3.4.4 Integrated system approach identifies correlated gene networks associated with TBI

To identify gene networks affected by TBI, we employed Weighted Gene Co-expression Network Analysis (WGCNA) [147,113]. We used datasets of the same APOE3 and APOE4 expressing mice, shown on Fig. 2 and 3. WGCNA clusters genes based on expression profiles into functional groups (referred to as modules) and the average expression profile is represented as a ‘module eigengene’ (ME), which is given an arbitrary color name. MEs were then correlated to the phenotype of each experimental group, namely APOE3-TBI, APOE4-TBI, APOE3-Sham and APOE4-Sham, allowing identification of the networks associated with them. We found no significant gender difference, therefore male and female mice were analyzed together. The relationship table (Fig. 4A) shows the Pearson correlation of each module to the phenotype. Additionally, the table visualizes the overall direction of expression for the genes within each module for each phenotype. We were most interested in modules that correlated significantly with either injury in both APOE isoforms or with APOE isoform. Thus, we chose to further characterize two networks that correlate to TBI (ME Brown and ME Green), and two to APOE genotype (ME Darkred and ME Salmon). Correlations between the modules are shown in Fig. 10; Suppl. Materials.

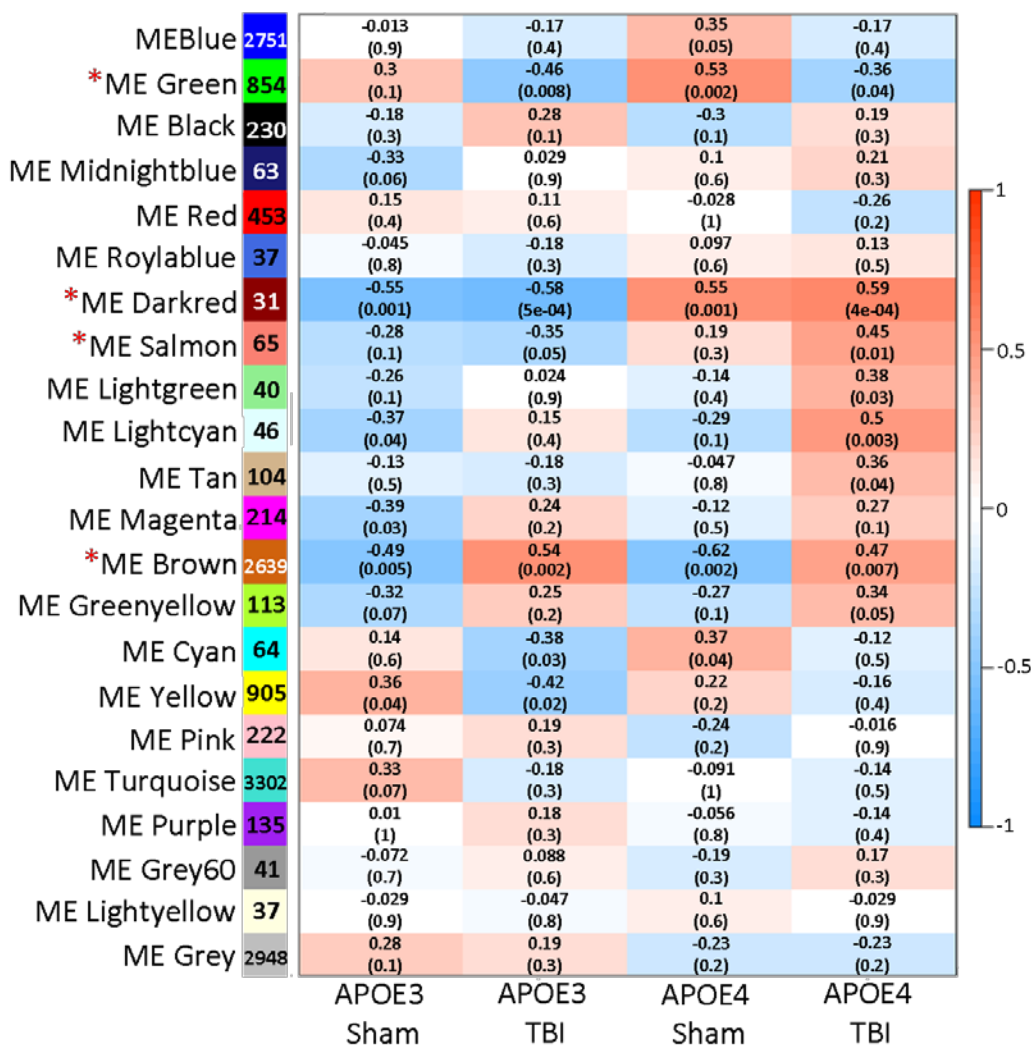


Figure 4. WGCNA identified modules that correlated to TBI and or APOE isoform.

WGCNA was used to determine the correlation of module eigengenes to Injury and APOE genotype. Each cell shows the correlation between the module eigengene (rows) and group (columns) with p-value. Red denotes a positive and blue is a negative correlation. Modules of interest are differentially expressed between trait conditions. Brown, and Green are modules associated with TBI, Darkred and Salmon – with APOE genotype.

ME Brown positively correlated to APOE3-TBI ($r=0.54$, $p=0.002$) and APOE4-TBI groups ($r=0.47$, $p=0.007$) and negatively correlated to sham treated mice. The interpretation of the positive correlation is that TBI increases the expression of genes, members of this module in mice expressing either isoform. This network is enriched with transcripts functionally associated

with “Immune Response” and “Innate Immunity” (Table 1). As seen in Fig. 11C and D; Suppl. Materials, the correlation between Module membership and Gene significance for genes within this network demonstrates that they strongly relate to the biological processes associated with this module. The expression levels for all genes in the network and for each sample are shown on Fig. 5A (heatmap and bar plot). The network (Fig. 5B) was built using hub genes associated with immune response and phagocytosis, such as *Trem2* (Triggering Receptor Expressed on Myeloid Cells 2), *Tyrobp*, *Clec7a*, *Cd68*, *Cx3cr1* and the transcripts connected to them. Hub genes of this network are highly enriched in microglia signature genes (fold enrichment 8.95), including *Grp34*, *Fcrls*, *Tmem119* and *Cx3cr1*. In the hub gene list, there were also astrocyte-specific genes such as *Gfap*, *Aqp4*, *Clu* (fold enrichment 8.69).

Table 1. Gene-network modules represent various biological functions associated with injury and APOE isoform.

Module Name	Effect	PValue	Gene Count	GO Terms	Enrichment Pvalue
Brown	Injury	1.0E-10	2639	Immune response	9.97E-41
				Innate immune response	1.16E-28
				Phagocytosis	2.61E-05
Green	Injury	5.0E-06	854	Transport	1.98E-04
				Phospholipid transport	0.0016
Darkred	Genotype	1.0E-23	31	Innate immune response	0.0428
				Complement Activation	0.0471
Salmon	Genotype	0.001	65	Myelination	3.73E-05
				Oligodendrocyte differentiation	1.06E-04

Networks of interest include ME Brown and ME Green, which are associated with injury, and ME Darkred and ME Salmon, which are associated with APOE isoform.

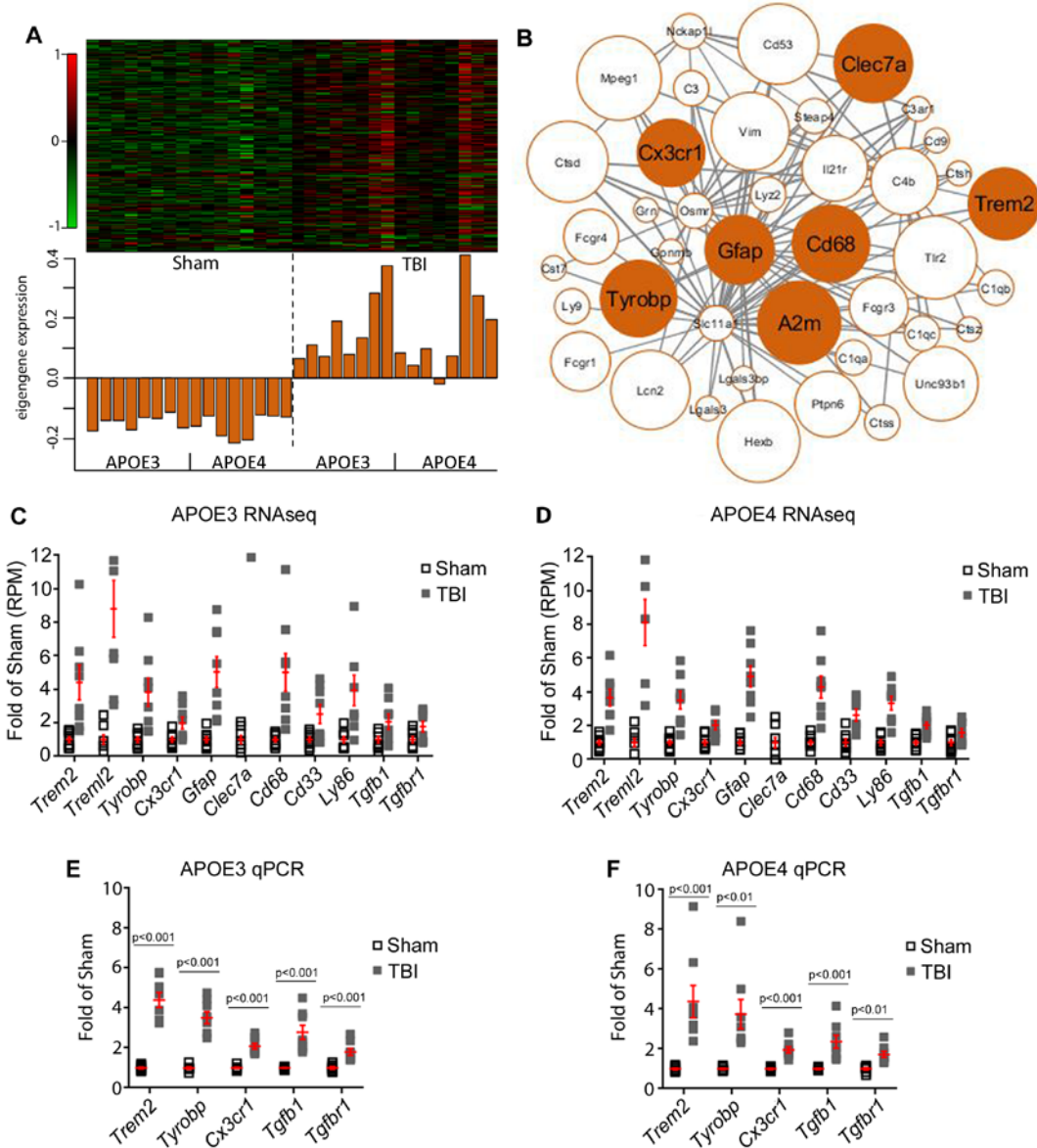


Figure 5. ME Brown correlates to TBI and is associated with Immune Response.

(A) Expression barplot shows the gene expression and eigengene expression within each sample. Within the heatmap, the rows denote genes and the columns correspond to samples, with the corresponding module eigengene value for each sample shown in the bar plot below. Red denotes over-expression and green under-expression of the gene within the sample. (B) Network of genes connected to hub genes *Trem2*, *Tyrobp*, *Clec7a*, *Cd68*, *Cx3cr1* representing immune response. Size of each gene was determined by modular membership value, and the weight determined edge width. (C-D) Average expression according to mRNA-seq results of genes modulated by TBI in “Immune response” category for (C) APOE3 and (D) APOE4 mice. The average expression was calculated as fold of Sham reads per million for each gene. Statistics is by edgeR, $p < 0.05$. (E-F) Validation of mRNA-seq results for *Trem2*, *Tyrobp*, *Cx3cr1*, *Tgfb1*, *Tgfb1* for (E) APOE3 and (F) APOE4 mice by qPCR. Statistics was determined by t-test.

To validate the mRNA-seq results shown on Fig. 5C and D, we performed RT-QPCR for several genes - *Trem2*, *Tyrobp*, *Cx3cr1*, *Tgfb1*, *Tgfbr1* (Fig. 5E and F). To confirm that mRNA expression levels correspond to an increase in the levels of the respective proteins, we chose three genes highly affected by TBI – *Trem2* and *Aif1/Iba-1* expressed in microglia and *Gfap* expressed in astrocytes. *Trem2* encodes a transmembrane protein that is expressed on myeloid lineage cells, including microglia and recent studies have shown that *Trem2* variants affect microglial functionality [30]. To analyze the impact of TBI on the protein level of TREM2, AIF1/IBA-1 and GFAP, we performed immunohistochemistry on brain sections from the same mice. As seen in Fig. 6A, sham animals showed relatively low-to-no TREM2 immunostaining. In contrast, TBI significantly increased presence of TREM2 around the injury site in both APOE3 (Fig. 6B) and APOE4 (Fig. 6C) mice ($p < 0.05$). IBA1 staining shown on Fig. 12; Suppl. Materials, is consistent with the increased intensity of TREM2 around the injury site and confirms microglia activation after TBI. For both TREM2 and IBA-1 staining, there was no significant difference between APOE3 and APOE4 injured animals. To validate the increased mRNA expression of GFAP, we performed immunohistochemistry against GFAP. As visible from Fig. 6E, sham animals show evenly distributed low levels of GFAP staining. In contrast, TBI animals show significantly higher levels of GFAP staining in both APOE3 and APOE4 when compared to their sham counterparts (Fig. 6F-G). As with TREM2 and IBA-1, there was no significant APOE isoform dependent difference in GFAP staining of either sham or TBI groups. The high levels of astrogliosis and microgliosis present at the injury site demonstrate a recruitment of these cell types to the injury.

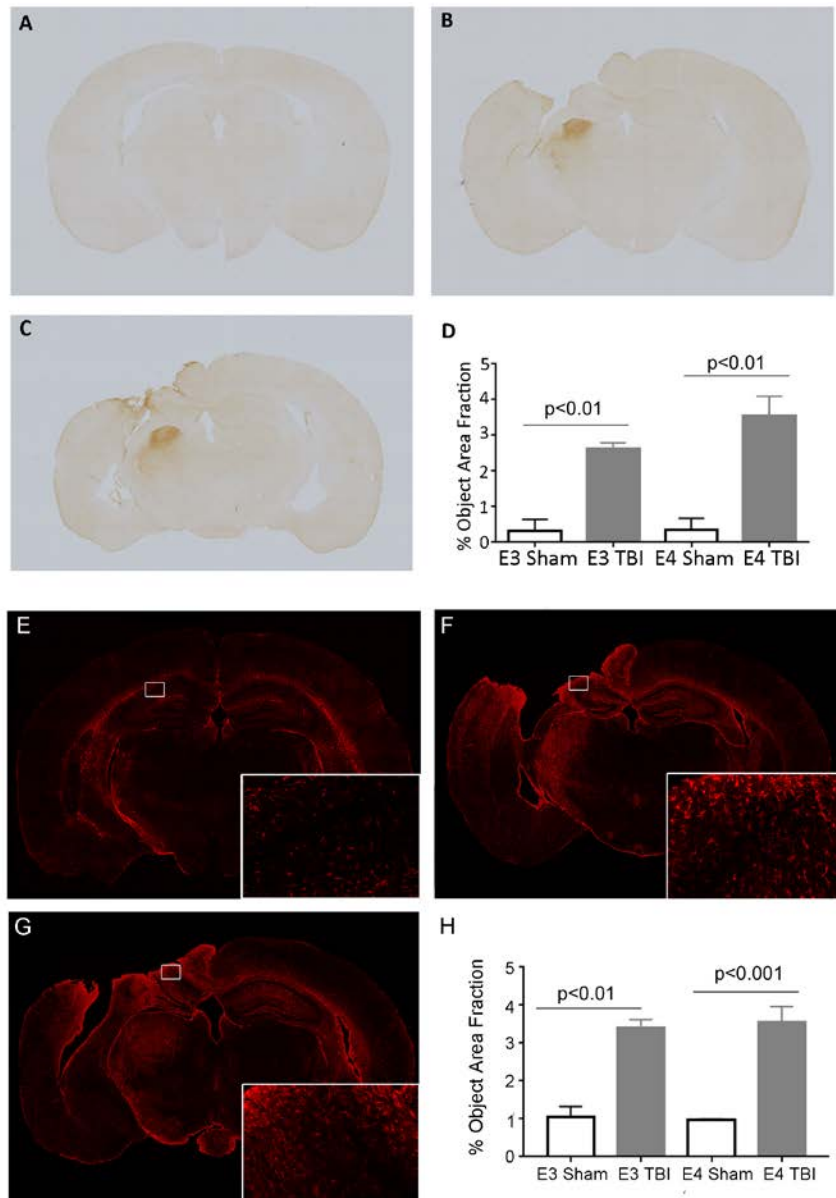


Figure 6. TREM2 protein level and Astrocytosis are increased by TBI.

Immunohistochemistry with anti-TREM2 antibody or anti-GFAP was performed in both sham and TBI mice ($n=3/\text{group}$). Percent intensity of Trem2 staining or GFAP staining was determined in the ipsilateral hemispheres. (A) Sham animals had low to no levels in Trem2. (B) APOE3 TBI and (C) APOE4 TBI animals had significantly higher levels of Trem2 when compared to their sham counterparts ($p < 0.01$ for both APOE3 and APOE4). (D) Analysis of object area fraction demonstrates a significant main effect of injury ($p < 0.001$), but not APOE isoform in Trem2 levels. Statistics is by Two-way ANOVA with post-hoc Tukey's multiple comparisons test. (E) Sham animals demonstrated low GFAP staining levels. (F) APOE3 and (G) APOE4 TBI animals show increased GFAP staining compared to their sham counterparts, particularly near the injury site (APOE3: $p < 0.01$; APOE4: $p < 0.001$). Insets taken from the injury visualize the increased staining at higher magnification (20X). (H) Analysis of object area fraction demonstrates a significant main effect of injury ($p < 0.001$), but not APOE isoform in GFAP levels. There was no significant difference between APOE3 and APOE4 animals, regardless of injury. Statistics is by Two-way ANOVA with post-hoc Tukey's multiple comparisons test.

The conclusion from these data is that, in both APOE isoforms, TBI affects resident microglia genes functionally related to immune response and phagocytosis, as well as astrocyte specific genes.

ME Green is negatively associated with injury suggesting that genes, members of this module are downregulated by TBI (Fig. 13; Suppl. Materials). The related biological process that represents this network (module size = 854) was associated with GO category “Transport” and is represented by *Camk2b*, *Pik3r2* and *Pld3* for which genetic variants are associated with an increased risk of Alzheimer’s disease [57,134] and functionally have a role in hippocampal plasticity, phospholipid metabolism, brain development, and APP processing [35].

3.4.5 Networks associated with expressed APOE isoform

As shown on Fig. 4, ME Darkred (Fig. 7, Fig. 14; Suppl. Materials) and Salmon (Fig. 8, Fig. 14; Suppl. Materials) are significantly associated with APOE isoform regardless of injury. On Fig. 7A, the heat-map and bar plot representing ME Darkred demonstrate an increased expression of genes associated with this network in APOE4 mice (TBI+Sham) and a decreased expression in APOE3 mice (TBI+Sham). The biological process associated with ME Darkred network (module size = 31) was the GO term “Innate immunity” (Fig. 7B). The heatmap (Fig. 7C) shows the highest 50 upregulated genes when comparing APOE3 and APOE4 mice. We were interested and further validated one of the hub genes associated with BP “Innate Immunity” - *Fyn* (*Fyn* proto-oncogene, Src family tyrosine kinase). *Fyn* is a major regulator of pro-inflammatory processes, specifically microglia mediated neuroinflammation [103]. mRNA-seq (Fig. 7D) and protein expression level for *Fyn* are shown on Fig. 7E and F. Three of *Serpina3* genes (*Serpina3m*, *Serpina3f* and *Serpina3h*) have been also identified as hub genes in this network.

ME Salmon positively correlated to APOE4-TBI mice and negatively to APOE3-TBI ($r=0.41$, $p=0.01$). Functionally, this module (module size = 65) is enriched in genes connected to the BP “Myelination” (Fig. 8 and Table 1). The network is significantly enriched with oligodendrocyte signature genes (18 genes out of 64 were oligodendrocyte specific). The representative network (Fig. 8B) was built using the hub genes *Car2*, *F2ah*, *Mbp* and *Plp1* that are all coding for major components of myelin [5,21] and together with cholesterol, are particularly important for myelin formation and remodeling in the context of axonal loss and repair after TBI [119,120]. Mutations in the majority of the genes within the network lead to demyelination and hypomyelinating inherited disorders [28,120,122,131], or have been implicated in neurodegeneration, including Alzheimer’s Disease. Alternatively, the high presence of myelin related proteins, including *Mag*, myelin associated glycoprotein, could be indicative of the formation of a glial scar [145,116]. Chronically, a glial scar could prevent axonal regeneration and potentially explain a worse outcome in APOE4 TBI mice. mRNA-seq results between APOE4 TBI and APOE3 TBI for selected hub genes are shown on Fig. 8C.

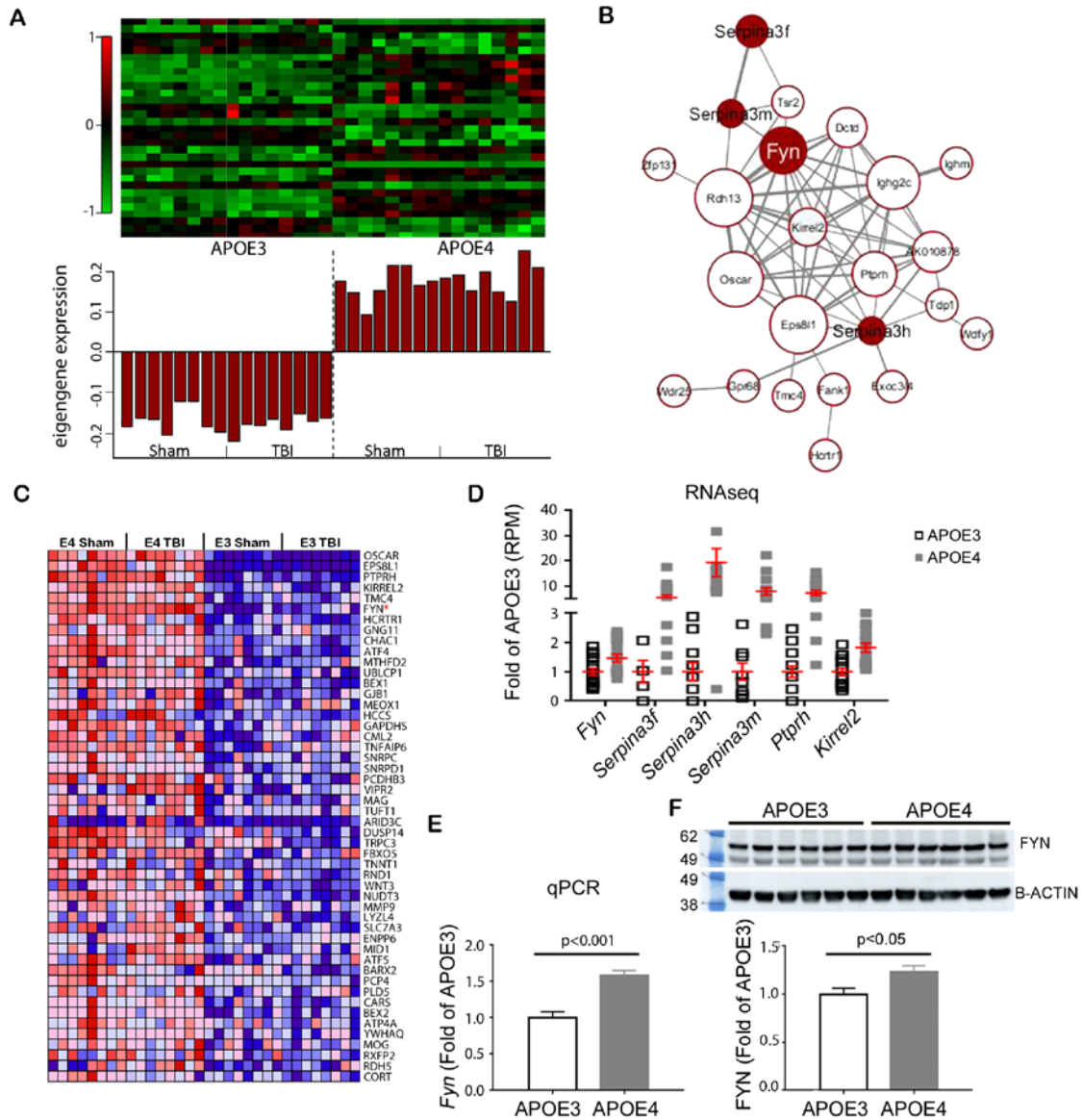


Figure 7. ME darkred correlates to APOE isoform and is associated with innate immunity.

(A) The expression bar plot shows the gene expression and eigengene expression within each sample. (B) Network of genes connected to the chosen hub gene *Fyn* representing innate immunity. (C) Heatmap of top 50 upregulated genes in comparing APOE3 to APOE4 mice. (D) mRNA-seq results for important genes within the network. The average expression was calculated as fold of APOE3 reads per million for each gene. Statistics is by edgeR, $p < 0.05$. (E) Validation of mRNA-seq results by qPCR. Statistics was determined by t-test. (F) Western blot results for APOE3 TBI versus APOE4 TBI animals for FYN and β -ACTIN validate mRNA-seq results. Proteins are normalized to levels of β -ACTIN and presented as fold of APOE3.

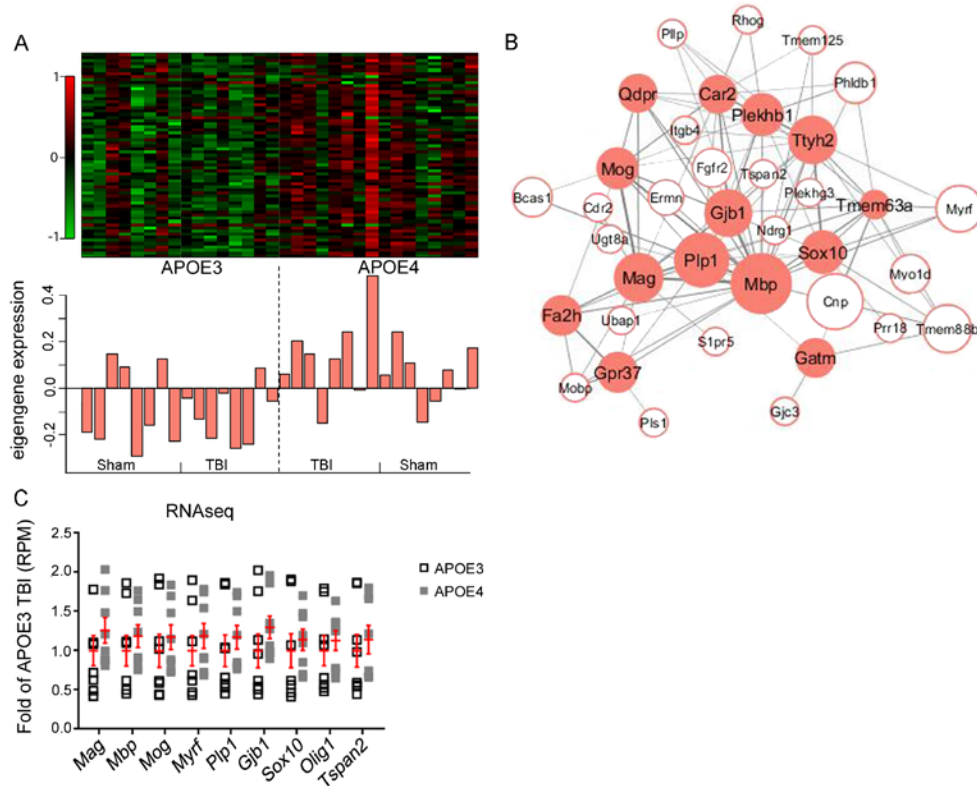


Figure 8. Gene-network module salmon correlates to APOE isoform in injury groups and is associated with myelination.

(A) The expression barplot shows the gene expression and eigengene expression within each sample. (B) Network of genes connected to hub genes Car2, F2ah, Mbp and Plp1 representing myelination. (C) mRNA-seq results for important genes within the network. The average expression was calculated as fold of APOE3 TBI reads per million for each gene. Statistics is by edgeR, $p < 0.05$. (D) Validation of mRNA-seq results by qPCR for Mbp and Plp1. The average expression was calculated as fold of all APOE3 TBI mice. Statistics was determined by t-test.

3.5 DISCUSSION

We examined the role of human APOE isoforms in the response to TBI in mice. Our study was designed with the goal to identify differences in cognitive performance, brain transcriptome and genome-wide correlated gene networks in adult (3-month-old) APOE targeted replacement mice, following CCI model of brain injury. We found that TBI significantly worsened performance in the anxiety-related EPM and the spatial learning task MWM, but the results showed no interaction of injury with APOE isoform. At baseline, animals expressing APOE4 had pre-

existing deficits compared to APOE3 animals, but both groups displayed similar responses to injury although in general APOE3 mice performed better. In mice expressing either isoform, TBI significantly changed the transcriptome, particularly increasing the expression of genes related to immune response and phagocytosis, such as *Trem2*, *Tyrobp*, *Clec7a*, *Cd68*, *Cx3cr1*, with low to no expression of peripheral macrophage genes, such as *Alox15* and *P2rx4*. We analyzed the effect of TBI on the transcriptome within each genotype and found similar biological processes affected, regardless of the genotype. The GO terms downregulated by TBI were also similar, with the top processes being regulation of transmembrane ion transport and potassium transport. We did identify an APOE isoform effect on the brain transcriptome in TBI mice, but this effect was entirely separate from the effect of injury.

Using WGCNA we identified correlated gene networks associated with TBI. We determined differential effects of two traits – genotype and type of injury, and identified gene networks throughout the entire genome, that correlated with injury and with the expressed APOE isoform. To a very significant extent, WGCNA results confirmed the GO terms identified through pathway analysis using the lists of differentially expressed genes in response to TBI. Most highly affected by TBI network was represented by “Immune Response”. Importantly, neither APOE3 or APOE4 isoform had a specific modulatory effect on this network: validations of several genes by RT-qPCR, including *Trem2* by IHC, found no differences between mice expressing APOE3 or APOE4 (Fig. 5 & 6). This network was highly enriched in microglia signature genes; among those, *Trem2*, *Clec7a* and *Hexb* were identified as hub genes suggesting that at our chosen time-point – 14 days post injury, the elevated immune response in the brain was predominantly a result of activated microglia and astrocytes, which was confirmed by immunohistochemistry and is consistent with TREM2 localization. Recently, human TREM2 has

come under scrutiny for its role in inflammation and neurodegeneration. *TREM2* is expressed solely in cells of myeloid lineage, including microglia, and *TREM2* mutations or mutations in the gene *TYROBP*, coding for its adaptor protein (aka *DAP12*) are linked to Nasu-Hakola disease [13]. Although its natural ligands are unknown, binding of TREM2 to negatively charged lipids, results in TYROBP phosphorylation, activation of intracellular spleen tyrosine kinase SYK, and thus SYK-RAS-ERK signaling pathway, actin remodeling and calcium mobilization needed for phagocytosis [30]. Using fluid percussion model of injury in *Trem2* deficient mice Lamb's group has recently shown that in injured mice there was a reduction of infiltrating macrophages, reduced inflammatory cytokines, less hippocampal volume loss and a rescue of spatial memory deficits [118]. Yet, a different study found that *Trem2*^{-/-} mice had decreased phagocytosis after stroke and worsened neurological outcomes [66]. Obviously, the contradictory results of these studies point to the need of standardized study designs and data collection to understand the role of TREM2 in the response to TBI and subsequent repair.

The “Transport” network, ME Green, was significantly affected and down-regulated by injury in both genotypes. The hub genes of this network include *Camk2b*, which is important for both hippocampal-dependent learning and long-term potentiation [17]. The kinase transcribed by *Camk2b* is necessary for the proper targeting of CAMK2a at the synapse for promotion of dendritic spines and synapse formation. *Pld3* is another gene in the “Transport” network, which is highly expressed in the brain and may be involved in synaptic transmission and signal transduction [35]. A rare missense variant of *PLD3* was linked to an increased risk of late onset AD and since a decreased expression of PLD3 is associated with higher levels of extracellular A β , PLD3 may have some role in APP processing [102].

In injured mice “Innate immunity” was the network of genes differentially affected by APOE isoform. The network was built of transcripts connected to *Fyn* and *Serpina3*. Since tau and *Fyn* have been shown to co-localize in dendrites, not surprisingly, recent studies have suggested a pathogenic role for *Fyn* in AD, [74]. FYN interacts with A β , which possibly serves as a critical step in triggering downstream neuronal pathology. Moreover, it has been suggested that binding of A β oligomer species to the neuronal membrane receptors at the post-synaptic terminal may activate FYN by phosphorylation, resulting in *N*-methyl-D-aspartate (NMDA) receptor phosphorylation, dendritic spine loss and tau phosphorylation [100]. *Serpina3m*, *Serpina3f* and *Serpina3h* - *Serpina3* genes identified as hub genes in ME Darkred, reside on mouse chromosome 12 (*I2F1* locus) and code for isoforms of the plasma protease inhibitor α 1-antichymotrypsin [48]. Initially, SERPINA3 binding to A β peptide and subsequent deposition of this complex in amyloid plaque has been linked to the progression of Alzheimer’s disease (see [1] for review). Genetic variants of α 1-antichymotrypsin have been considered as increasing the risk of LOAD, or a modifier of the risk imposed by *APOE4* [50,64]. Results of more recent studies, however, have demonstrated a neuroprotective effect of the protein SERPINA3 in *in vitro* and *in vivo* models of multiple sclerosis, as well as accelerated tissue repair in a diabetic mouse model [58,53].

The “myelination” network represented by ME salmon was differentially affected by APOE isoform within only the injury groups. ME Salmon was upregulated in APOE4 TBI mice and downregulated in APOE3 TBI mice, and not significant in sham groups. The network was built on several myelin related proteins, such as *Car2*, *F2ah*, *Mbp* and *Plp1*, and was also highly enriched in oligodendrocyte specific markers. The presence of oligodendrocytes after injury is not surprising, as myelin and cholesterol would both be necessary components for axonal repair

and regeneration [119,120]. However, myelin related proteins, particularly *Mag*, which was identified as a hub gene within the network, have been associated with inhibited axonal outgrowth and the formation of a glial scar [145]. The role of this network in repair and scar formation could provide a mechanism for worse outcome in APOE4 isoform after TBI that is temporally dependent.

The underlying molecular mechanisms by which human APOE isoforms, globally expressed in a mouse, affect the outcome of TBI are not clear, and in general are poorly understood. While controversial in their findings and final interpretation, many studies have suggested, so far, that the inheritance of *APOE4* allele in humans or the expression of APOE4 in animal models would result in a worse outcome following brain injury. Several human studies, however, have shown that APOE4 had no effect on outcome of TBI [26,90]. In contrast, the majority of animal studies, mostly in AD mouse models expressing human APP, have demonstrated APOE4 plays a significant role in determining the pathology and recovery following TBI, possibly in an age dependent manner [12,86,14]. The animal models of TBI obviously do not, and cannot, represent all aspects of brain pathology as a response to brain trauma at molecular, cellular and organ levels. Moreover the lack of standardized study design and data collection makes it extraordinarily difficult to compare the results of the studies performed so far and to draw definitive conclusions. The results of our study did not suggest a major role for APOE3 or APOE4 isoforms in modulating the response to TBI. We identified, however, networks of genes in brains of APOE3 and APOE4 injured mice that have clearly pointed out to genes, and thus their proteins, with a potential to become useful and rational targets for future research and drug discovery relevant to TBI.

The major physiological role of APOE, as a principal apolipoprotein of HDL-like particles in brain, is to transport cholesterol and phospholipids in brain interstitial space/fluid. Thus, it is reasonable to assume that other genes/proteins, involved in brain cholesterol metabolism with a regulatory role in *APOE* expression or in the brain cell type specific transport of cholesterol may play an equally significant, if not a larger role in the response to injury. In our sequencing datasets and validation assays we found that following injury *Abca1* mRNA and ABCA1 protein levels were increased. An increased ABCA1 protein level in a rat model of TBI has already been reported [22]. Thus, the elevated expression of ABCA1 following TBI could be a response to the increased demand for cholesterol and phospholipids, necessary for axonal repair. The hub genes in ME Salmon provide additional support that a correlated response to TBI includes upregulation of network of genes relevant to cholesterol transport and myelin formation. While in normal conditions in adult, developed brain oligodendrocytes synthesize cholesterol and do not depend on cholesterol transported by APOE particles, they express LDL-R and receptor mediated endocytosis of lipoproteins, APOE included, is a very important transport mechanism for cholesterol supply in traumatized brain areas with axonal damage and undergoing myelination/myelin remodeling. APOE mediated stimulation of Neural Stem Cells and enhanced oligodendrogenesis, which require sufficient amounts of cholesterol and phospholipids, and to some extent APOE/LDL-R interaction for activation of downstream signaling cascades, most probably have an important role for improved myelination and axonal restoration as part of the recovery process.

In conclusion, we found that APOE3 and APOE4 targeted replacement mice demonstrate similar cognitive impairment following moderate TBI with differences reflecting the preexisting deficits in APOE4 mice at baseline. Transcriptional profiling 14 days following TBI revealed a

clear separation between sham and injured animals without a difference based on APOE isoform. Top up-regulated categories in both genotypes were highly consistent and were associated with Immune System, Innate Immune and Inflammatory Responses. Ion and Potassium Transport categories were downregulated, similarly in both genotypes. Using WGCNA, we determined that TBI and APOE affected separate networks independently. Immune Response was the most affected network driven by TBI in both genotypes, while both sham and injured animals were differentially affected by APOE isoform, with increased expression of genes associated with functional groups/modules representing Innate Immunity. The network representing Myelination was affected by APOE isoform across the injury groups, demonstrating a difference in response to injury between APOE3 and APOE4 mice. The results of this study indicate that distinct cellular pathways/networks drive the APOE isoform specific phenotype and the response to TBI at this acute time point.

3.6 SUPPLEMENTAL MATERIALS & FIGURES

3.6.1 TBI consistently affects biological processes in both APOE isoforms

Table 2a-b show several genes of interest differentially expressed between TBI versus Sham, as well as APOE4 versus APOE3. We were interested if there was a similarity between the biological processes affected by TBI in APOE3 and E4 mice. Top up-regulated categories in both genotypes were highly consistent and were associated with “immune system process”, “innate immune response” and “inflammatory response”(Table 3a-b). Top down-regulated categories in both genotypes were also similar including “regulation of ion transmembrane

transport”, and “potassium ion transport” (Table 4a-b). Interestingly, one category down-regulated by TBI in APOE4 mice was associated with cholesterol and lipid metabolism including genes such as 3-Hydroxy-3-Methylglutaryl-CoA Reductase (*Hmgcr*) and NPC1 like intracellular cholesterol transporter 1 (*Npc1l1*). In APOE3 mice, categories also affected were “regulation of synaptic plasticity” and “long-term potentiation”.

Table 2. Differentially expressed genes of interest and their corresponding coefficients.

A. TBI versus Sham				
	Gene	APOE3	APOE4	
Up in TBI	<i>Abca1</i>	1.78	1.83	
	<i>ApoD</i>	1.02	0.96	
	<i>Axl</i>	0.72	0.71	
	<i>Cd33</i>	1.25	1.36	
	<i>Cd68</i>	2.22	1.96	
	<i>Clec7a</i>	5.26	5.84	
	<i>Clu</i>	0.79	0.70	
	<i>Cx3cr1</i>	0.94	0.94	
	<i>Gfap</i>	2.29	2.24	
	<i>Itgam</i>	1.16	1.11	
	<i>Itgax</i>	4.15	4.05	
	<i>Ly86</i>	1.87	1.67	
	<i>Spi1</i>	1.47	1.65	
	<i>Tgfb1</i>	0.95	0.93	
	<i>Tgfb1</i>	0.81	0.61	
	<i>Trem2</i>	2.03	1.79	
	<i>Trem2</i>	2.99	2.81	
	<i>Tyrobp</i>	1.84	1.69	
	Down in TBI	<i>Atp1b1</i>	-0.17	-0.18
		<i>Bdnf</i>	-0.77	-0.58
<i>Egr1</i>		-0.95	-0.72	
<i>Epha1</i>		-0.47	-0.32	
<i>Grin2a</i>		-0.70	nf	
<i>Ldlr</i>		-0.63	-0.37	
<i>Stx1a</i>		-0.28	-0.32	

B. APOE4 versus APOE3			
	Gene	Sham	TBI
Up in APOE4	<i>Abca7</i>	0.12	nf
	<i>Plp1</i>	0.14	0.32
	<i>Ptprh</i>	3.15	2.78
	<i>Serpina3f</i>	2.80	2.07
	<i>Serpina3h</i>	4.37	3.73
	<i>Serpina3m</i>	4.45	2.59
	<i>Wnt3</i>	0.36	0.88
	<i>Fyn</i>	0.69	0.59
	<i>Kirrel2</i>	0.88	1.06
	<i>Mag</i>	nf	0.42
	<i>Mbp</i>	0.23	0.34
	<i>Mog</i>	0.22	0.31
	<i>Picalm</i>	nf	0.13
Down in APOE4	<i>Wnt2</i>	-0.54	-0.52
	<i>Pcdh11x</i>	-0.40	nf
	<i>Gpr68</i>	-0.34	-0.57
	<i>Celf1</i>	-0.12	nf
	<i>Celf2</i>	-0.12	nf
	<i>Apoc1</i>	-0.45	nf

a Several significant transcripts both up- and down-regulated are shown beside corresponding coefficients for APOE3 mice, TBI versus sham and APOE4 mice, TBI versus sham. b Several significant transcripts both up- and down-regulated in APOE4 are shown beside corresponding coefficients for Sham, APOE4 versus APOE3 and TBI, APOE4 versus APOE3.

Table 3. TBI increases the expression of genes related to immune response and inflammation in both APOE3 and APOE4 mice.

A.	Term	Count	%	PValue	FE	Benjamini
	GO:0002376~immune system process	97	19.52	1.51E-71	10.63	3.28E-68
	GO:0045087~innate immune response	85	17.10	3.60E-55	8.83	3.91E-52
	GO:0006954~inflammatory response	62	12.47	3.51E-35	7.42	2.53E-32
	GO:0006955~immune response	50	10.06	1.17E-25	6.53	6.36E-23
	GO:0051607~defense response to virus	37	7.44	3.05E-24	9.20	1.32E-21
	GO:0009615~response to virus	24	4.83	2.33E-18	11.79	8.40E-16
	GO:0006935~chemotaxis	27	5.43	3.68E-18	9.56	1.14E-15
	GO:0030593~neutrophil chemotaxis	21	4.23	2.22E-16	12.18	6.02E-14
	GO:0071346~cellular response to interferon-gamma	19	3.82	1.92E-14	11.67	4.63E-12
	GO:0071222~cellular response to lipopolysaccharide	30	6.04	6.89E-14	5.72	1.49E-11
	GO:0019886~antigen processing and presentation of exogenous peptide antigen via MHC class II	10	2.01	4.20E-12	29.84	8.27E-10
	GO:0050729~positive regulation of inflammatory response	16	3.22	2.57E-11	10.28	4.65E-09
	GO:0070374~positive regulation of ERK1 and ERK2 cascade	25	5.03	3.58E-11	5.44	5.96E-09

B.	Term	Count	%	PValue	FE	Benjamini
	GO:0002376~immune system process	100	20.12	3.38E-75	10.94	7.14E-72
	GO:0045087~innate immune response	82	16.50	9.21E-52	8.50	9.73E-49
	GO:0006954~inflammatory response	68	13.68	2.81E-41	8.12	1.98E-38
	GO:0051607~defense response to virus	40	8.05	1.56E-27	9.92	8.27E-25
	GO:0006955~immune response	50	10.06	1.30E-25	6.51	5.51E-23
	GO:0009615~response to virus	26	5.23	8.36E-21	12.75	2.95E-18
	GO:0006935~chemotaxis	29	5.84	2.31E-20	10.24	6.98E-18
	GO:0030593~neutrophil chemotaxis	22	4.43	1.35E-17	12.73	3.56E-15
	GO:0050729~positive regulation of inflammatory response	19	3.82	8.30E-15	12.18	1.96E-12
	GO:0071222~cellular response to lipopolysaccharide	28	5.63	3.05E-12	5.33	6.45E-10
	GO:0071346~cellular response to interferon-gamma	17	3.42	4.16E-12	10.42	8.00E-10
	GO:0070374~positive regulation of ERK1 and ERK2 cascade	26	5.23	5.85E-12	5.64	1.03E-09
	GO:0042742~defense response to bacterium	26	5.23	8.28E-12	5.56	1.35E-09

Top upregulated functional annotation terms were determined using DAVID for a APOE and b APOE4 sham versus injury mice using a gene list with a cut-off at $p < 0.05$. Common GO terms between the genotypes are listed in bold. FE, fold enrichment.

Table 4. TBI decreases the expression of genes related to transport and ion transmembrane transport in APOE3 and APOE4 mice.

A.	Term	Count	%	PValue	FE	Benjamini
	GO:0034765~regulation of ion transmembrane transport	26	5.24	4.32E-16	8.42	9.17E-13
	GO:0006813~potassium ion transport	25	5.04	1.60E-15	8.48	1.60E-12
	GO:0071805~potassium ion transmembrane transport	21	4.23	1.16E-14	10.16	8.02E-12
	GO:0006811~ion transport	49	9.88	1.78E-14	3.64	9.17E-12
	GO:0042391~regulation of membrane potential	16	3.23	6.35E-09	7.10	2.62E-06
	GO:0055085~transmembrane transport	26	5.24	1.37E-06	3.08	4.73E-04
	GO:0048791~calcium ion-regulated exocytosis of neurotransmitter	8	1.61	2.65E-06	12.30	7.81E-04
	GO:0007612~learning	11	2.22	2.65E-06	7.18	6.85E-04
	GO:0035556~intracellular signal transduction	27	5.44	3.21E-06	2.86	7.36E-04
	GO:0048167~regulation of synaptic plasticity	9	1.81	4.60E-06	9.23	9.49E-04
	GO:0060291~long-term synaptic potentiation	9	1.81	1.52E-05	7.91	2.86E-03
	GO:0007156~homophilic cell adhesion via plasma membrane adhesion molecules	15	3.02	2.72E-05	3.96	4.67E-03
	GO:0006810~transport	69	13.91	4.90E-05	1.63	7.75E-03
	GO:0060052~neurofilament cytoskeleton organization	5	1.01	5.34E-05	21.53	7.85E-03

B.	Term	Count	%	PValue	FE	Benjamini
	GO:0034765~regulation of ion transmembrane transport	23	4.66	3.79E-13	7.50	7.73E-10
	GO:0006813~potassium ion transport	20	4.05	9.54E-11	6.83	9.74E-08
	GO:0006695~cholesterol biosynthetic process	11	2.23	1.53E-09	14.91	1.04E-06
	GO:0008202~steroid metabolic process	15	3.04	6.86E-09	7.74	3.50E-06
	GO:0006811~ion transport	38	7.69	2.33E-08	2.84	9.50E-06
	GO:0016126~sterol biosynthetic process	9	1.82	7.97E-08	15.01	2.71E-05
	GO:0071805~potassium ion transmembrane transport	14	2.83	1.21E-07	6.82	3.52E-05
	GO:0008203~cholesterol metabolic process	12	2.43	6.10E-06	5.85	1.56E-03
	GO:0008299~isoprenoid biosynthetic process	6	1.21	3.10E-05	15.31	7.00E-03
	GO:0006694~steroid biosynthetic process	9	1.82	8.36E-05	6.30	1.69E-02
	GO:0051480~regulation of cytosolic calcium ion concentration	7	1.42	1.11E-04	8.93	2.05E-02
	GO:0006629~lipid metabolic process	25	5.06	1.78E-04	2.36	2.98E-02
	GO:0042391~regulation of membrane potential	10	2.02	3.96E-04	4.47	6.04E-02
	GO:0006816~calcium ion transport	12	2.43	4.23E-04	3.69	5.99E-02

Top downregulated functional annotation terms were determined using DAVID in a APOE3 and b APOE4 sham versus injury mice using a gene list with a cut-off at $p < 0.05$. Common GO terms between the genotypes are listed in bold. FE, fold enrichment.

3.6.2 Gene Set Enrichment Analysis identifies biological processes commonly effected by injury in both isoforms

To further identify enriched pathways commonly affected by TBI in both isoforms, we used Gene Set Enrichment Analysis (GSEA) assessing all transcripts without a cutoff [126]. To examine the effect of injury on transcriptome, we combined the results for both isoforms in TBI group (E3-TBI+E4-TBI) and compared them to sham treated (E3-sham + E4-sham). The bubble plot shown on Fig. 9a visualizes the biological process categories upregulated by TBI and amongst them are “Immune System Response”, “Receptor Activity”, “Cysteine Type Endopeptidase Activity”, “G Protein-coupled Receptor Binding” and “Chemokine Receptor Binding”. Top downregulated categories are “Synaptic Transmission” and “Potassium Ion Transport” but they were not statistically significant.

On Fig. 9 are shown the enplots and heatmaps for the top upregulated categories by TBI namely “Immune System Response” (NES=1.60, $p<0.002$, Fig. 9b-c) and “Receptor Activity” (NES=1.55, $p<0.013$, Supplementary Fig. 9e-f), as well as the RNA-seq results on chosen genes from these categories (Supplementary Fig. 9d and g). To confirm the results we validated several of these genes by qPCR or Western blotting.

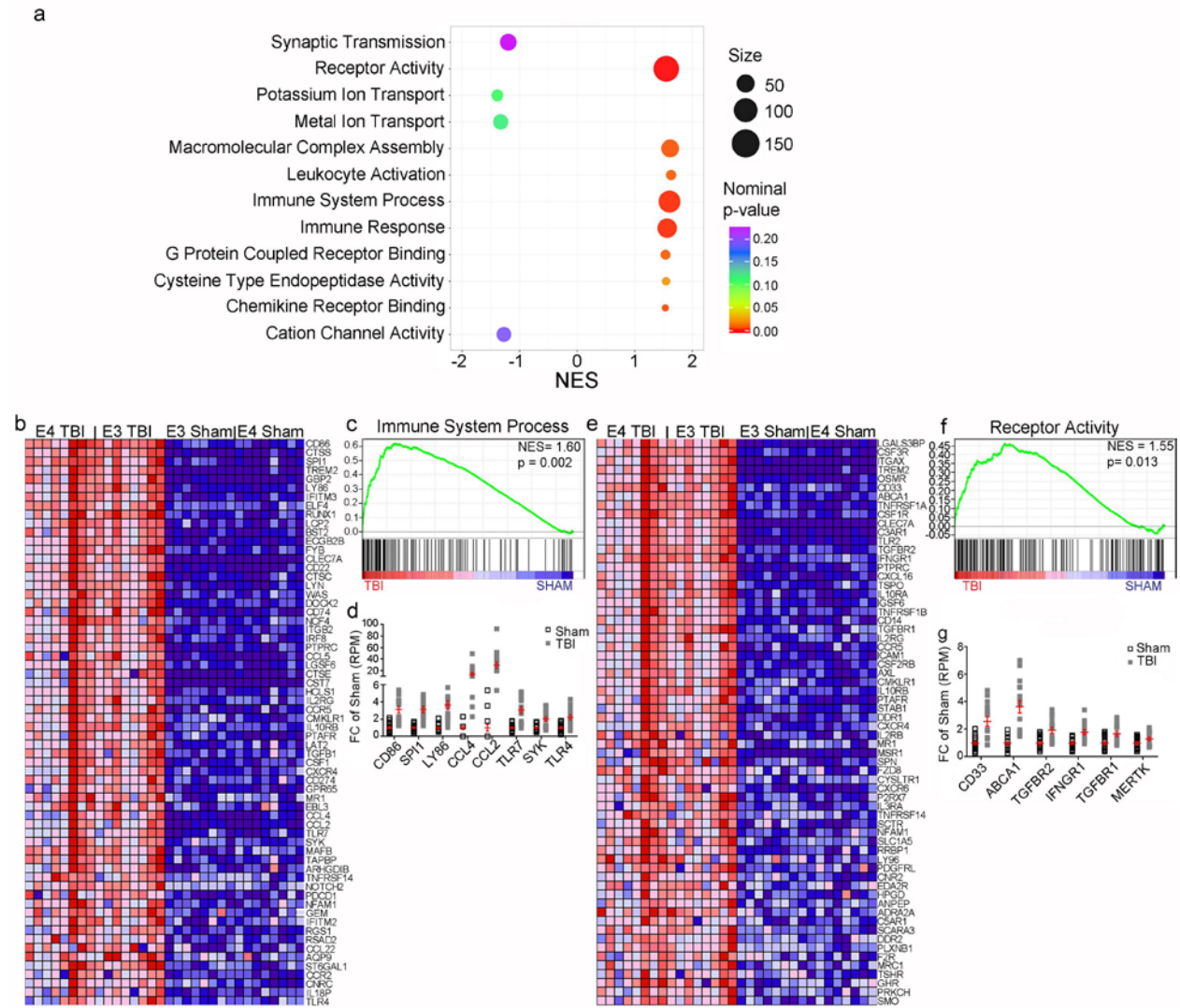


Figure 9. Gene set enrichment analysis of injury.

Compared are all TBI mice (APOE3-TBI+APOE4-TBI) versus all Sham mice (APOE3-Sham + APOE4-Sham). a The bubble plot shows top ranked GO terms affected by the injury. Color indicates normalized p value and size of bubble indicates the number of genes assigned to the GO term. b Heatmap and c enrichment score curve (enplot) provided by the GSEA analysis for “Immune System Process”. The upregulated genes are represented in red and downregulated genes are represented in blue. d RNA-seq results for selected genes from the GO term “Immune System Process” are shown as normalized to the average of sham. e Heatmap and f enplot provided by the GSEA analysis for “Receptor Activity”. g RNA-seq results for selected genes from the GO term “Receptor Activity” are shown as normalized to the average of sham.

3.6.3 WGCNA identifies correlations between modules

Fig. 10A depicts a hierarchical clustering dendrogram of the eigengenes indicating modules with similar expression profiles. The heatmap represents the adjacency between modules (Fig. 10B).

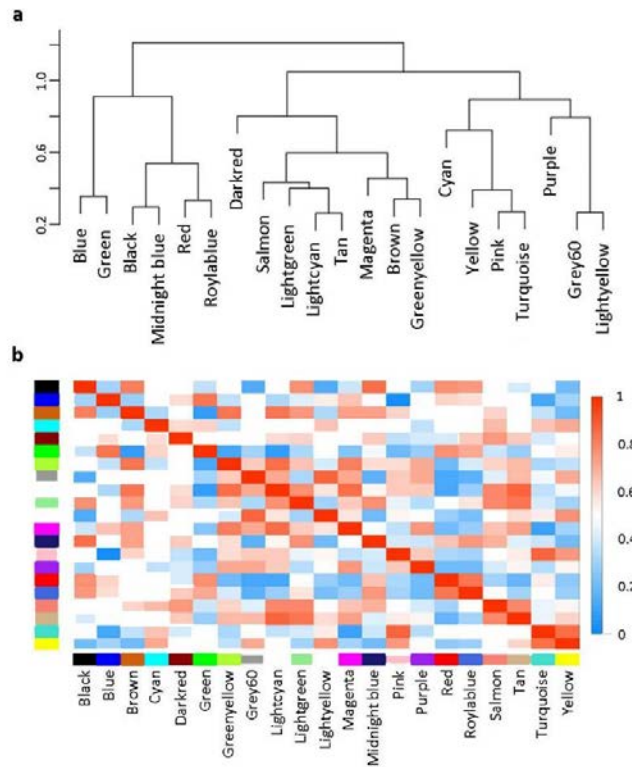


Figure 10. (Related to Fig. 4) WGCNA identified correlations between modules.

a Hierarchical clustering dendrogram of the eigengenes showing the level of similarity and dissimilarity of eigengenes. b Heatmap of modules showing level of adjacency, with red indicating high level and blue indicating low level.

3.6.4 ME brown strongly correlates with injury regardless of APOE isoform

In Fig. 11a and b, the scatterplot showing the correlation between connectivity and Gene significance (GS) is shown for each isoform. This demonstrates the functional relationship between the genes within the module. As seen in Fig. 11c and d, the correlation between Module membership (MM) and GS for genes within ME brown demonstrates how strongly they relate to the biological process the module represents, “immune response and “innate immune response” for each isoform. The bar plot of module significance for each isoform demonstrates the ME brown is strongly associated with injury regardless of APOE isoform (Fig. 11e and f).

3.6.5 Microglia localize to the injury site in TBI brains

To visualize recruitment of microglia to the site of injury, we performed immunohistochemistry against Iba1 (Fig. 12). Sham mice showed little Iba1 staining in both APOE3 (Fig. 12a) and APOE4 (Fig. 12b) isoforms. In comparing between TBI and sham, both APOE3 (Suppl. Fig. 12c; $p=0.04$) and APOE4 (Fig. 12d, $p=0.007$) mice had significantly higher levels of Iba1 staining. These results demonstrate the significant microglia presence around the injury site, consistent with TREM2 localization.

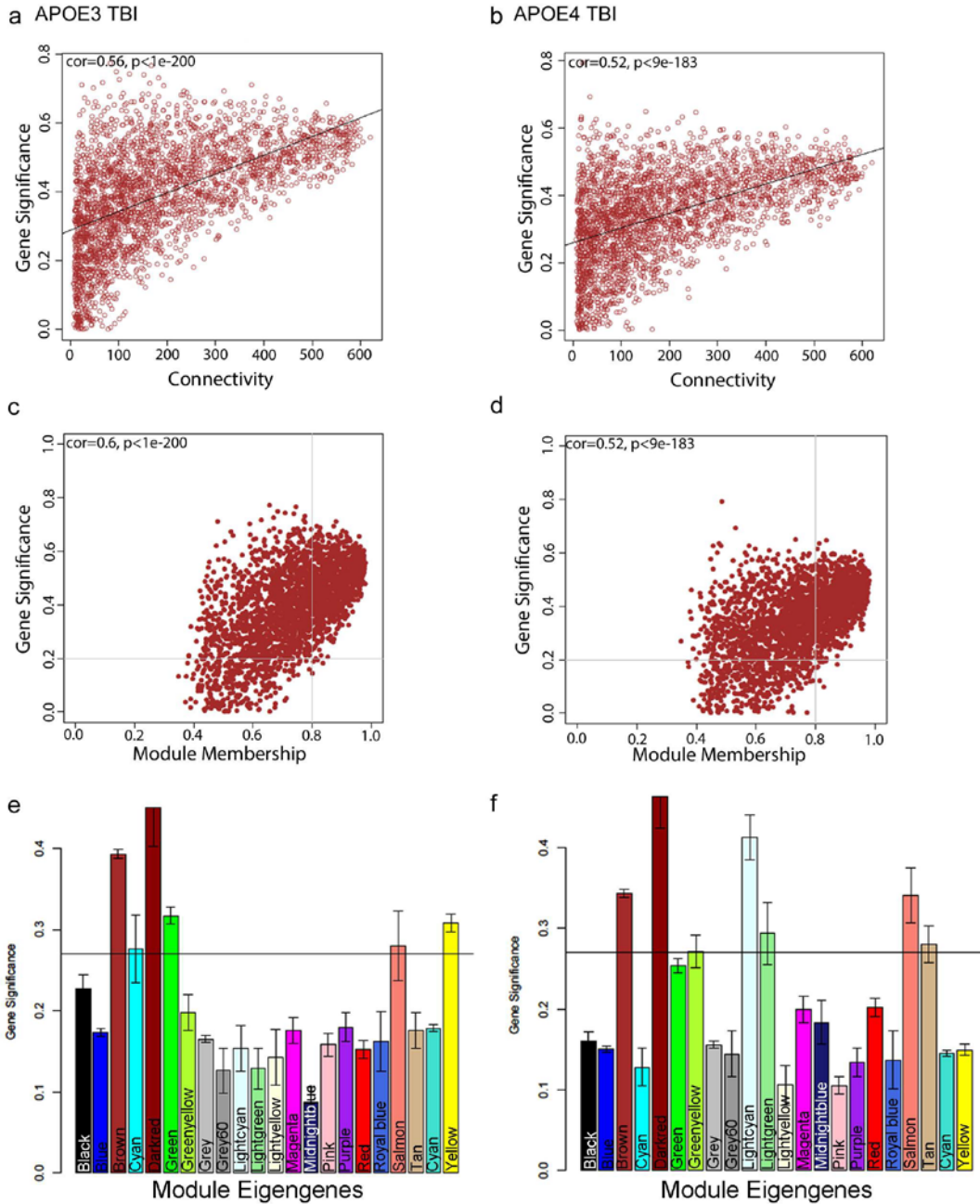


Figure 11. (Related to Fig. 5) Module related to injury was identified by relationship between gene significance and module membership.

a Scatter plot showing the correlation between connectivity and gene significance (GS) for the brown module for APOE3-TBI mice. Correlation value and p value are indicated in the plot. b Scatter plot for brown module for APOE4-TBI mice. c Scatter plot for brown module showing the correlation between module membership (MM) and GS for APOE3-TBI mice. The degree of association between MM and GS was evaluated by Pearson correlation. Correlation value and p value are indicated in the plot. d Scatter plot showing the correlation between MM and GS brown module for APOE4-TBI mice. e Bar plot of module significance (MS) for all module eigengenes for APOE3-TBI mice. MS denotes mean of the absolute value of gene significance across modules for APOE isoform. f Bar plot of MS for all module eigengenes for APOE4-TBI mice.

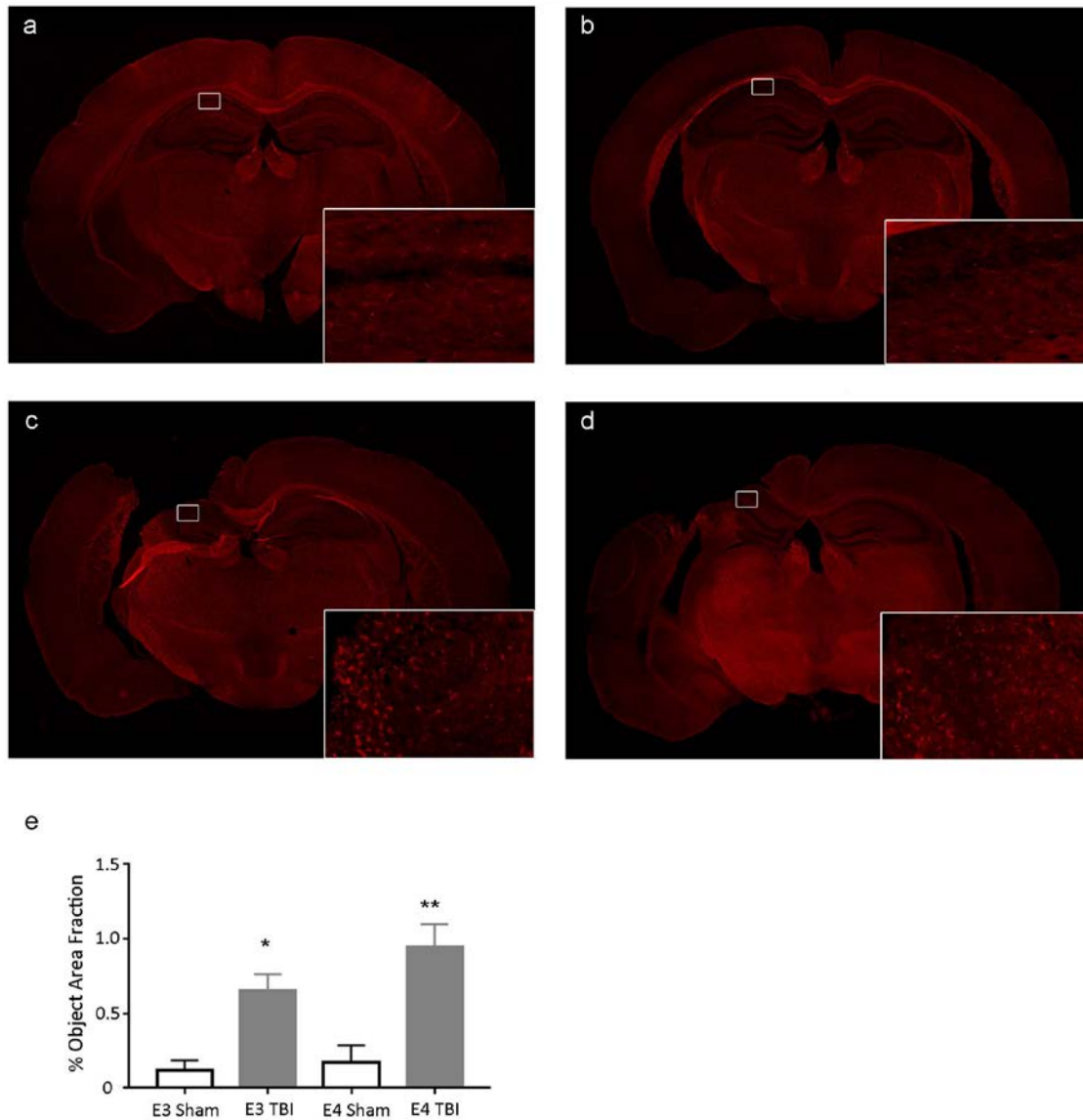


Figure 12. Microglia are significantly higher in TBI animals and concentrated at the injury site.

Immunohistochemistry with anti-Iba1 antibody was performed in both sham and TBI mice (n=3/group). Percent intensity of Iba1 staining was determined in the ipsilateral hemisphere. a APOE3 and b APOE4 sham animals demonstrated low Iba1 staining levels. c APOE3 and d APOE4 TBI animals show increased GFAP staining compared to their sham counterparts, particularly near the injury site (APOE3: $p=0.049$; APOE4: $p=0.007$). Insets taken from the injury visualize the increased staining at higher magnification (20X). e Analysis of object area fraction demonstrates a significant main effect of injury ($p=0.0005$), but not APOE isoform in Iba1 levels. There was no significant difference between APOE3 and APOE4 animals, regardless of injury. Statistics is by Two-way ANOVA with post-hoc Tukey's multiple comparisons test.

3.6.6 Gene-network associated with ‘transport’ is downregulated in injured mice

We found that ME green is negatively associated with injury suggesting that genes members of this module are downregulated in TBI. As seen in Fig. 13a, module eigengene expression is consistently downregulated in TBI animals. The related biological process that represents the genes within this network (module size = 854) was associated with GO category “transport”. We were most interested in hub genes connected to this network such as calcium/calmodulin-dependent protein kinase 2B (*Camk2b*), and phosphatidylinositol 3-kinase regulatory subunit 2 (*Pik3r2*) (Fig. 13b). Interestingly, the network also includes the gene phospholipase D family member 3 (*Pld3*), for which several variants are associated with an increased risk of Alzheimer’s disease [57,134]. RNA-seq results for important genes within the network are shown (Fig. 13c).

3.6.7 ME Darkred and ME Salmon both correlate with APOE isoform

Fig. 14a shows the bar plot of module significance (MS) for all groups. MS denotes mean of the absolute value of gene significance across modules for APOE isoform. Darkred and Salmon module show the highest gene significance, implying that gene expression of these modules is strongly associated with APOE isoform. Scatter plots are shown for the correlation between connectivity and GS of ME darkred (Fig. 14b) and ME salmon (Fig. 14c) for all mice. Additionally, scatter plots showing the correlation between MM and GS are shown for ME darkred (Fig. 14d) and ME salmon (Fig. 14e).

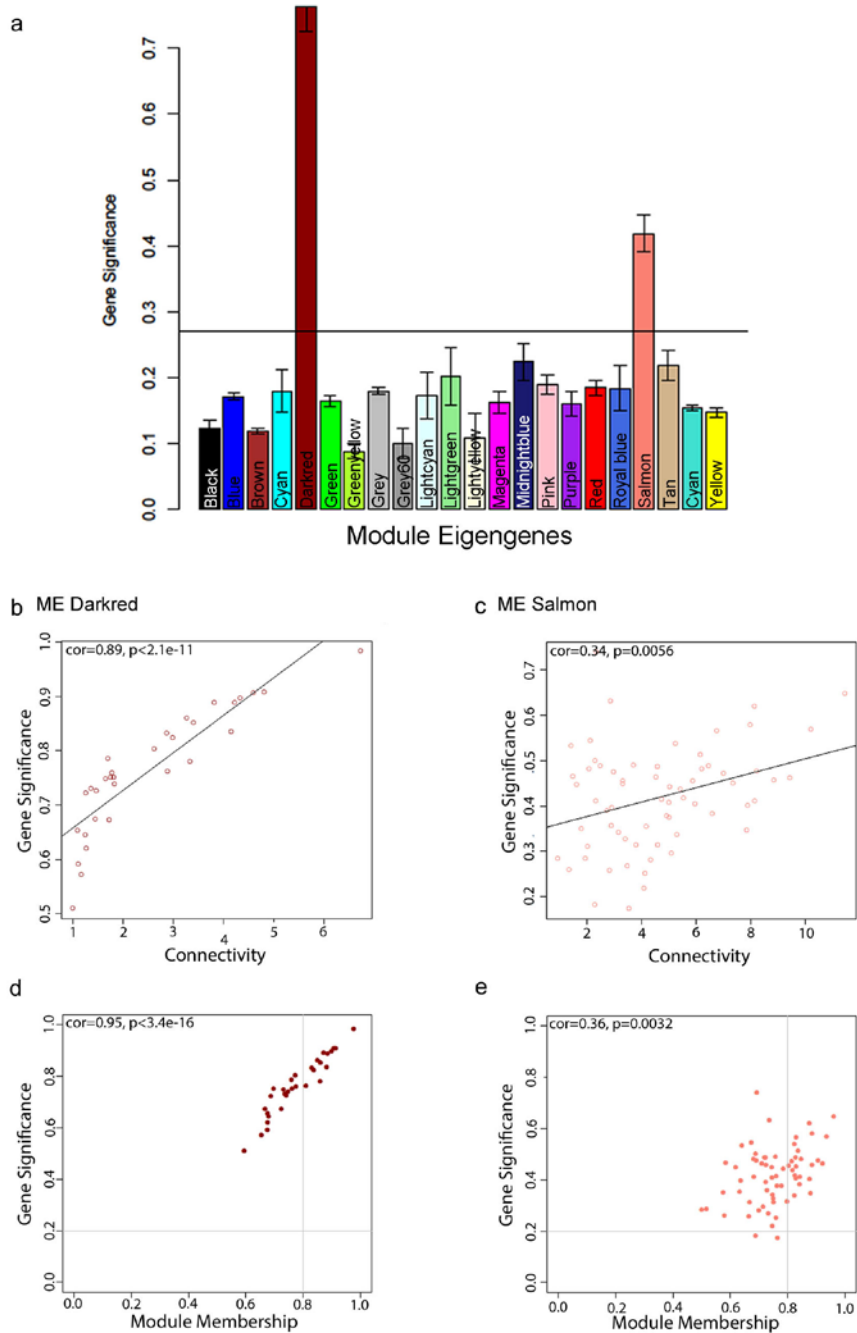


Figure 14. (Related to Figure 7-8). Modules related to APOE isoform were identified by relationship between gene significance and module membership.

a Bar plot of module significance (MS) for each Module eigengene (ME). b Scatter plot showing the correlation between connectivity and gene significance (GS) of ME darkred for all mice. Correlation value and p value are indicated in the plot. c Scatter plot for ME salmon. d Scatter plot for ME darkred module showing the correlation between module membership (MM) and GS. The degree of association between MM and GS was evaluated by Pearson correlation. Correlation value and p value are indicated in the plot. e Scatter plot showing the correlation between MM and GS of ME salmon.

4.0 ABCA1 HAPLODEFICIENCY AFFECTS THE BRAIN TRANSCRIPTOME FOLLOWING TRAUMATIC BRAIN INJURY IN MICE EXPRESSING HUMAN APOE ISOFORMS

The data presented in this article has been accepted to *Acta Neuropathol Commun.* (2018).

Emilie L. Castranio¹, Cody M. Wolfe¹, Kyong Nyon Nam¹, Florent Letronne¹, Nicholas F. Fitz¹,
Iliya Lefterov¹, Radosveta Koldamova¹

¹ Department of Environmental and Occupational Health, University of Pittsburgh, PA 15261, USA

4.1 ABSTRACT

Expression of human Apolipoprotein E (*APOE*) modulates the inflammatory response in an isoform specific manner, with *APOE4* isoform eliciting a stronger pro-inflammatory response, suggesting a possible mechanism for worse outcome following traumatic brain injury (TBI). *APOE* lipidation and stability is modulated by ATP-binding cassette transporter A1 (*ABCA1*), a transmembrane protein that transports lipids and cholesterol onto *APOE*. We examined the impact of *Abca1* deficiency and *APOE* isoform expression on the response to TBI using 3-months-old, human *APOE3*^{+/+} (*E3/Abca1*^{+/+}) and *APOE4*^{+/+} (*E4/Abca1*^{+/+}) targeted replacement

mice, and *APOE3*^{+/+} and *APOE4*^{+/+} mice with only one functional copy of the *Abca1* gene (*E3/Abca1*^{+/-}; *E4/Abca1*^{+/-}). TBI-treated mice received a craniotomy followed by a controlled cortical impact (CCI) brain injury in the left hemisphere; sham-treated mice received the same surgical procedure without the impact. We performed RNA-seq using samples from cortices and hippocampi followed by genome-wide differential gene expression analysis. We found that TBI significantly impacted unique transcripts within each group, however, the proportion of unique transcripts was highest in *E4/Abca1*^{+/-} mice. Additionally, we found that *Abca1* haplodeficiency increased the expression of microglia sensome genes among only *APOE4* injured mice, a response not seen in injured *APOE3* mice, nor in either group of sham-treated mice. To identify gene networks, or modules, correlated to TBI, *APOE* isoform and *Abca1* haplodeficiency, we used weighted gene co-expression network analysis (WGCNA). The module that positively correlated to TBI groups was associated with immune response and featured hub genes that were microglia-specific, including *Trem2*, *Tyrobp*, *Cd68* and *Hexb*. The modules positively correlated with *APOE4* isoform and negatively to *Abca1* haplodeficient mice represented “protein translation” and “oxidation-reduction process”, respectively. Our results reveal *E4/Abca1*^{+/-} TBI mice have a distinct response to injury, and unique gene networks are associated with *APOE* isoform, *Abca1* insufficiency and injury.

4.2 INTRODUCTION

Traumatic brain injury (TBI) is a significant public health concern; it is a major cause of death and disability in the United States, and its occurrence is highest among multiple vulnerable populations, including the elderly, young adults, and military personnel [42]. No treatment

currently exists for the approximately 2 million cases of TBI sustained each year in the United States, and the costs of medical care for 2010 were estimated at \$76.5 billion annually [25].

TBI is caused by an initial external force, whether a physical object or inertia, contacting the head [80]. The impact and initial mechanical stress placed on the cells constitute the primary injury, whereas the secondary injury occurs after the inciting traumatic event, and involves multiple pathways and signaling cascades that can cause further damage [125,8,37]. Inflammation is a major component of the secondary injury. Inflammation is present in every case of TBI and may be a driving force for secondary pathology [37]. Chronic neuroinflammation following TBI was closely associated with neuronal death and impaired cell proliferation in locations both immediately adjacent to, and more distant from, the site of injury [3]. Many studies have shown that levels of inflammation and inflammatory molecules are strongly correlated with multiple measures of outcome in patients, including neurobehavioral impairments and survival rates [91,144]. Microglia are the brain's main form of immune response to infection, disease, and injury, as well as the source of inflammation. As such, inflammation and microglia have been recent concentrations of research as a means of developing therapies and improving outcomes of TBI.

Outcomes of TBI include possible changes in cognition, behavior, emotion, and sensory processing, all of which are influenced by injury severity and location [105,49,11]. Additionally, research has linked TBI to the risk of developing neurodegenerative diseases, including chronic traumatic encephalopathy and Alzheimer's disease (AD) [109]. The high level of heterogeneity in outcomes suggests a significant role for genetic influence on brain susceptibility and recovery [40,141]. The apolipoprotein E (*APOE*) gene has been frequently studied to determine its role in TBI and its isoform-dependent impact on outcome. The *APOE* ϵ 4 allele is the strongest genetic

risk factor for late onset AD, and is thought to confer worse outcome after TBI [6]. *APOEε4* carriers have been found to have slower recovery, increased risk of posttraumatic seizures, and worse memory performance after TBI [38,34,6]. However, multiple studies also show that *APOEε4* carriers did not differ from non-carriers in cognitive performance, functional outcomes or recovery after TBI [111,26]. The contradictory results so far emphasize the need for more research on APOE and TBI.

APOE is involved in several pathways after a TBI occurs, including inflammation [68]. Inheritance of the *APOEε4* allele is associated with increased inflammatory responses, including after TBI [86]. APOE4 may induce a more robust pro-inflammatory reaction from microglia and may suppress anti-inflammatory signaling [77,10,79,73]. This may be a result of decreased stability and faster catabolic degradation of APOE4, compared to the other isoforms, which is possibly due to its lower lipidation levels [68]. APOE is secreted as nonlipidated apolipoprotein, cholesterol and phospholipid efflux to lipid-poor APOE is mediated by ATP Binding Cassette Transporter A1 (ABCA1) [20]. *Abca1* deficiency results in decreased APOE lipidation and APOE levels [71,46]. ABCA1 may also play a role in modulating the inflammatory response in the brain. Mice lacking brain ABCA1 saw increased inflammatory gene expression, and the microglia cultured from these mice exhibited an increased pro-inflammatory response, as seen by higher levels of TNF α secretion and lower phagocytic activity, in response to lipopolysaccharide administration [65]. It is not known how *Abca1* haploinsufficiency may influence TBI.

We recently performed transcriptional profiling of APOE expressing mice after TBI using Next Generation Sequencing [24]. Using a network-based approach, we were able to identify distinct modules correlated to injury and APOE isoform, as well as a module driven by APOE isoform across TBI groups. The aim of this study was to examine the effect of *Abca1*

haploinsufficiency on gene expression induced by TBI in APOE targeted replacement mice using transcriptional profiling and a network-based approach. We used 3-month-old mice expressing human *APOE3*^{+/+} and *APOE4*^{+/+} isoforms (*E3/Abca1*^{+/+} and *E4/Abca1*^{+/+}, respectively), and compared them to their *Abca1* haploinsufficient counterparts (*E3/Abca1*^{+/-} and *E4/Abca1*^{+/-}, respectively), after performing a controlled cortical impact. Transcriptional profiling of hippocampal and cortical tissue from the injury site was performed using RNA-sequencing (RNA-seq). *E4/Abca1*^{+/-} mice had higher expression levels of the common up-regulated transcripts after TBI, which included genes related to the immune response and inflammatory response. We then examined how ABCA1 insufficiency impacted expression of the microglia sensome genes, and found that *E4/Abca1*^{+/-} TBI mice expressed these genes higher than *E4/Abca1*^{+/+} TBI mice, whereas no difference was found when comparing sham *Abca1*^{+/-} to *Abca1*^{+/+} mice of either isoform. There was no effect of *Abca1* haploinsufficiency on the expression of microglia genes in *APOE3* TBI mice. We were able to correlate the transcriptome to each phenotype using a network-based approach, Weighted Gene Co-expression Network Analysis (WGCNA). We found that the immune response module, although correlated positively to all TBI groups regardless of APOE isoform or *Abca1* copy number, consisted of genes expressed at higher levels in *E4/Abca1*^{+/-} TBI mice, and featured microglia-specific hub genes, including *Trem2*, *Tyrobp*, *Hexb*, and *Cd68*. Our results demonstrate an effect of ABCA1 deficiency on microglia gene expression after TBI in *APOE4* mice.

4.3 MATERIALS & METHODS

4.3.1 Animals

All animal experiments were approved through the University of Pittsburgh Institutional Animal Care and Use Committee and carried out in accordance with PHS policies on the use of animals in research. Human *APOE3*^{+/+} and *APOE4*^{+/+} targeted replacement mice (referred to as *E3/Abca1*^{+/+} and *E4/Abca1*^{+/+}) were bred to *Abca1*^{+/-} mice to generate *APOE3*^{+/+}/*Abca1*^{+/-} and *APOE4*^{+/+}/*Abca1*^{+/-} (referred to *E3/Abca1*^{+/-} and *E4/Abca1*^{+/-}, respectively) [23,46]. All mice were on the C57BL/6 genetic background and experimental groups consisted of both genders. Experimental mice were kept on a 12 h light-dark cycle with *ad libitum* access to food and water. At 3 months of age, these mice were randomly assigned to either sham or controlled cortical impact (CCI) experimental group. Mice were handled for 2 days (5 min per day) prior to surgical procedures. All materials were purchased through ThermoFisher Scientific, unless otherwise noted.

4.3.2 Traumatic Brain Injury

CCI model of brain injury was performed as previously described [24]. Anesthesia was induced using 5% isoflurane, after which it was maintained at 1.5% isoflurane. The head was secured using a stereotaxic frame, and core body temperature was held at 37°C using a heating pad. After shaving the heads, two separate iodine - alcohol washes were performed to sterilize the surgical site. A 50% mixture of bupivacaine and lidocaine was applied to the area and ophthalmic ointment was applied to the eyes. The scalp was opened with a midline incision exposing the

dorsal aspect of the skull and the skull leveled. A 4.5 mm diameter craniotomy was performed over the left parietal cortex using a dental drill. Once the bone flap was removed, mice in the CCI group received a single impact at 1.0 mm depth with a 3.0 mm diameter metal tip onto the cortex (3 m/s, 100 ms dwell time; Impact One, Leica). Sham mice received identical anesthesia and craniotomy, but did not receive impact and are considered negative controls. Following the impact, the surgical site was sutured, triple antibiotic cream applied, Buprenex (0.1 mg/kg; IP) provided for analgesia, and sterile saline administered for rehydration. Mice were allowed to recover on heating pad, until freely mobile, before returning to their home cage.

4.3.3 Tissue Processing

Fourteen days post-injury, mice were anesthetized using Avertin (250 mg/kg of body weight, i.p.) and perfused transcardially with 20mL of cold 0.1M PBS pH 7.4 [95,24]. Brains were rapidly removed and a 1.5 mm coronal section of the brain, including the injury site, taken by slicing the brain at -2.5 mm and -4.0 mm from bregma. Within the coronal slice, the hemispheres were separated, and the subcortical tissue was dissected out; hippocampal and cortical tissue were snap-frozen together for RNA isolation and RNA-seq.

4.3.4 RNA Isolation and RNA Sequencing

All procedures were performed as before [96,24]. CCI and sham mice consisting of both genders for each genotype were used for RNA-seq. RNA was isolated from frozen cortices and hippocampi at the injury site and purified using RNeasy kit (Qiagen) according to the manufacturer recommendations. Quality control of all RNA samples was performed on a 2100

Bioanalyzer instrument (Agilent Technologies) and samples with RIN > 8 were further used for library construction using RNA Library Prep Reagent Set (Illumina). Libraries for Next Generation Sequencing were generated by PCR enrichment including incorporation of barcodes to enable multiplexing. Sequencing was performed by the Next Generation Sequencing Center (University of Pennsylvania, <https://ngsc.med.upenn.edu/>) on HiSeq 2500 machine. Following initial processing and quality control, the sequencing datasets were further analyzed for differential gene expression, which in all cases was calculated using Subread/featureCounts (v1.5.0; <https://sourceforge.net/projects/subread/files/subread-1.5.0/>) for read alignment and summarization and statistical package edgeR (v3.14.0; <https://bioconductor.org/packages/release/bioc/html/edgeR.html>). Lists of differentially expressed genes are further analyzed as described in the following section.

4.3.5 Weighted Gene Co-expression Network Analysis (WGCNA)

Network analysis was performed using WGCNA (v.1.51; <https://cran.r-project.org/web/packages/WGCNA/index.html>) [149,97]. Libraries are clustered by gene expression enabling the detection of outliers and the power is determined by scale free topology model. Modules were generated automatically using a soft thresholding power, $\beta=10$, a minimum module size of 18 genes and a minimum module merge cut height of 0.25. Modules were named by conventional color scheme and then correlated with trait data using Pearson's correlation (APOE isoform, Injury, *Abca1* copy number). Statistical significance was determined by student's *t*-test, $p<0.05$. All modules were summarized by module eigengenes (ME), the first principle component of each module that was calculated as a synthetic gene representing the expression profile of all genes within a given module.

Representative networks were built using hub genes and the transcripts connected to them. Hub genes were identified using cutoffs of their interconnectivity within the module (module membership, >0.8), and the correlation between expression level and trait (gene significance, >0.2). Once the hub genes are selected, the connections to other transcripts are sorted by weight, with the first 150 connections used for visualization. Gene-association networks of interest were visualized using Cytoscape (v3.3.0). Unsupervised hierarchical clustering was performed on ME turquoise using pheatmap (v1.0.10; <https://cran.r-project.org/web/packages/pheatmap/index.html>) to identify 2 sub-modules. A representative network was built for each sub-module consisting of only genes within the sub-module.

4.3.6 Functional Pathway Analysis

Functional annotation clustering was performed using the Database for Annotation, Visualization and Integrated Discovery (DAVID v6.8, <https://david.ncifcrf.gov>) [78].

4.4 RESULTS

4.4.1 TBI induces changes to the transcriptome that are common among both *Abca1*^{+/-} and *Abca1*^{+/+} mice expressing human APOE isoforms

To examine the effect of TBI on gene expression in the brains of *Abca1*^{+/-} and *Abca1*^{+/+} mice expressing human APOE isoforms (E3/*Abca1*^{+/-}, E4/*Abca1*^{+/-}, E3/*Abca1*^{+/+}, E4/*Abca1*^{+/+}), we collected hippocampal and cortical tissue from the injury site at 14 days post-injury. Total RNA

was isolated from these tissues and used for RNA-sequencing. As shown in Fig. 15A-D, TBI significantly affected the transcriptome within each genotype. We highlighted several genes of interest on the scatterplots increased by TBI, and while they were differentially expressed within all the groups, the group with the highest CPM values was the E4/Abca1^{+/-} TBI mice. To determine what similarities existed among the affected biological processes, we examined the differentially expressed genes that were significant and common among the 4 genotypes. The expression levels of the top 100 up- and down-regulated genes are shown in the heatmap (Fig. 15E). Although the genes are common, the E4/Abca1^{+/-} mice show the highest expression levels of the upregulated genes. Fig. 15F shows the biological processes associated with the common, upregulated genes. There were 1,196 up-regulated genes common to all the groups and the top Gene Ontology (GO) terms derived from these genes were “immune system process”, “innate immune response”, and “inflammatory response”. In comparison, Fig. 15G shows the biological processes associated with the common, downregulated genes. There were 579 downregulated genes common to the groups, and these genes were functionally associated with “regulation of ion transmembrane transport”, and “potassium ion transport”.

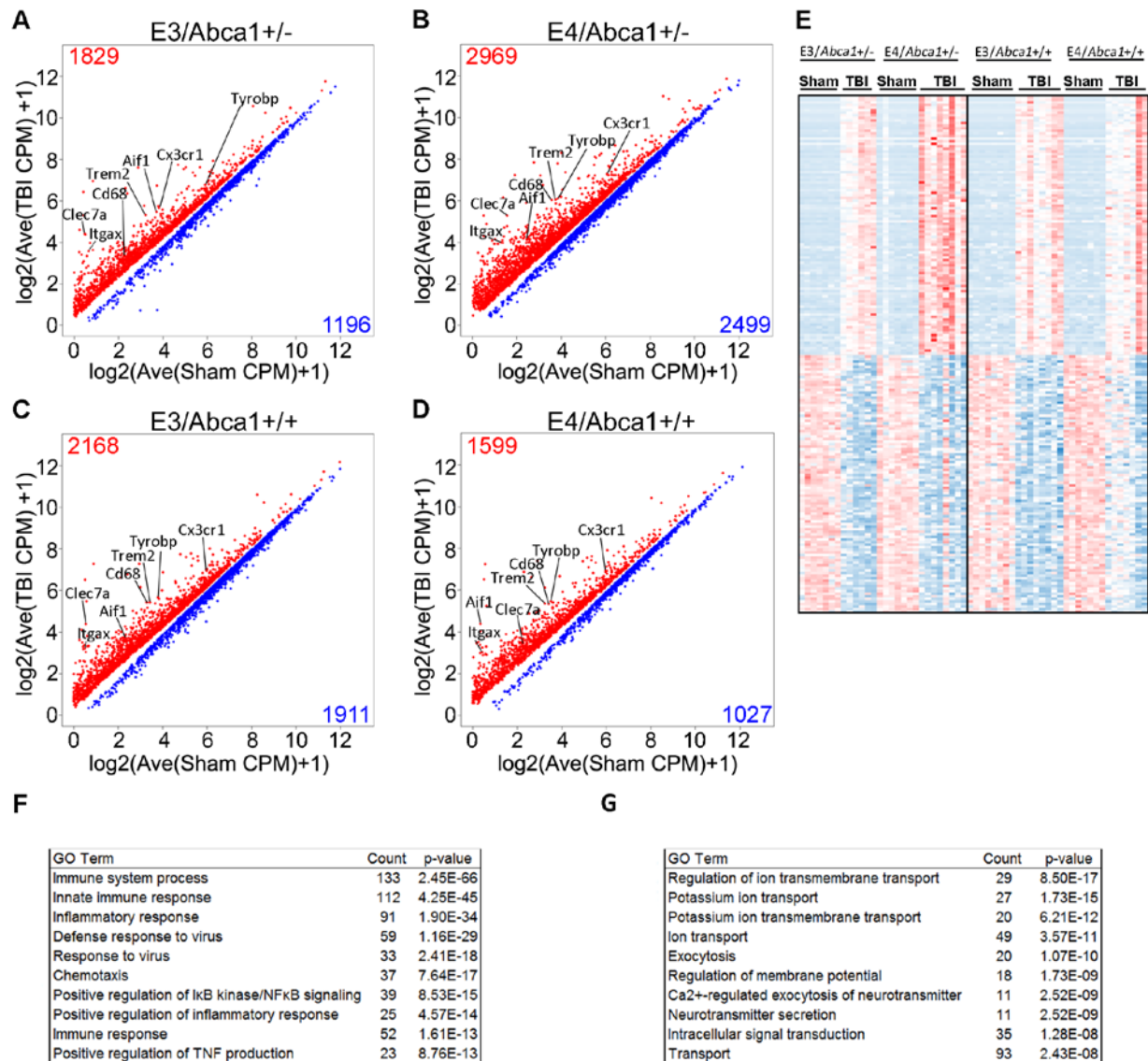


Figure 15. TBI increases the expression of genes associated with immune response, and decreases the expression of genes connected to ion transmembrane transport.

RNA was isolated from the hippocampal and cortical tissues collected 14 days after injury from *Abca1*^{+/-} and *Abca1*^{+/+} mice of both *APOE* isoforms and was then used to perform RNA-seq, N=6-8 mice per group of both genders. (A-D) Scatter plots represent the RNA-seq results for differentially expressed genes. EdgeR analysis between sham and injured mice identified significant affected transcripts in (A) *APOE3/Abca1*^{+/-}, (B) *APOE4/Abca1*^{+/-}, (C) *APOE3/Abca1*^{+/+} and (D) *APOE4/Abca1*^{+/+} mice. Red denotes up-regulated, and blue denotes down-regulated genes, *p*<0.05. (E) Heatmap of the top 100 upregulated and downregulated genes by TBI is shown. (F) A table shows the top annotated GO terms derived from the common, upregulated genes (total = 1,215 genes). (G) A table shows the top annotated GO terms derived from the common, downregulated genes (total = 531 genes).

4.4.2 TBI significantly alters the expression of transcripts unique to each genotype, with the highest proportion of unique transcripts among *E4/Abca1*^{+/-} mice

We were interested in whether the response to TBI was specifically influenced by each genotype, particularly by *Abca1* haplodeficiency in conjunction with *APOE4* isoform. To do this, we determined the proportion of genes that were differentially expressed, either in common among several of the groups or were uniquely expressed in only one group. These proportions are shown for each genotype in the donut plots in Fig. 16. As seen in Fig. 16A, *E4/Abca1*^{+/-} mice have a higher proportion of unique transcripts (26%) that are up-regulated by TBI than the other genotypes (*E3/Abca1*^{+/-}: 5.5%; *E3/Abca1*^{+/+}: 10%; *E4/Abca1*^{+/+}: 5.0%). The biological processes derived from the unique genes of the *E4/Abca1*^{+/-} mice, include “positive regulation of neuroblast differentiation” and “positive regulation of apoptotic process”. The biological functions associated with the unique, upregulated genes within each group differ greatly; the other top terms include “determination of left/right symmetry”, “negative regulation of cell proliferation”, and “inner dynein arm assembly” for *E3/Abca1*^{+/-}, *E3/Abca1*^{+/+}, *E4/Abca1*^{+/+} respectively. Expression plots show the distinct upregulation in *E4/Abca1*^{+/-} TBI mice of several genes, including *Plekho1*, which has been shown to promote apoptosis (Fig. 16C) [148].

E4/Abca1^{+/-} mice, again, have a higher proportion of unique, significant down-regulated transcripts (30%) than the other genotypes (*E3/Abca1*^{+/-}: 10%; *E3/Abca1*^{+/+}: 13%; *E4/Abca1*^{+/+}: 9.4%) (Fig. 16B). The top GO terms derived from the unique down-regulated genes for each group are “transcription, DNA-templated”, “covalent chromatin modification”, “GPI anchor biosynthetic process”, and “Protein K63-linked ubiquitination” for *E3/Abca1*^{+/-}, *E4/Abca1*^{+/-}, *E3/Abca1*^{+/+}, *E4/Abca1*^{+/+}, respectively.

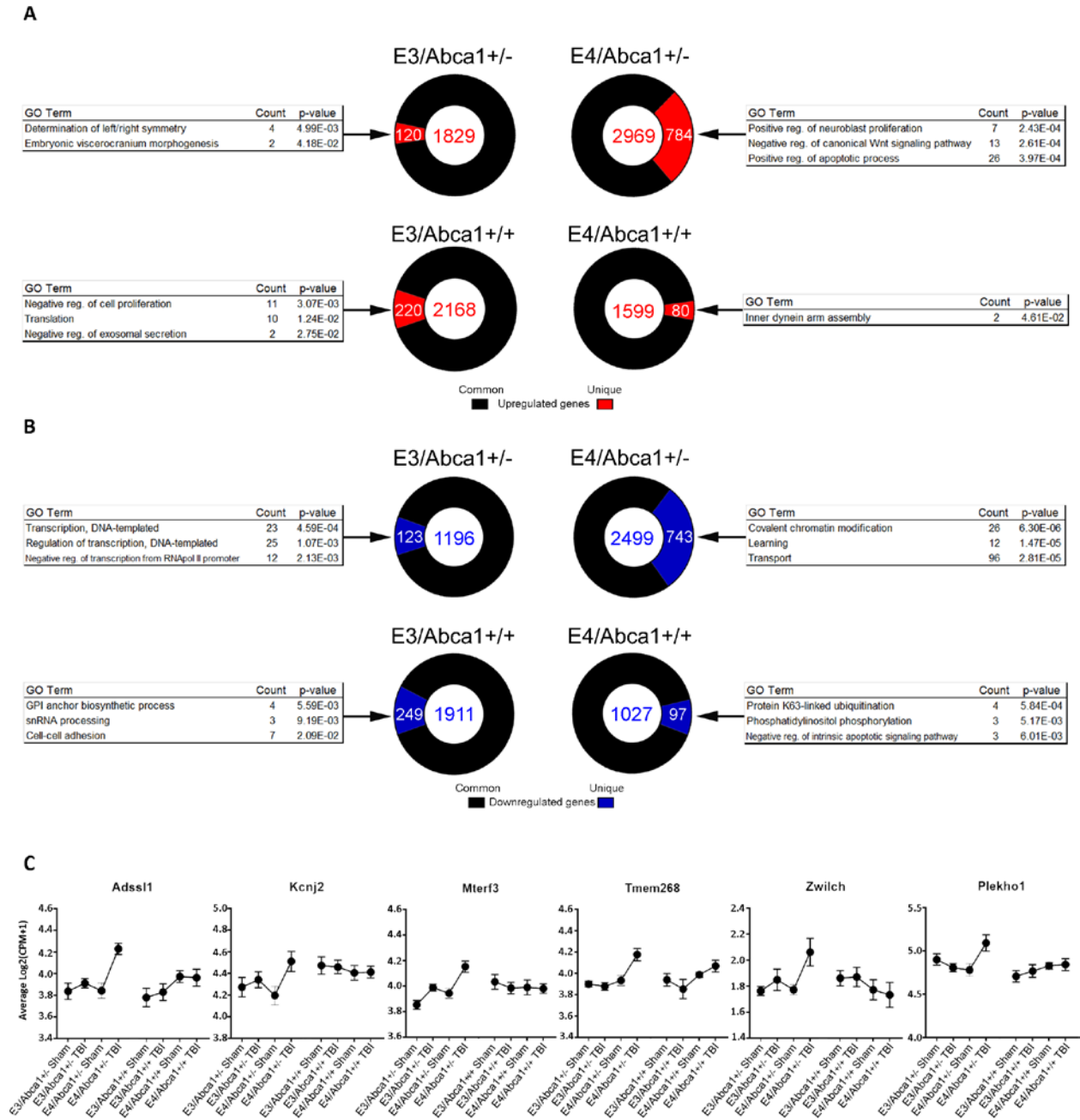


Figure 16. TBI affects a greater proportion of unique genes in E4/Abca1^{+/-} mice.

(A-B) Donut plots for each genotype indicate the proportion of significantly (A) up- or (B) down-regulated genes that are either expressed in common among 2 or more groups (black), or unique to that group (A: red and B: blue). The total number of genes are shown within the center of the plot for each genotype. The top 3 GO terms for the unique genes in each genotype are shown to either side. (C) Expression plots for unique transcripts upregulated in E4/Abca1^{+/-} mice are shown.

4.4.3 *Abca1* haploinsufficiency upregulates microglia sensome genes in injured APOE4 mice

To determine if there was any effect of *Abca1* haploinsufficiency on gene expression changes induced by injury, we examined the expression of microglial sensome genes. Although a clear effect of TBI is present in the differential expression of the microglia sensome by *Abca1* genotype, the heatmap also shows that *E4/Abca1*^{+/-} TBI mice have higher expression levels of microglial sensome genes than the other groups (Fig. 17A). In contrast, there is no effect of *Abca1* copy number on synaptic transmission genes (Fig. 17B), although an injury effect on expression is still visible. We examined the expression levels of the microglia sensome genes within each *APOE* isoform, separated by injury status, for the effect of *Abca1* genotype. Sham mice in both *APOE* isoforms (Fig. 17C-D) and injured *APOE3* mice (Fig. 17E) have no significant changes in microglia sensome gene expression due to *Abca1* haploinsufficiency. In comparison, the injured *E4/Abca1*^{+/-} mice demonstrate significant expression of the microglia sensome compared to *E4/Abca1*^{+/+} TBI mice (Fig. 17F). In conclusion, these results demonstrate an effect of *Abca1* haploinsufficiency on the microglia sensome in *APOE4* mice after TBI.

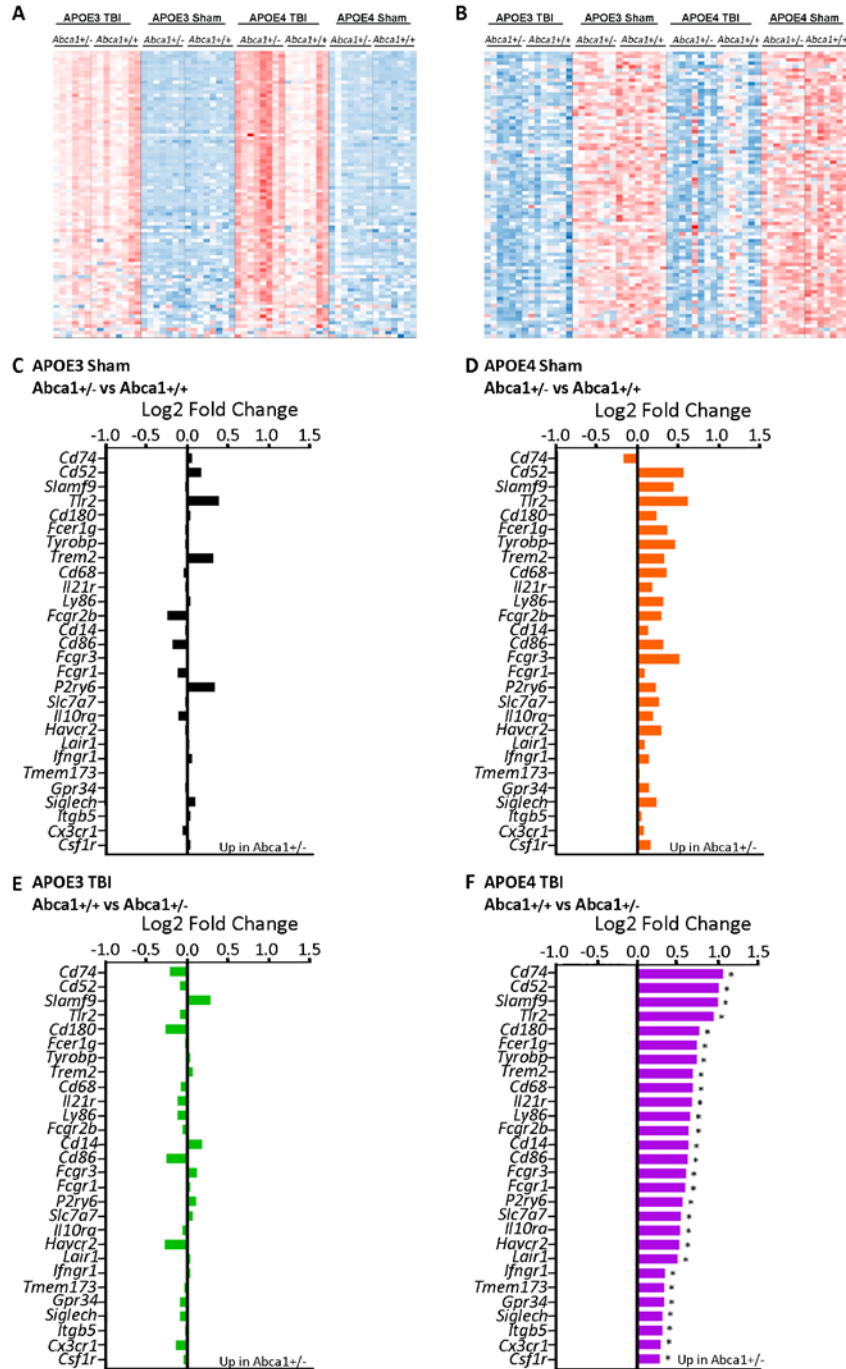


Figure 17. Abca1 deficiency affects the microglial response to TBI in an APOE isoform-dependent manner. (A-B) Heatmaps were generated using normalized *Abca1*^{+/-} versus *Abca1*^{+/-} CPM values for each group for (A) microglia sensome genes and (B) synaptic transmission genes. Red denotes higher expression values, and blue denotes lower expression values. n=6-8 per group, including both males and females. (C, E) Selected genes from the microglia sensome of *APOE3/Abca1*^{+/-} and *APOE3/Abca1*^{+/-} mice are compared separately for (C) sham (black bars) and (E) TBI groups (green bars). Shown are the Log2-fold change values for each gene. (D, F) Selected genes from the microglia sensome of *APOE4/Abca1*^{+/-} and *APOE4/Abca1*^{+/-} mice are compared separately for (D) sham (orange bars) and TBI groups (purple bars). Shown are the Log2-fold change values. *: *p*<0.05.

4.4.4 WGCNA reveals interconnected gene clusters associated with each trait of interest- *APOE* isoform, *Abca1* copy number, and injury status

To identify interconnected gene clusters, or modules, associated within each trait of interest, we employed WGCNA. We were interested in the modules that were differentially expressed across our traits of interest - injury status, *APOE* isoform and *Abca1* copy number. The relationship table (Fig. 18A) shows the MEs of interest and the corresponding correlation coefficients per group.

ME tan (module size=182 genes) correlated across the groups depending on *APOE* isoform, regardless of either injury status, or *Abca1* copy number. It positively correlated to *APOE4* groups and negatively with *APOE3* groups. As seen in the module heatmap (Fig. 18A; far right), the gene members are generally increased in *APOE4* mice and decreased in *APOE3* mice. The GO terms associated with the module genes were “tRNA aminoacylation for translation”, “RNA processing”, and “translation”. We built a representative network using the hub genes associated with “tRNA aminoacylation for translation”, such as *Yars*, *Gars*, and *Nars*, which are aminoacyl-tRNA synthetases.

ME pink correlated with injury status, however, it negatively correlated to TBI groups and positively correlated with sham groups. The biological processes associated with ME pink (module size=518 genes) included “synaptic vesicle docking”, “long-term synaptic potentiation”, and “chemical synaptic transmission”, which suggests that injury decreases synaptic transmission. The representative network (Fig. 18C) was built around several hub genes related with synaptic transmission, including *Stx1a*, *Snap25*, and *Lamp5*, which are all associated with synaptic vesicle docking and neurotransmitter release. *Lamp5*, in particular, is associated with

GABAergic synaptic transmission and short-term synaptic plasticity [129]. Another hub gene is *Prkcz*, which is necessary for long-term potentiation in hippocampal CA1 pyramidal cells [135].

ME grey60 correlated with *Abca1* copy number, specifically, it negatively correlated with *Abca1*^{+/-} mice and positively correlated with *Abca1*^{+/+} mice, regardless of injury or *APOE* isoform. As seen in Fig. 18D, the network was built around hub genes, which represented GO terms “oxidation-reduction process”, “transport”, and “aging”. These hub genes included a number of the NADH hydrogenase subunits, such as *ND1*, *ND2*, *ND4*, *ND5* and *ND6*. Other hub genes were *COX1*, *Atp5j2*, and *CYTB*. All of these hub genes are involved in the mitochondrial respiratory chain [146].

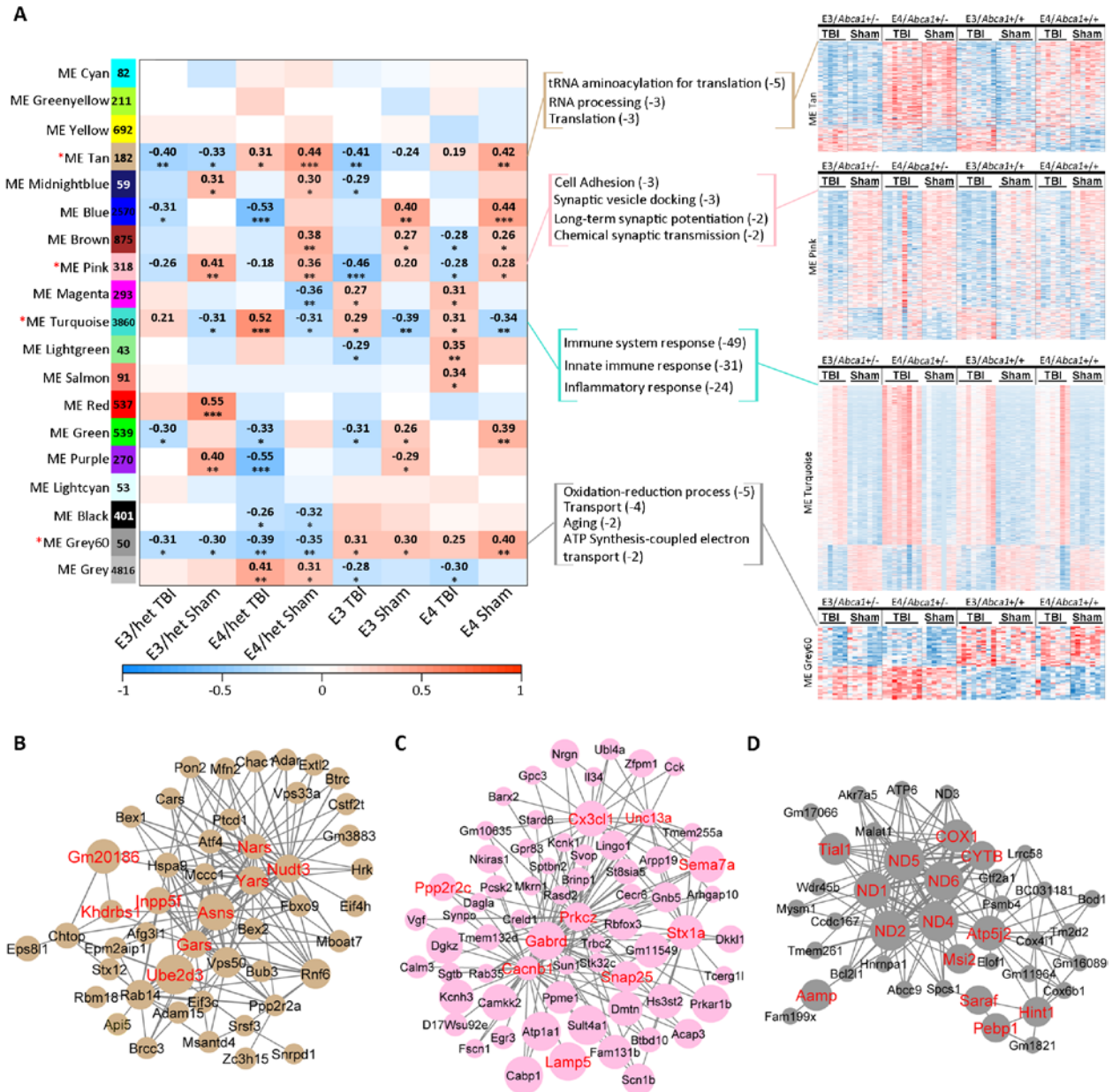


Figure 18. WGCNA identified modules correlated to TBI and *Abca1* haploinsufficiency.

WGCNA was used to determine the correlation of module eigengenes to Injury and *Abca1* genotype. (A) The relationship tables shows the correlation between the module eigengene (rows) and group (columns) with p-value. Red denotes a positive, and blue is a negative correlation. Modules of interest are differentially expressed between trait conditions. MEs turquoise and pink correlated with TBI in opposite directions, ME tan correlated with *APOE* isoform, and ME grey60 with *Abca1* genotype. Top assigned GO terms and their log₁₀ of the p-values are shown to the right of the table, aside heatmaps of the genes within each module, for each animal. Red denotes higher expression values, and blue denotes lower expression values. (B-D) Representative networks for (B) ME tan, (C) ME pink, and (D) ME grey60 were built using module hub genes. Hub genes are identified in red font. Size of the nodes represents the module membership value and width of edge, the interaction between genes shown as connecting lines, represents the weight of the connection.

ME turquoise strongly correlated with injury status, however, unlike ME pink, it correlated positively to TBI groups and negatively to sham groups. The genes within ME turquoise are strongly connected and related to the module biological process, as seen in the module membership and gene significance scatterplot (Fig. 19A). Due to the size (module size = 3860 genes), we were interested in further separating the module. To do this, we ran a heatmap function on the genes within the module, which aggregates the genes using hierarchical clustering. As shown in Fig. 19B, the heatmap separated the module into 2 distinct clusters based on injury status and direction of expression. Additionally, the heatmap shows the expression for all the genes in ME turquoise and the eigengene expression for each sample. The first cluster, Cluster 1, (size = 2605 genes) consisted of genes upregulated in TBI groups and downregulated in sham groups. The heatmap suggests a stronger response of the cluster 1 genes within the *E4/Abca1*^{+/-} mice, which is consistent with the correlation of ME turquoise to this group in the relationship table. The GO terms derived from Cluster 1 were “immune system response”, “innate immune response”, and “inflammatory response”. Additionally, among the top 10 GO terms was “lipid metabolic process”. The representative network (Fig. 19C) was built around hub genes associated with immune response, such as *Clec7a*, *Clqc*, and microglia-specific genes, *Trem2*, *Tyrobp*, *Hexb*, and *Cd68*.

The second cluster, Cluster 2, (size = 1111 genes) featured genes downregulated in the TBI mice, upregulated in the sham mice. Functionally, this cluster is enriched in genes connected to the GO term “transport”, other transport-associated terms, such as “vesicle-mediated transport”, but also GO terms “sterol biosynthetic process” and “cholesterol biosynthetic process”. The network (Fig. 18D) built for Cluster 2 excluded any genes from Cluster 1, and functionally represents transport, however, while hub genes, *Gabrb2*, *Gabrg2*, and *Atp1b1* all

relate directly to the transport of ions across the membrane, through this mechanism, these genes are also strongly associated with synaptic transmission. In conclusion, ME turquoise strongly correlated to injury status, but hierarchical clustering of the genes revealed two distinct clusters associated with the gene expression direction. Cluster 1 was larger and featured genes related to immune response and was more strongly upregulated in *E4/Abca1^{+/-}* mice, while cluster 2 featured genes downregulated in TBI groups and represented transport, but functionally are also involved in synaptic transmission.

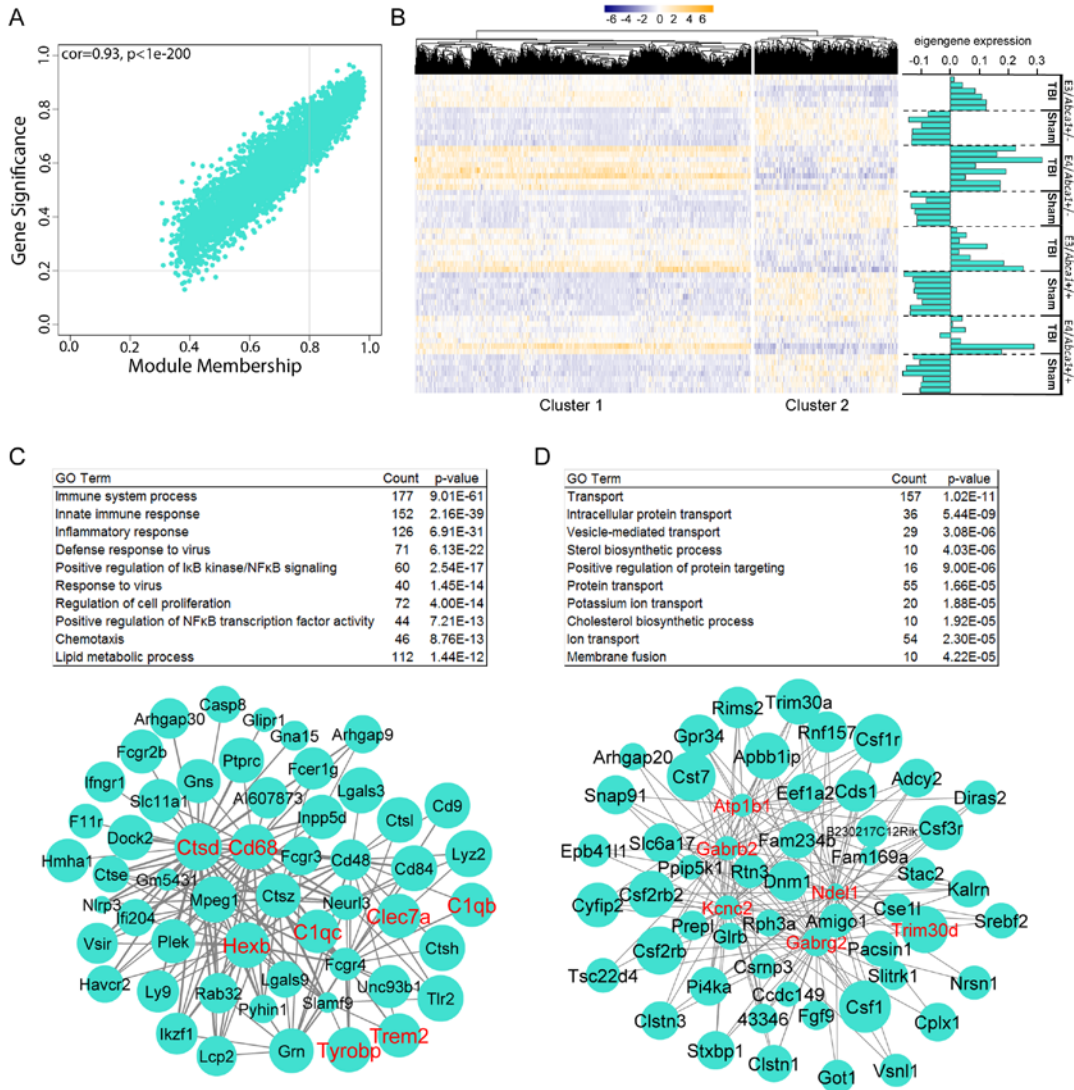


Figure 19. ME turquoise consists of two sub-modules correlated to injury status.

(A) Scatter plot for ME turquoise module showing the correlation between module membership and gene significance. The degree of association between MM and GS was evaluated by Pearson correlation. Correlation value and p value are indicated in the plot. (B) The heatmap shows normalized gene expression values beside module eigengene expression values for each sample for ME turquoise. The heatmap function aggregated the module into 2 sub-modules (Cluster 1 and Cluster 2) by hierarchical clustering. (C-D) Tables of top assigned GO terms are shown above representative networks for (C) cluster 1 and (D) cluster 2. Hub genes are identified in red font. Size of the nodes represents the module membership value and width of the edge represents the weight of the connection.

4.5 DISCUSSION

We examined the impact of *Abca1* deficiency and *APOE* isoform expression on the response to traumatic brain injury. Our goal was to identify differences in the transcriptional response and trait-associated genome-wide correlated gene networks between *Abca1*^{+/+} and *Abca1*^{+/-} mice following a controlled cortical impact in human *APOE3*^{+/+} and *APOE4*^{+/+} targeted replacement mice. We found that the four groups within our study -*E3/Abca1*^{+/-}, *E4/Abca1*^{+/-}, *E3/Abca1*^{+/+}, and *E4/Abca1*^{+/+} - had common and distinct responses to TBI. *E4/Abca1*^{+/-} mice had the highest proportion of unique transcripts affected by TBI, suggesting that *E4/Abca1*^{+/-} mice are more disposed to changes in gene expression by TBI than the other groups, and demonstrate possible pathways that could be associated with worsened outcome, such as downregulated genes associated with learning. The common, up-regulated genes were associated with biological processes related to immune response, innate immune response and inflammatory response. While, these genes were common among the four groups, the *E4/Abca1*^{+/-} mice had higher expression levels of the genes upregulated by TBI compared to the other groups, suggesting a role for *APOE* isoform and ABCA1 in the expression of inflammatory genes after TBI. Consequently, we examined the effect of *Abca1* insufficiency on microglia sensome genes by injury status and *APOE* isoform. When comparing injured *Abca1*^{+/-} to *Abca1*^{+/+} mice, we found *E4/Abca1*^{+/-} TBI mice had increased expression of the microglia sensome genes. In contrast, there was no effect of *Abca1* copy number in *APOE3* mice, sham or TBI. These results suggest that *Abca1* haploinsufficiency may influence the inflammatory response following TBI, particularly through an impact on microglia and their gene expression. This effect is seen only among *APOE4* mice, not *APOE3* mice; this response may be related to the isoform-specific effect on inflammation. Additionally, the *APOE4* isoform may be more vulnerable to the

consequences of *Abca1* haploinsufficiency due to a gene-gene interaction, a result also demonstrated by data from AD-model mice [46]. These results suggest a possible mechanism for worse outcome after TBI associated with *APOE4* isoform.

Using WGCNA, we identified modules associated with each trait – injury, *APOE* isoform and *Abca1* copy number. ME tan was associated with *APOE* isoform; the module positively correlated with *APOE4* mice and negatively correlated with *APOE3* mice, regardless of *Abca1* copy number or injury status. The representative network was associated with the GO term “tRNA aminoacylation for translation”, and included hub genes *Yars*, *Gars*, and *Nars*, which are aminoacyl-tRNA synthetases. Mutations in these genes are associated with Charcot-Marie-Tooth disease, one of the most commonly inherited neurological disorders [16]. Additionally, a metabolomics study on AD patient CSF and plasma found that a pathway significantly affected in plasma by AD severity was aminoacyl-tRNA biosynthesis, however, the mechanisms associated with altered aminoacyl-tRNA synthetases and AD remain unknown [130].

The “synaptic transmission” module, ME pink was significantly correlated and down-regulated by injury across the groups. The network represented GO terms “synaptic vesicle docking”, “long-term synaptic potentiation”, and “chemical synaptic transmission”. The hub genes featured in the representative network, included *Stx1a*, *Snap25*, and *Lamp5*, which are all associated with synaptic vesicle docking and neurotransmitter release. *Lamp5* localizes in the synapse, where it may play a regulatory role in GABAergic synaptic transmission [129]. Another hub gene in this network, *Prkcz*, has an important role in hippocampal long term potentiation and learning [135]. Its expression mediates the storage of specific forms of long term memory [124]. The negative association between this network and injury is consistent with the impact that TBI is known to have on memory.

The network representing ME grey60 was associated with “oxidation-reduction process” and “aging”. This module was differentially expressed dependent on *Abca1* copy number; the module was downregulated in *Abca1*^{+/-} mice, and upregulated in *Abca1*^{+/+} mice. The network was built around hub genes involved in the mitochondrial respiratory chain, including a number of the NADH hydrogenase subunits, such as *ND1*, *ND2*, *ND4*, *ND5* and *ND6*, as well as, *COX1*, *Atp5j2*, and *CYTB*. Mitochondrial dysfunction and dysfunctional energy metabolism are early pathological features of multiple neurological diseases, including Alzheimer’s disease, Parkinson’s disease and Huntington’s disease [146,104]. Perturbations in the mitochondrial respiratory chain results in decreased ATP synthesis, the generation of free radicals and oxidative damage resulting in neuronal dysfunction and apoptosis [93]. HDL and HDL-associated lipids play key roles in the regulation and preservation of mitochondrial function [140]. ABCA1 is an essential mediator of HDL formation, which may explain the negative correlation between *Abca1*^{+/-} mice and this network.

ME turquoise correlated with the groups by injury status, however, the module separated into distinct gene clusters representing unique biological processes. Using the heatmap function, we were able to separate ME turquoise into 2 sub-modules by hierarchical clustering. The clusters were separated based on injury status and the direction of gene expression. The first cluster was larger and consisted of genes upregulated by injury. This cluster represented the “immune response” and the network was built from several microglia-specific genes including *Trem2*, *Tyrobp*, *Hexb*, and *Cd68*. Although there was no specific modulatory effect of *APOE* isoform or *Abca1* copy number on the module, the expression of the module genes was much higher in *E4/Abca1*^{+/-} injured mice, which is consistent with our other results.

ABCA1 is a major regulator of cholesterol transport and an essential mediator of high density lipoprotein generation [70]. ABCA1 may have a crucial role in the response to TBI by providing essential cholesterol and phospholipids required for repair. However, ABCA1 may also influence the TBI response through its modulatory effects on the inflammatory response. Mice lacking brain ABCA1 exhibit increased neuroinflammation, and in particular have an increased microglial pro-inflammatory response [65]. The effect of ABCA1 on inflammation could also occur through its functional role in mediating cholesterol efflux onto lipid-poor apolipoprotein, including APOE. It was previously shown that the loss of ABCA1 function results in a reduction of APOE, and data from experimental animals show that *Abca1* deficiency abolishes the lipidation of APOE [71]. The isoform-dependent effect of APOE is possibly driven by lipidation status, which has been shown to affect its stability and degradation rate. Our study shows that ABCA1 haploinsufficiency increased expression of the microglia sensome genes in an APOE isoform dependent manner, which suggests gene-gene interactions as a possible mechanism for worsened outcomes after TBI in *APOEε4* carriers.

4.6 CONCLUSIONS

Our results suggest a possible role for *Abca1* haploinsufficiency on the response to TBI in *APOE4* TBI mice at a transcriptional level. When we compared *Abca1*^{+/+} mice to *Abca1*^{+/-} mice by injury status and isoform, we found that the lack of one copy of *Abca1* significantly increased the expression of microglia sensome genes only in *APOE4* TBI mice. This was consistent with the higher expression of the common, upregulated genes, which were associated with immune response. Furthermore, *E4/Abca1*^{+/-} showed the highest expression of the immune response gene

network, which also included microglia-specific hub genes, *Trem2*, *Tyrobp*, *Hexb*, and *Cd68*. Our results suggest that gene-gene interactions can modify the response of *APOE4* mice to harmful effects.

5.0 FINAL CONCLUSIONS

5.1 GENERAL SUMMARY

Our original hypothesis was that there was an isoform-specific response to TBI, specifically that mice expressing human APOE4 would have worsened outcomes and would be modulated by *Abca1* deficiency. We addressed this hypothesis through two separate aims. In the first aim (Chapter 3), we examined the role of human APOE isoforms in the response to TBI [24]. We examined cognitive performance, brain transcriptome and genome-wide correlated gene networks in 3-month old APOE-TR mice. We found that TBI significantly worsened anxiety and spatial learning, as seen through the elevated plus maze and Morris Water Maze tests, however there was no interaction with APOE isoform. TBI significantly impacted the transcriptome, particularly increasing genes related to the immune response, including *Trem2*, *Tyrobp*, *Cd68*, and *Cx3cr1*. We examined what cell type was responsible for the inflammatory response in the brain at 14 days post-injury by comparing expression of microglia sensome genes to those of peripheral macrophages, and determined that resident microglia are the predominant source of the inflammatory response in the brain at this time point. Overall, the effect of TBI on the transcriptome was similar between the genotypes, with similar biological processes affected. Although there was an APOE isoform effect on the brain transcriptome in TBI mice, this effect was entirely separate from the effect of injury.

Using WGCNA, we identified correlated gene networks associated with each trait, injury and genotype. The results largely confirmed the GO terms identified through pathway analysis. The gene network that correlated most with TBI represented the immune response, and importantly, there was no isoform-specific modulatory effect on this network. We did identify one network that was differentially affected by APOE isoform within only the injury groups. This network represented the biological process “myelination” and featured several myelin related proteins, included *Mbp* and *Plp*. Additionally, the network was also highly enriched in oligodendrocyte specific markers. While myelin and cholesterol would both be necessary components for axonal repair and regeneration, several myelin related proteins have been associated with the formation of a glial scar and inhibited axonal outgrowth [119,120,145]. The positive correlation of this network with APOE4 injured mice could provide a potential mechanism for worse outcome after TBI that is temporally dependent.

In the second aim (Chapter 4), we compared mice expressing human APOE isoforms to their *Abca1* haplodeficient counterparts. We examined differences in the transcriptional response to injury between *Abca1*^{+/+} and *Abca1*^{+/-} mice following a controlled cortical impact in human APOE3^{+/+} and APOE4^{+/+} targeted replacement mice. Our results suggested a role for *Abca1* haploinsufficiency on the transcriptional response to TBI in APOE4 mice. E4/*Abca1*^{+/-} mice had the highest proportion of unique transcripts affected by TBI than the other groups, suggesting that these mice are more vulnerable to changes in gene expression induced by TBI and identifying possible pathways associated with worsened outcome, such as the downregulated GO term “learning”. The common, upregulated genes were associated with immune response, and inflammatory response, however, several of these genes were expressed at higher levels in E4/*Abca1*^{+/-} TBI mice. As a result, we examined whether ABCA1 insufficiency influenced the

expression of microglia sensome genes in either isoform. When comparing *Abca1*^{+/+} and *Abca1*^{+/-} mice by injury status and isoform, we found that *Abca1* haplodeficiency significantly increased the expression of microglia sensome genes in APOE4 TBI mice, but not in APOE3 TBI mice, nor either sham group. Our results suggested a possibly mechanism for worsened outcomes after TBI in *APOEε4* carriers.

In both studies, the immune response and inflammatory response were strongly upregulated after TBI. These processes were the most significant as determined by functional pathway analysis and the associated modules were also the most strongly correlated to injury status. In both studies, the “immune response” module featured microglia-specific genes as the hub genes, including *Trem2*, *Tyrobp*, *Cd68*, and *Hexb*. Although there was no isoform-specific effect on these genes in the first study, which was also validated by immunohistochemistry for TREM2 and IBA1, our second study demonstrated a significant effect of *Abca1* deficiency on the expression of microglia sensome genes in APOE4 mice. Our results confirm the significant role of microglia and inflammation after TBI, and future research is needed to analyze the role of ABCA1 in modulating the inflammatory response in APOE isoforms.

5.1.1 Strengths and Limitations

To our knowledge, we are the first to perform transcriptional profiling of APOE expressing mice using Next Generation Sequencing. We are also the first to examine the effect of *Abca1* haplodeficiency on the gene expression induced by TBI in APOE-TR mice. Additionally, using WGCNA, we were able to correlate gene networks to each phenotype, identifying genes, and thus their proteins, with a potential to become useful and rational targets for future research and drug discovery relevant to TBI.

One limitation of our studies is the lack of multiple time-points. TBI patients commonly develop symptoms months, and even years, after the injury occurred. While the differential effects of the APOE-ABCA1 interaction may occur at early stages of brain injury, characterization of both short- and long-term consequences is likely necessary to design and implement therapeutic strategies. Our studies featured only a single time-point and it is acute. At an entirely different time-point, these mice could demonstrate different cognitive outcomes, and transcriptional profiles. Having multiple time-points would allow for a more complete characterization of the impact of APOE isoform and *Abca1* deficiency on TBI outcomes.

More research is needed to fully determine the role of APOE, and in particular, its regulation by ABCA1, on TBI outcomes. The pathophysiological heterogeneity of TBI is due to a wide array of factors, including injury location, and severity, as well as individual characteristics, such as age, gender, health and genetics. Animal models of TBI are designed to produce a homogenous injury, with all other factors well controlled. As such, the animal models of TBI do not recapitulate all aspects of brain pathology as a response to brain trauma. Moreover the lack of standardized study design and data collection makes it extraordinarily difficult to compare the results of the studies performed so far and to draw definitive conclusions. Our results suggest a complex relationship between APOE isoform and TBI that is potentially modulated by ABCA1, however, further research is necessary to fully characterize this relationship.

BIBLIOGRAPHY

1. Abraham CR (2001) Reactive astrocytes and alpha1-antichymotrypsin in Alzheimer's disease. *Neurobiol Aging* 22:931-936
2. Acosta SA, Tajiri N, Shinozuka K, Ishikawa H, Grimmig B, Diamond DM, Diamond D, Sanberg PR, Bickford PC, Kaneko Y, Borlongan CV (2013) Long-term upregulation of inflammation and suppression of cell proliferation in the brain of adult rats exposed to traumatic brain injury using the controlled cortical impact model. *PLoS one* 8:e53376-e53376
3. Acosta SA, Tajiri N, Shinozuka K, Ishikawa H, Grimmig B, Diamond DM, Sanberg PR, Bickford PC, Kaneko Y, Borlongan CV (2013) Long-term upregulation of inflammation and suppression of cell proliferation in the brain of adult rats exposed to traumatic brain injury using the controlled cortical impact model. *PLoS One* 8:e53376. doi:10.1371/journal.pone.0053376
4. Aitken ME, McCarthy ML, Slomine BS, Ding R, Durbin DR, Jaffe KM, Paidas CN, Dorsch AM, Christensen JR, Mackenzie EJ (2009) Family burden after traumatic brain injury in children. *Pediatrics* 123:199-206. doi:10.1542/peds.2008-0607
5. Alderson NL, Maldonado EN, Kern MJ, Bhat NR, Hama H (2006) FA2H-dependent fatty acid 2-hydroxylation in postnatal mouse brain. *J Lipid Res* 47:2772-2780. doi:10.1194/jlr.M600362-JLR200
6. Alexander S, Kerr ME, Kim Y, Kamboh MI (2007) Apolipoprotein E4 allele presence and functional outcome after severe traumatic brain injury. *Journal of Neurotrauma* 24:790-797
7. American Psychiatric A, American Psychiatric A, Force DSMT (2013) Diagnostic and statistical manual of mental disorders : DSM-5.
8. Anthony-muthu TS, Kenny EM, Bayir H (2016) Therapies targeting lipid peroxidation in traumatic brain injury. *Brain Res* 1640:57-76. doi:10.1016/j.brainres.2016.02.006
9. Bales KR, Verina T, Dodel RC, Du Y, Altstiel L, Bender M, Hyslop P, Johnstone EM, Little SP, Cummins DJ, Piccardo P, Ghetti B, Paul SM (1997) Lack of apolipoprotein E dramatically reduces amyloid beta-peptide deposition. *NatGenet* 17:263-264
10. Barger SW, Harmon AD (1997) Microglial activation by Alzheimer amyloid precursor protein and modulation by apolipoprotein E. *Nature* 388:878-881. doi:10.1038/42257
11. Bazarian JJ, Cernak I, Noble-Haeusslein L, Potolicchio S, Temkin N (2009) Long-term neurologic outcomes after traumatic brain injury. *J Head Trauma Rehabil* 24:439-451. doi:10.1097/HTR.0b013e3181c15600
12. Bennett RE, Esparza TJ, Lewis HA, Kim E, Mac Donald CL, Sullivan PM, Brody DL (2013) Human apolipoprotein E4 worsens acute axonal pathology but not amyloid-beta

- immunoreactivity after traumatic brain injury in 3xTG-AD mice. *J Neuropathol Exp Neurol* 72:396-403. doi:10.1097/NEN.0b013e31828e24ab
13. Bianchin MM, Capella HM, Chaves DL, Steindel M, Grisard EC, Ganev GG, da Silva Junior JP, Neto Evaldo S, Poffo MA, Walz R, Carlotti Junior CG, Sakamoto AC (2004) Nasu-Hakola disease (polycystic lipomembranous osteodysplasia with sclerosing leukoencephalopathy--PLOSL): a dementia associated with bone cystic lesions. From clinical to genetic and molecular aspects. *Cell Mol Neurobiol* 24:1-24
 14. Bird SM, Sohrabi HR, Sutton TA, Weinborn M, Rainey-Smith SR, Brown B, Patterson L, Taddei K, Gupta V, Carruthers M, Lenzo N, Knuckey N, Bucks RS, Verdile G, Martins RN (2016) Cerebral amyloid-beta accumulation and deposition following traumatic brain injury--A narrative review and meta-analysis of animal studies. *Neurosci Biobehav Rev* 64:215-228. doi:10.1016/j.neubiorev.2016.01.004
 15. Bjorkhem I, Meaney S (2004) Brain cholesterol: long secret life behind a barrier. *Arterioscler Thromb Vasc Biol* 24:806-815. doi:10.1161/01.ATV.0000120374.59826.1b
 16. Blocquel D, Li S, Wei N, Daub H, Sajish M, Erfurth ML, Kooi G, Zhou J, Bai G, Schimmel P, Jordanova A, Yang XL (2017) Alternative stable conformation capable of protein misinteraction links tRNA synthetase to peripheral neuropathy. *Nucleic acids research* 45:8091-8104. doi:10.1093/nar/gkx455
 17. Borgesius NZ, van Woerden GM, Buitendijk GH, Keijzer N, Jaarsma D, Hoogenraad CC, Elgersma Y (2011) betaCaMKII plays a nonenzymatic role in hippocampal synaptic plasticity and learning by targeting alphaCaMKII to synapses. *J Neurosci* 31:10141-10148. doi:10.1523/JNEUROSCI.5105-10.2011
 18. Bramlett HM, Dietrich WD (2015) Long-Term Consequences of Traumatic Brain Injury: Current Status of Potential Mechanisms of Injury and Neurological Outcomes. *J Neurotrauma* 32:1834-1848. doi:10.1089/neu.2014.3352
 19. Brody DL, Mac Donald C, Kessens CC, Yuede C, Parsadonian M, Spinner M, Kim E, Schwetye KE, Holtzman DM, Bayly PV (2007) Electromagnetic controlled cortical impact device for precise, graded experimental traumatic brain injury. *J Neurotrauma* 24:657-673. doi:10.1089/neu.2006.0011
 20. Brooks-Wilson A, Marcil M, Clee SM, Zhang LH, Roomp K, van Dam M, Yu L, Brewer C, Collins JA, Molhuizen HO, Loubser O, Ouellette BF, Fichter K, Ashbourne-Excoffon KJ, Sensen CW, Scherer S, Mott S, Denis M, Martindale D, Frohlich J, Morgan K, Koop B, Pimstone S, Kastelein JJ, Hayden MR (1999) Mutations in ABC1 in Tangier disease and familial high-density lipoprotein deficiency. *Nature Genet* 22:336-345
 21. Bujalka H, Koening M, Jackson S, Perreau VM, Pope B, Hay CM, Mitew S, Hill AF, Lu QR, Wegner M, Srinivasan R, Svaren J, Willingham M, Barres BA, Emery B (2013) MYRF is a membrane-associated transcription factor that autoproteolytically cleaves to directly activate myelin genes. *PLoS Biol* 11:e1001625. doi:10.1371/journal.pbio.1001625
 22. Cartagena CM, Ahmed F, Burns MP, Pajoohesh-Ganji A, Pak DT, Faden AI, Rebeck GW (2008) Cortical injury increases cholesterol 24S hydroxylase (Cyp46) levels in the rat brain. *J Neurotrauma* 25:1087-1098. doi:10.1089/neu.2007.0444
 23. Carter AY, Letronne F, Fitz NF, Mounier A, Wolfe CM, Nam KN, Reeves VL, Kamboh H, Lefterov I, Koldamova R (2017) Liver X receptor agonist treatment significantly affects phenotype and transcriptome of APOE3 and APOE4 Abca1 haplo-deficient mice. *PLoS One* 12:e0172161. doi:10.1371/journal.pone.0172161

24. Castranio EL, Mounier A, Wolfe CM, Nam KN, Fitz NF, Letronne F, Schug J, Koldamova R, Lefterov I (2017) Gene co-expression networks identify Trem2 and Tyrobp as major hubs in human APOE expressing mice following traumatic brain injury. *Neurobiol Dis* 105:1-14. doi:10.1016/j.nbd.2017.05.006
25. Centers for Disease C, Prevention (2013) CDC grand rounds: reducing severe traumatic brain injury in the United States. *MMWR Morb Mortal Wkly Rep* 62:549-552
26. Chamelian L, Reis M, Feinstein A (2004) Six-month recovery from mild to moderate Traumatic Brain Injury: the role of APOE-epsilon4 allele. *Brain* 127:2621-2628. doi:10.1093/brain/awh296
27. Chauhan NB (2014) Chronic neurodegenerative consequences of traumatic brain injury. *Restor Neurol Neurosci* 32:337-365. doi:10.3233/RNN-130354
28. Chrast R, Saher G, Nave KA, Verheijen MH (2011) Lipid metabolism in myelinating glial cells: lessons from human inherited disorders and mouse models. *J Lipid Res* 52:419-434. doi:10.1194/jlr.R009761
29. Cirrito JR, Deane R, Fagan AM, Spinner ML, Parsadanian M, Finn MB, Jiang H, Prior JL, Sagare A, Bales KR, Paul SM, Zlokovic BV, Piwnica-Worms D, Holtzman DM (2005) P-glycoprotein deficiency at the blood-brain barrier increases amyloid-beta deposition in an Alzheimer disease mouse model. *J Clin Invest* 115:3285-3290
30. Colonna M, Wang Y (2016) TREM2 variants: new keys to decipher Alzheimer disease pathogenesis. *Nat Rev Neurosci* 17:201-207. doi:10.1038/nrn.2016.7
31. Coronado VG, Xu L, Basavaraju SV, McGuire LC, Wald MM, Faul MD, Guzman BR, Hemphill JD, Centers for Disease C, Prevention (2011) Surveillance for traumatic brain injury-related deaths--United States, 1997-2007. *MMWR Surveill Summ* 60:1-32
32. Corrigan JD, Selassie AW, Orman JA (2010) The epidemiology of traumatic brain injury. *J Head Trauma Rehabil* 25:72-80. doi:10.1097/HTR.0b013e3181ccc8b4
33. Crawford F, Wood M, Ferguson S, Mathura V, Gupta P, Humphrey J, Mouzon B, Laporte V, Margenthaler E, O'Steen B, Hayes R, Roses A, Mullan M (2009) Apolipoprotein E-genotype dependent hippocampal and cortical responses to traumatic brain injury. *Neuroscience* 159:1349-1362. doi:10.1016/j.neuroscience.2009.01.033
34. Crawford FC, Vanderploeg RD, Freeman MJ, Singh S, Waisman M, Michaels L, Abdullah L, Warden D, Lipsky R, Salazar A, Mullan MJ (2002) APOE genotype influences acquisition and recall following traumatic brain injury. *Neurology* 58:1115-1118
35. Cruchaga C, Karch CM, Jin SC, Benitez BA, Cai Y, Guerreiro R, Harari O, Norton J, Budde J, Bertelsen S, Jeng AT, Cooper B, Skorupa T, Carrell D, Levitch D, Hsu S, Choi J, Ryten M, Consortium UKBE, Hardy J, Ryten M, Trabzuni D, Weale ME, Ramasamy A, Smith C, Sassi C, Bras J, Gibbs JR, Hernandez DG, Lupton MK, Powell J, Forabosco P, Ridge PG, Corcoran CD, Tschanz JT, Norton MC, Munger RG, Schmutz C, Leary M, Demirci FY, Bamne MN, Wang X, Lopez OL, Ganguli M, Medway C, Turton J, Lord J, Braae A, Barber I, Brown K, Alzheimer's Research UKC, Passmore P, Craig D, Johnston J, McGuinness B, Todd S, Heun R, Kolsch H, Kehoe PG, Hooper NM, Vardy ER, Mann DM, Pickering-Brown S, Brown K, Kalsheker N, Lowe J, Morgan K, David Smith A, Wilcock G, Warden D, Holmes C, Pastor P, Lorenzo-Betancor O, Brkanac Z, Scott E, Topol E, Morgan K, Rogaeva E, Singleton AB, Hardy J, Kamboh MI, St George-Hyslop P, Cairns N, Morris JC, Kauwe JS, Goate AM (2014) Rare coding variants in the phospholipase D3 gene confer risk for Alzheimer's disease. *Nature* 505:550-554. doi:10.1038/nature12825

36. Dalgard CL, Cole JT, Kean WS, Lucky JJ, Sukumar G, McMullen DC, Pollard HB, Watson WD (2012) The cytokine temporal profile in rat cortex after controlled cortical impact. *Frontiers in molecular neuroscience* 5:6-6
37. Das M, Mohapatra S, Mohapatra SS (2012) New perspectives on central and peripheral immune responses to acute traumatic brain injury. *J Neuroinflammation* 9:236. doi:10.1186/1742-2094-9-236
38. Diaz-Arrastia R, Gong Y, Fair S, Scott KD, Garcia MC, Carlile MC, Agostini MA, Van Ness PC (2003) Increased risk of late posttraumatic seizures associated with inheritance of APOE epsilon4 allele. *Arch Neurol* 60:818-822. doi:10.1001/archneur.60.6.818
39. Donat CK, Scott G, Gentleman SM, Sastre M (2017) Microglial Activation in Traumatic Brain Injury. *Front Aging Neurosci* 9:208. doi:10.3389/fnagi.2017.00208
40. Draper K, Ponsford J (2008) Cognitive functioning ten years following traumatic brain injury and rehabilitation. *Neuropsychology* 22:618-625. doi:10.1037/0894-4105.22.5.618
41. Fagan AM, Holtzman DM, Munson G, Mathur T, Schneider D, Chang LK, Getz GS, Reardon CA, Lukens J, Shah JA, LaDu MJ (1999) Unique lipoproteins secreted by primary astrocytes from wild type, apoE (-/-), and human apoE transgenic mice. *J Biol Chem* 274:30001-30007
42. Faul M, Coronado V (2015) Epidemiology of traumatic brain injury. *Handb Clin Neurol* 127:3-13. doi:10.1016/B978-0-444-52892-6.00001-5
43. Ferreira LCB, Regner A, Miotto KDL, Moura Sd, Ikuta N, Vargas AE, Chies JAB, Simon D (2014) Increased levels of interleukin-6, -8 and -10 are associated with fatal outcome following severe traumatic brain injury. *Brain injury* 28:1311-1316
44. Fitz NF, Cronican A, Pham T, Fogg A, Fauq AH, Chapman R, Lefterov I, Koldamova R (2010) Liver X receptor agonist treatment ameliorates amyloid pathology and memory deficits caused by high-fat diet in APP23 mice. *J Neurosci* 30:6862-6872
45. Fitz NF, Cronican AA, Lefterov I, Koldamova R (2013) Comment on "ApoE-directed therapeutics rapidly clear beta-amyloid and reverse deficits in AD mouse models". *Science* 340:924-c. doi:10.1126/science.1235809
46. Fitz NF, Cronican AA, Saleem M, Fauq AH, Chapman R, Lefterov I, Koldamova R (2012) Abca1 deficiency affects Alzheimer's disease-like phenotype in human ApoE4 but not in ApoE3-targeted replacement mice. *J Neurosci* 32:13125-13136. doi:10.1523/JNEUROSCI.1937-12.2012
47. Fitz NF, Tapias V, Cronican AA, Castranio EL, Saleem M, Carter AY, Lefterova M, Lefterov I, Koldamova R (2015) Opposing effects of Apoe/Apoa1 double deletion on amyloid-beta pathology and cognitive performance in APP mice. *Brain* 138:3699-3715. doi:10.1093/brain/awv293
48. Forsyth S, Horvath A, Coughlin P (2003) A review and comparison of the murine alpha1-antitrypsin and alpha1-antichymotrypsin multigene clusters with the human clade A serpins. *Genomics* 81:336-345
49. Ghroubi S, Feki I, Chelly H, Elleuch MH (2016) Neuropsychological and behavioral disorders and their correlations with the severity of the traumatic brain injury. *Ann Phys Rehabil Med* 59S:e134-e135. doi:10.1016/j.rehab.2016.07.302
50. Guan F, Gu J, Hu F, Zhu Y, Wang W (2012) Association between alpha1-antichymotrypsin signal peptide -15A/T polymorphism and the risk of Alzheimer's disease: a meta-analysis. *Mol Biol Rep* 39:6661-6669. doi:10.1007/s11033-012-1472-8

51. Gyoneva S, Ransohoff RM (2015) Inflammatory reaction after traumatic brain injury: therapeutic potential of targeting cell-cell communication by chemokines. *Trends in pharmacological sciences* 36:471-480
52. Gyoneva S, Ransohoff RM (2015) Inflammatory reaction after traumatic brain injury: therapeutic potential of targeting cell-cell communication by chemokines. *Trends Pharmacol Sci* 36:471-480. doi:10.1016/j.tips.2015.04.003
53. Haile Y, Carmine-Simmen K, Olechowski C, Kerr B, Bleackley RC, Giuliani F (2015) Granzyme B-inhibitor serpinA3n induces neuroprotection in vitro and in vivo. *J Neuroinflammation* 12:157. doi:10.1186/s12974-015-0376-7
54. Hauser PS, Narayanaswami V, Ryan RO (2011) Apolipoprotein E: from lipid transport to neurobiology. *Prog Lipid Res* 50:62-74. doi:10.1016/j.plipres.2010.09.001
55. Hickman SE, Kingery ND, Ohsumi TK, Borowsky ML, Wang LC, Means TK, El Khoury J (2013) The microglial sensome revealed by direct RNA sequencing. *Nat Neurosci* 16:1896-1905. doi:10.1038/nn.3554
56. Holmin S, Mathiesen T, Shetye J, Biberfeld P (1995) Intracerebral inflammatory response to experimental brain contusion. *Acta neurochirurgica* 132:110-119
57. Hooli BV, Lill CM, Mullin K, Qiao D, Lange C, Bertram L, Tanzi RE (2015) PLD3 gene variants and Alzheimer's disease. *Nature* 520:E7-8. doi:10.1038/nature14040
58. Hsu I, Parkinson LG, Shen Y, Toro A, Brown T, Zhao H, Bleackley RC, Granville DJ (2014) SerpinA3n accelerates tissue repair in a diabetic mouse model of delayed wound healing. *Cell Death Dis* 5:e1458. doi:10.1038/cddis.2014.423
59. Hua F, Wang J, Ishrat T, Wei W, Atif F, Sayeed I, Stein DG (2011) Genomic profile of Toll-like receptor pathways in traumatically brain-injured mice: effect of exogenous progesterone. *Journal of neuroinflammation* 8:42-42
60. Huang Y, Mahley RW (2014) Apolipoprotein E: structure and function in lipid metabolism, neurobiology, and Alzheimer's diseases. *Neurobiol Dis* 72 Pt A:3-12. doi:10.1016/j.nbd.2014.08.025
61. Jay TR, Miller CM, Cheng PJ, Graham LC, Bemiller S, Broihier ML, Xu G, Margevicius D, Karlo JC, Sousa GL, Cotleur AC, Butovsky O, Bekris L, Staugaitis SM, Leverenz JB, Pimplikar SW, Landreth GE, Howell GR, Ransohoff RM, Lamb BT (2015) TREM2 deficiency eliminates TREM2+ inflammatory macrophages and ameliorates pathology in Alzheimer's disease mouse models. *J Exp Med* 212:287-295. doi:10.1084/jem.20142322
62. Jordan BD (2007) Genetic influences on outcome following traumatic brain injury. *Neurochem Res* 32:905-915. doi:10.1007/s11064-006-9251-3
63. Jordan BD (2014) Chronic traumatic encephalopathy and other long-term sequelae. *Continuum (Minneapolis)* 20:1588-1604. doi:10.1212/01.CON.0000458972.94013.e1
64. Kamboh MI, Sanghera DK, Ferrell RE, DeKosky ST (1995) APOE*4-associated Alzheimer's disease risk is modified by alpha 1-antichymotrypsin polymorphism. *Nat Genet* 10:486-488. doi:10.1038/ng0895-486
65. Karasinska JM, de Haan W, Franciosi S, Ruddell P, Fan J, Kruit JK, Stukas S, Lutjohann D, Gutmann DH, Wellington CL, Hayden MR (2013) ABCA1 influences neuroinflammation and neuronal death. *Neurobiol Dis* 54:445-455. doi:10.1016/j.nbd.2013.01.018
66. Kawabori M, Kacimi R, Kauppinen T, Calosing C, Kim JY, Hsieh CL, Nakamura MC, Yenari MA (2015) Triggering receptor expressed on myeloid cells 2 (TREM2) deficiency

- attenuates phagocytic activities of microglia and exacerbates ischemic damage in experimental stroke. *J Neurosci* 35:3384-3396. doi:10.1523/JNEUROSCI.2620-14.2015
67. Kelley BJ, Lifshitz J, Povlishock JT (2007) Neuroinflammatory responses after experimental diffuse traumatic brain injury. *Journal of neuropathology and experimental neurology* 66:989-1001
 68. Kim J, Basak JM, Holtzman DM (2009) The role of apolipoprotein E in Alzheimer's disease. *Neuron* 63:287-303. doi:10.1016/j.neuron.2009.06.026
 69. Koldamova R, Fitz NF, Lefterov I (2010) The role of ATP-binding cassette transporter A1 in Alzheimer's disease and neurodegeneration. *Biochim Biophys Acta* 1801:824-830. doi:10.1016/j.bbaliip.2010.02.010
 70. Koldamova R, Fitz NF, Lefterov I (2014) ATP-binding cassette transporter A1: from metabolism to neurodegeneration. *Neurobiol Dis* 72 Pt A:13-21. doi:10.1016/j.nbd.2014.05.007
 71. Koldamova R, Staufenbiel M, Lefterov I (2005) Lack of ABCA1 considerably decreases brain ApoE level and increases amyloid deposition in APP23 mice. *J Biol Chem* 280:43224-43235. doi:10.1074/jbc.M504513200
 72. Langlois JA, Kegler SR, Butler JA, Gotsch KE, Johnson RL, Reichard AA, Webb KW, Coronado VG, Selassie AW, Thurman DJ (2003) Traumatic brain injury-related hospital discharges. Results from a 14-state surveillance system, 1997. *MMWR Surveill Summ* 52:1-20
 73. Laskowitz DT, Fillit H, Yeung N, Toku K, Vitek MP (2006) Apolipoprotein E-derived peptides reduce CNS inflammation: implications for therapy of neurological disease. *Acta Neurol Scand Suppl* 185:15-20. doi:10.1111/j.1600-0404.2006.00680.x
 74. Lau DH, Hogseth M, Phillips EC, O'Neill MJ, Pooler AM, Noble W, Hanger DP (2016) Critical residues involved in tau binding to fyn: implications for tau phosphorylation in Alzheimer's disease. *Acta Neuropathol Commun* 4:49. doi:10.1186/s40478-016-0317-4
 75. Leduc V, Jasmin-Belanger S, Poirier J (2010) APOE and cholesterol homeostasis in Alzheimer's disease. *Trends Mol Med* 16:469-477. doi:10.1016/j.molmed.2010.07.008
 76. Lefterov I, Fitz NF, Cronican AA, Fogg A, Lefterov P, Kodali R, Wetzel R, Koldamova R (2010) Apolipoprotein A-I deficiency increases cerebral amyloid angiopathy and cognitive deficits in APP/PS1DeltaE9 mice. *Journal of Biological Chemistry* 285:36945-36957
 77. Li X, Montine KS, Keene CD, Montine TJ (2015) Different mechanisms of apolipoprotein E isoform-dependent modulation of prostaglandin E2 production and triggering receptor expressed on myeloid cells 2 (TREM2) expression after innate immune activation of microglia. *FASEB J* 29:1754-1762. doi:10.1096/fj.14-262683
 78. Liliang PC, Liang CL, Weng HC, Lu K, Wang KW, Chen HJ, Chuang JH (2010) Tau proteins in serum predict outcome after severe traumatic brain injury. *J Surg Res* 160:302-307. doi:10.1016/j.jss.2008.12.022
 79. Lynch JR, Morgan D, Mance J, Matthew WD, Laskowitz DT (2001) Apolipoprotein E modulates glial activation and the endogenous central nervous system inflammatory response. *J Neuroimmunol* 114:107-113
 80. Maas AI, Stocchetti N, Bullock R (2008) Moderate and severe traumatic brain injury in adults. *Lancet Neurol* 7:728-741. doi:10.1016/s1474-4422(08)70164-9
 81. Mahley RW (1988) Apolipoprotein E: cholesterol transport protein with expanding role in cell biology. *Science* 240:622-630

82. Mahley RW (2016) Apolipoprotein E: from cardiovascular disease to neurodegenerative disorders. *J Mol Med (Berl)* 94:739-746. doi:10.1007/s00109-016-1427-y
83. Mahley RW, Huang Y (1999) Apolipoprotein E: from atherosclerosis to Alzheimer's disease and beyond. *Curr Opin Lipidol* 10:207-217
84. Mahley RW, Rall SC, Jr. (2000) Apolipoprotein E: far more than a lipid transport protein. *Annu Rev Genomics Hum Genet* 1:507-537. doi:10.1146/annurev.genom.1.1.507
85. Mannix R, Meehan WP, Mandeville J, Grant PE, Gray T, Berglass J, Zhang J, Bryant J, Rezaie S, Chung JY, Peters NV, Lee C, Tien LW, Kaplan DL, Feany M, Whalen M (2013) Clinical correlates in an experimental model of repetitive mild brain injury. *Ann Neurol* 74:65-75. doi:10.1002/ana.23858
86. Mannix RC, Zhang J, Park J, Zhang X, Bilal K, Walker K, Tanzi RE, Tesco G, Whalen MJ (2011) Age-dependent effect of apolipoprotein E4 on functional outcome after controlled cortical impact in mice. *J Cereb Blood Flow Metab* 31:351-361. doi:10.1038/jcbfm.2010.99
87. Mannix RC, Zhang J, Park J, Zhang X, Bilal K, Walker K, Tanzi RE, Tesco G, Whalen MJ (2016) Age-dependent effect of apolipoprotein E4 on functional outcome after controlled cortical impact in mice. *Journal of Cerebral Blood Flow & Metabolism* 31:351-361
88. McKee AC, Cairns NJ, Dickson DW, Folkerth RD, Keene CD, Litvan I, Perl DP, Stein TD, Vonsattel JP, Stewart W, Tripodis Y, Crary JF, Bieniek KF, Dams-O'Connor K, Alvarez VE, Gordon WA, group TC (2016) The first NINDS/NIBIB consensus meeting to define neuropathological criteria for the diagnosis of chronic traumatic encephalopathy. *Acta Neuropathol* 131:75-86. doi:10.1007/s00401-015-1515-z
89. Mootha VK, Lepage P, Miller K, Bunkenborg J, Reich M, Hjerrild M, Delmonte T, Villeneuve A, Sladek R, Xu F, Mitchell GA, Morin C, Mann M, Hudson TJ, Robinson B, Rioux JD, Lander ES (2003) Identification of a gene causing human cytochrome c oxidase deficiency by integrative genomics. *Proc Natl Acad Sci U S A* 100:605-610. doi:10.1073/pnas.242716699
90. Moran L, Taylor H, Ganesalingam K, Gastier-Foster J, Frick J, Bangert B, Dietrich A, Nuss K, Rusin J, Wright M, Yeates K (2009) Apolipoprotein E4 as a predictor of outcomes in pediatric mild traumatic brain injury. *J Neurotraum* 26:1489-1495
91. Morganti JM, Jopson TD, Liu S, Riparip L-K, Guandique CK, Gupta N, Ferguson AR, Rosi S (2015) CCR2 antagonism alters brain macrophage polarization and ameliorates cognitive dysfunction induced by traumatic brain injury. *The Journal of neuroscience : the official journal of the Society for Neuroscience* 35:748-760
92. Morrow JA, Segall ML, Lund-Katz S, Phillips MC, Knapp M, Rupp B, Weisgraber KH (2000) Differences in stability among the human apolipoprotein E isoforms determined by the amino-terminal domain. *Biochemistry* 39:11657-11666
93. Muller WE, Eckert A, Kurz C, Eckert GP, Leuner K (2010) Mitochondrial dysfunction: common final pathway in brain aging and Alzheimer's disease--therapeutic aspects. *Mol Neurobiol* 41:159-171. doi:10.1007/s12035-010-8141-5
94. Nagata KO, Nakada C, Kasai RS, Kusumi A, Ueda K (2013) ABCA1 dimer-monomer interconversion during HDL generation revealed by single-molecule imaging. *Proc Natl Acad Sci U S A* 110:5034-5039. doi:10.1073/pnas.1220703110
95. Nam KN, Mounier A, Fitz NF, Wolfe C, Schug J, Lefterov I, Koldamova R (2016) RXR controlled regulatory networks identified in mouse brain counteract deleterious effects of Abeta oligomers. *Sci Rep* 6:24048. doi:10.1038/srep24048

96. Nam KN, Mounier A, Wolfe CM, Fitz NF, Carter AY, Castranio EL, Kamboh HI, Reeves VL, Wang J, Han X, Schug J, Lefterov I, Koldamova R (2017) Effect of high fat diet on phenotype, brain transcriptome and lipidome in Alzheimer's model mice. *Sci Rep* 7:4307. doi:10.1038/s41598-017-04412-2
97. Nam KN, Wolfe CM, Fitz NF, Letronne F, Castranio EL, Mounier A, Schug J, Lefterov I, Koldamova R (2018) Integrated approach reveals diet, APOE genotype and sex affect immune response in APP mice. *Biochim Biophys Acta* 1864:152-161. doi:10.1016/j.bbadis.2017.10.018
98. Nayak D, Roth TL, McGavern DB (2014) Microglia development and function. *Annual review of immunology* 32:367-402. doi:10.1146/annurev-immunol-032713-120240
99. Nizamutdinov D, Shapiro LA (2017) Overview of Traumatic Brain Injury: An Immunological Context. *Brain Sci* 7. doi:10.3390/brainsci7010011
100. Nygaard HB, van Dyck CH, Strittmatter SM (2014) Fyn kinase inhibition as a novel therapy for Alzheimer's disease. *Alzheimers Res Ther* 6:8. doi:10.1186/alzrt238
101. Oram JF, Vaughan AM (2006) ATP-Binding cassette cholesterol transporters and cardiovascular disease. *Circulation research* 99:1031-1043. doi:10.1161/01.RES.0000250171.54048.5c
102. Osisami M, Ali W, Frohman MA (2012) A role for phospholipase D3 in myotube formation. *PLoS One* 7:e33341. doi:10.1371/journal.pone.0033341
103. Panicker N, Saminathan H, Jin H, Neal M, Harischandra DS, Gordon R, Kanthasamy K, Lawana V, Sarkar S, Luo J, Anantharam V, Kanthasamy AG, Kanthasamy A (2015) Fyn Kinase Regulates Microglial Neuroinflammatory Responses in Cell Culture and Animal Models of Parkinson's Disease. *J Neurosci* 35:10058-10077. doi:10.1523/JNEUROSCI.0302-15.2015
104. Pathania D, Millard M, Neamati N (2009) Opportunities in discovery and delivery of anticancer drugs targeting mitochondria and cancer cell metabolism. *Advanced drug delivery reviews* 61:1250-1275. doi:10.1016/j.addr.2009.05.010
105. Perez-Garcia G, Gama Sosa MA, De Gasperi R, Lashof-Sullivan M, Maudlin-Jeronimo E, Stone JR, Haghghi F, Ahlers ST, Elder GA (2016) Chronic post-traumatic stress disorder-related traits in a rat model of low-level blast exposure. *Behav Brain Res.* doi:10.1016/j.bbr.2016.09.061
106. Pfrieger FW (2010) Role of glial cells in the formation and maintenance of synapses. *Brain Res Rev* 63:39-46. doi:10.1016/j.brainresrev.2009.11.002
107. Pitas RE, Boyles JK, Lee SH, Foss D, Mahley RW (1987) Astrocytes synthesize apolipoprotein E and metabolize apolipoprotein E-containing lipoproteins. *Biochim Biophys Acta* 917:148-161
108. Pitas RE, Boyles JK, Lee SH, Hui D, Weisgraber KH (1987) Lipoproteins and their receptors in the central nervous system. Characterization of the lipoproteins in cerebrospinal fluid and identification of apolipoprotein B,E(LDL) receptors in the brain. *J Biol Chem* 262:14352-14360
109. Plassman BL, Grafman J (2015) Traumatic brain injury and late-life dementia. *Handb Clin Neurol* 128:711-722. doi:10.1016/B978-0-444-63521-1.00044-3
110. Ponsford J, Draper K, Schonberger M (2008) Functional outcome 10 years after traumatic brain injury: its relationship with demographic, injury severity, and cognitive and emotional status. *J Int Neuropsychol Soc* 14:233-242. doi:10.1017/S1355617708080272

111. Ponsford J, Rudzki D, Bailey K, Ng KT (2007) Impact of apolipoprotein gene on cognitive impairment and recovery after traumatic brain injury. *Neurology* 68:619-620. doi:10.1212/01.wnl.0000254609.04330.9d
112. Povlishock JT, Christman CW (1995) The pathobiology of traumatically induced axonal injury in animals and humans: a review of current thoughts. *J Neurotrauma* 12:555-564. doi:10.1089/neu.1995.12.555
113. Richter F, Gao F, Medvedeva V, Lee P, Bove N, Fleming SM, Michaud M, Lemesre V, Patassini S, De La Rosa K, Mulligan CK, Sioshansi PC, Zhu C, Coppola G, Bordet T, Pruss RM, Chesselet MF (2014) Chronic administration of cholesterol oximes in mice increases transcription of cytoprotective genes and improves transcriptome alterations induced by alpha-synuclein overexpression in nigrostriatal dopaminergic neurons. *Neurobiol Dis* 69:263-275. doi:10.1016/j.nbd.2014.05.012
114. Rodriguez GA, Burns MP, Weeber EJ, Rebeck GW (2013) Young APOE4 targeted replacement mice exhibit poor spatial learning and memory, with reduced dendritic spine density in the medial entorhinal cortex. *Learn Mem* 20:256-266. doi:10.1101/lm.030031.112
115. Rodriguez GA, Tai LM, LaDu MJ, Rebeck GW (2014) Human APOE4 increases microglia reactivity at Abeta plaques in a mouse model of Abeta deposition. *J Neuroinflammation* 11:111. doi:10.1186/1742-2094-11-111
116. Rolls A, Shechter R, Schwartz M (2009) The bright side of the glial scar in CNS repair. *Nat Rev Neurosci* 10:235-241. doi:10.1038/nrn2591
117. Ruff RL, Blake K (2016) Pathophysiological links between traumatic brain injury and post-traumatic headaches. *F1000Res* 5. doi:10.12688/f1000research.9017.1
118. Saber M, Kokiko-Cochran O, Puntambekar SS, Lathia JD, Lamb BT (2016) Triggering Receptor Expressed on Myeloid Cells 2 Deficiency Alters Acute Macrophage Distribution and Improves Recovery after Traumatic Brain Injury. *J Neurotrauma*. doi:10.1089/neu.2016.4401
119. Saher G, Brugger B, Lappe-Siefke C, Mobius W, Tozawa R, Wehr MC, Wieland F, Ishibashi S, Nave KA (2005) High cholesterol level is essential for myelin membrane growth. *Nat Neurosci* 8:468-475. doi:10.1038/nn1426
120. Saher G, Stumpf SK (2015) Cholesterol in myelin biogenesis and hypomyelinating disorders. *Biochim Biophys Acta* 1851:1083-1094. doi:10.1016/j.bbali.2015.02.010
121. Savage JC, Jay T, Goduni E, Quigley C, Mariani MM, Malm T, Ransohoff RM, Lamb BT, Landreth GE (2015) Nuclear receptors license phagocytosis by trem2+ myeloid cells in mouse models of Alzheimer's disease. *J Neurosci* 35:6532-6543. doi:10.1523/JNEUROSCI.4586-14.2015
122. Schiza N, Sargiannidou I, Kagiava A, Karaiskos C, Nearchou M, Kleopa KA (2015) Transgenic replacement of Cx32 in gap junction-deficient oligodendrocytes rescues the phenotype of a hypomyelinating leukodystrophy model. *Hum Mol Genet* 24:2049-2064. doi:10.1093/hmg/ddu725
123. Selassie AW, Zaloshnja E, Langlois JA, Miller T, Jones P, Steiner C (2008) Incidence of long-term disability following traumatic brain injury hospitalization, United States, 2003. *J Head Trauma Rehabil* 23:123-131. doi:10.1097/01.HTR.0000314531.30401.39
124. Shema R, Sacktor TC, Dudai Y (2007) Rapid erasure of long-term memory associations in the cortex by an inhibitor of PKM zeta. *Science* 317:951-953. doi:10.1126/science.1144334

125. Simon DW, McGeachy MJ, Bayir H, Clark RS, Loane DJ, Kochanek PM (2017) The far-reaching scope of neuroinflammation after traumatic brain injury. *Nat Rev Neurol* 13:171-191. doi:10.1038/nrneurol.2017.13
126. Subramanian A, Tamayo P, Mootha VK, Mukherjee S, Ebert BL, Gillette MA, Paulovich A, Pomeroy SL, Golub TR, Lander ES, Mesirov JP (2005) Gene set enrichment analysis: a knowledge-based approach for interpreting genome-wide expression profiles. *Proc Natl Acad Sci U S A* 102:15545-15550. doi:10.1073/pnas.0506580102
127. Susarla BT, Villapol S, Yi JH, Geller HM, Symes AJ (2014) Temporal patterns of cortical proliferation of glial cell populations after traumatic brain injury in mice. *ASN Neuro* 6:159-170. doi:10.1042/an20130034
128. Tang C, Oram JF (2009) The cell cholesterol exporter ABCA1 as a protector from cardiovascular disease and diabetes. *Biochim Biophys Acta* 1791:563-572. doi:10.1016/j.bbaliip.2009.03.011
129. Tiveron MC, Beurrier C, Ceni C, Andriambao N, Combes A, Koehl M, Maurice N, Gatti E, Abrous DN, Kerkerian-Le Goff L, Pierre P, Cremer H (2016) LAMP5 Fine-Tunes GABAergic Synaptic Transmission in Defined Circuits of the Mouse Brain. *PLoS One* 11:e0157052. doi:10.1371/journal.pone.0157052
130. Trushina E, Dutta T, Persson XM, Mielke MM, Petersen RC (2013) Identification of altered metabolic pathways in plasma and CSF in mild cognitive impairment and Alzheimer's disease using metabolomics. *PLoS One* 8:e63644. doi:10.1371/journal.pone.0063644
131. Tsai PC, Yang DM, Liao YC, Chiu TY, Kuo HC, Su YP, Guo YC, Soong BW, Lin KP, Liu YT, Lee YC (2016) Clinical and biophysical characterization of 19 GJB1 mutations. *Ann Clin Transl Neurol* 3:854-865. doi:10.1002/acn3.347
132. Venables WN, Ripley BD (2002) *Modern Applied Statistics with S. Statistics and Computing*, 4 edn. Springer-Verlag New York,
133. Walker WC, Pickett TC (2007) Motor impairment after severe traumatic brain injury: A longitudinal multicenter study. *J Rehabil Res Dev* 44:975-982
134. Wang C, Tan L, Wang HF, Yu WJ, Liu Y, Jiang T, Tan MS, Hao XK, Zhang DQ, Yu JT, Alzheimer's Disease Neuroimaging I (2015) Common Variants in PLD3 and Correlation to Amyloid-Related Phenotypes in Alzheimer's Disease. *J Alzheimers Dis* 46:491-495. doi:10.3233/JAD-150110
135. Wang S, Sheng T, Ren S, Tian T, Lu W (2016) Distinct Roles of PKC α and PKM ζ in the Initiation and Maintenance of Hippocampal Long-Term Potentiation and Memory. *Cell reports* 16:1954-1961. doi:10.1016/j.celrep.2016.07.030
136. Wang Y, Cella M, Mallinson K, Ulrich JD, Young KL, Robinette ML, Gilfillan S, Krishnan GM, Sudhakar S, Zinselmeyer BH, Holtzman DM, Cirrito JR, Colonna M (2015) TREM2 lipid sensing sustains the microglial response in an Alzheimer's disease model. *Cell* 160:1061-1071. doi:10.1016/j.cell.2015.01.049
137. Washington PM, Forcelli PA, Wilkins T, Zapple DN, Parsadanian M, Burns MP (2012) The effect of injury severity on behavior: a phenotypic study of cognitive and emotional deficits after mild, moderate, and severe controlled cortical impact injury in mice. *J Neurotrauma* 29:2283-2296. doi:10.1089/neu.2012.2456
138. Weisgraber KH (1990) Apolipoprotein E distribution among human plasma lipoproteins: role of the cysteine-arginine interchange at residue 112. *J Lipid Res* 31:1503-1511
139. Weisgraber KH (1994) Apolipoprotein E: structure-function relationships. *Adv Protein Chem* 45:249-302

140. White CR, Datta G, Giordano S (2017) High-Density Lipoprotein Regulation of Mitochondrial Function. *Adv Exp Med Biol* 982:407-429. doi:10.1007/978-3-319-55330-6_22
141. Whitnall L, McMillan TM, Murray GD, Teasdale GM (2006) Disability in young people and adults after head injury: 5-7 year follow up of a prospective cohort study. *J Neurol Neurosurg Psychiatry* 77:640-645. doi:10.1136/jnnp.2005.078246
142. Willemsse-van Son AHP, Ribbers GM, Hop WCJ, van Duijn CM, Stam HJ (2008) Association between apolipoprotein-epsilon4 and long-term outcome after traumatic brain injury. *Journal of neurology, neurosurgery, and psychiatry* 79:426-430
143. Xiong Y, Mahmood A, Chopp M (2013) Animal models of traumatic brain injury. *Nat Rev Neurosci* 14:128-142. doi:10.1038/nrn3407
144. Yang SH, Gangidine M, Pritts TA, Goodman MD, Lentsch AB (2013) Interleukin 6 mediates neuroinflammation and motor coordination deficits after mild traumatic brain injury and brief hypoxia in mice. *Shock (Augusta, Ga)* 40:471-475
145. Yiu G, He Z (2006) Glial inhibition of CNS axon regeneration. *Nat Rev Neurosci* 7:617-627. doi:10.1038/nrn1956
146. Yu H, Lin X, Wang D, Zhang Z, Guo Y, Ren X, Xu B, Yuan J, Liu J, Spencer PS, Wang JZ, Yang X (2018) Mitochondrial Molecular Abnormalities Revealed by Proteomic Analysis of Hippocampal Organelles of Mice Triple Transgenic for Alzheimer Disease. *Front Mol Neurosci* 11:74. doi:10.3389/fnmol.2018.00074
147. Zhang B, Horvath S (2005) A general framework for weighted gene co-expression network analysis. *Statistical applications in genetics and molecular biology* 4:Article17-Article17
148. Zhang L, Xing G, Tie Y, Tang Y, Tian C, Li L, Sun L, Wei H, Zhu Y, He F (2005) Role for the pleckstrin homology domain-containing protein CKIP-1 in AP-1 regulation and apoptosis. *The EMBO journal* 24:766-778. doi:10.1038/sj.emboj.7600532
149. Zhao W, Langfelder P, Fuller T, Dong J, Li A, Hovarth S (2010) Weighted gene coexpression network analysis: state of the art. *J Biopharm Stat* 20:281-300. doi:10.1080/10543400903572753
150. Zhong N, Weisgraber KH (2009) Understanding the association of apolipoprotein E4 with Alzheimer disease: clues from its structure. *J Biol Chem* 284:6027-6031. doi:10.1074/jbc.R800009200